UNIVERSITY OF NOVI SAD | FACULTY OF SCIENCES
DEPARTMENT OF GEOGRAPHY, TOURISM & HOTEL MANAGEMENT

INTERNATIONAL SCIENTIFIC JOURNAL

GEOGRAPHICA PANNONICA

Volume 30, Issue 2, June 2026

ISSN 0354-8724 (hard copy) | ISSN 1820-7138 (online) | UDC 05:91(497.1)=20

ISSN 0354-8724 (hard copy) | ISSN 1820-7138 (online) | UDC 05:91(497.1)=20

INTERNATIONAL SCIENTIFIC JOURNAL

GEOGRAPHICA PANNONICA

UNIVERSITY OF NOVI SAD | FACULTY OF SCIENCES | DEPARTMENT OF GEOGRAPHY, TOURISM & HOTEL MANAGEMENT

EDITOR IN CHIEF

Lazar Lazić, lazarus@uns.ac.rs

EDITORS

Jasmina Đorđević, jasminadjordjevic@live.com
Imre Nagy, nagyi@rkk.hu
Milka Bubalo Živković, milka.bubalo.zivkovic@dgt.uns.ac.rs
Aleksandra Dragin, sadragin@gmail.com
Mlađen Jovanović, mladjenov@gmail.com
Minučer Mesaroš, minucher@gmail.com

TECHNICAL EDITOR

Dragan Milošević, dragan.milosevic@dgt.uns.ac.rs
Jelena Dunjić, dunjicjelena1@gmail.com
Zorica Pogrmić, zorica.pogrmic@dgt.uns.ac.rs

EDITORIAL BOARD

Armelle Decaulne
CNRS UMR6042 - GEOLAB
Clermont-Ferrand cedex, Paris, France &
Natural Research Centre of North-western Iceland
Saudarkrokur, Iceland

Slobodan B. Marković
University of Novi Sad
Faculty of Science
Novi Sad, Serbia

Tobias Heckmann
Department of Geography, Physical Geography
Catholic University Eichstaett-Ingolstadt
Eichstätt, Germany

János Kovács
University of Pécs
Faculty of Science
Department of Geology
Pécs, Hungary

Petru Urdea
West University of Timişoara
Department of Geography
Timişoara, Romania

Péter Domonkos
University Rovira i Virgili de Tarragona
Geography Department
Center on Climate Change (C3)
Tarragona, Spain

Tamás Weidinger
Eötvös Loránd University
Institute of Geography and Earth Science
Department of Meteorology
Budapest, Hungary

Thomas Borén
Department of Human Geography
Stockholm University
Stockholm, Sweden

Tadeusz Stryjakiewicz
Adam Mickiewicz University
Institute of Socio-Economic Geography and Spatial Management
Poznań, Poland

Marko Krevs
University of Ljubljana
Faculty of Art, Department of Geography
Ljubljana, Slovenia

Horst Förster
Universität Tübingen
Geographisches Institut
Tübingen, Germany

Károly Kocsis
Geographical Research Institute
of the Hungarian Academy of Sciences
Budapest, Hungary

Konstantinos Andriotis
Cyprus University of Technology
Department of Hotel & Tourism Management
Cyprus

Jung Sung-Chae
Honam University
Department of Tourism Management
Gwangju, South Korea

ADVISORY BOARD

Ulrich Hambach
Geowissenschaften Universität Bayreuth
LS Geomorphologie
Bayreuth, Germany

Milivoj Gavrilov
University of Novi Sad
Faculty of Science
Novi Sad, Serbia

Darko Ogrin
University of Ljubljana
Faculty of Art, Department of Geography
Ljubljana, Slovenia

Nina Nikolova
"St. Kliment Ohridski" University of Sofia
Faculty of Geology and Geography
Department of Climatology, Hydrology and Geomorphology
Sofia, Bulgaria

Anna Leonowicz
University of Zurich
Department of Geography
Geographic Information Science (GIS)
Zurich, Switzerland

Zorana Lužanin
University of Novi Sad
Faculty of Science
Novi Sad, Serbia

Carlos Ferrás Sexto
University of Santiago de Compostela
Geography Department
Santiago de Compostela, Spain

Lajos Boros
University of Szeged
Department of Economic and Social Geography
Szeged, Hungary

Elena Matei
Bucharest University
Faculty of Geography
Bucharest, Romania

Yoel Mansfeld
University of Haifa
Department of Geography and Environmental Studies
Center for Tourism, Pilgrimage & Recreation Research
Haifa, Israel

Klodiana Gorica
University of Tirana
Faculty of Economics, Department of Marketing
Tirana, Albania

Damir Demonja
Institute for Development
and International Relations, IRMO,
Zagreb, Croatia

Praveen Kumar Rai
Banaras Hindu University
Department of Geography
Varanasi, India

EDITORIAL OFFICE

Faculty of Sciences
Department of Geography, Tourism and Hotel Management Trg
Dositeja Obradovića 3, 21000 Novi Sad, Serbia
tel. +381 21 450-105
fax +381 21 459-696
Official site: www.dgt.uns.ac.rs

CONTACTS

Lazar Lazić, PhD, full professor
Department of Geography, Tourism and Hotel Management, Serbia, lazarus@uns.ac.rs

Dragan Milošević, teaching assistant
Department of Geography, Tourism and Hotel Management, Serbia, dragan.milosevic@dgt.uns.ac.rs

Official mail of the Journal
gpscijournal@gmail.com

Internet portal
www.dgt.uns.ac.rs/pannonica.html

Instructions to authors
www.dgt.uns.ac.rs/pannonica/instructions.htm

Contents

Demir Šaćirović, Elvir Muslić, Fadil Novalić

Geographic Literacy and Spatial Thinking Among Primary School Teachers in Serbia.....88
DOI: 10.5937/gp30-65526

Utkarsha Pramod Dhurve, Sameer Deshkar

Tracing Integrative Pathways: A Bibliometric Analysis of Ecosystem Services in Landscape Planning.....101
DOI: 10.5937/gp30-63135

Lidiane da Silva Araújo, Antonio Samuel Alves da Silva, Rodrigo Luiz Costa Cavalcanti, Thiago Matheus Paiva do Passo, Matheus Dias Aguiar, Rosendo Chagas de Albuquerque, Ivana Tošić, Tatijana Stosic

Analysis of Concentration and Seasonality of Precipitation in Recife - Pernambuco, Brazil.....123
DOI: 10.5937/gp30-64717

Jean A. Doumit

Decoding Landscape Evolution: A Geomorphometric Approach to the Lebanese Terrain.....136
DOI: 10.5937/gp30-64913

Rasyiida Acintya, Tjahyo Nugroho Adji, Ahmad Cahyadi, Wafiq Nur Azizah, Akhmad Singgih

Epikarst Springs as Atmospheric CO_2 Sinks in a Tropical Karst Environment: Evidence from the Gunungsewu Karst, Indonesia.....153
DOI: 10.5937/gp30-66090

INTERNATIONAL SCIENTIFIC JOURNAL | GEOGRAPHICA PANNONICA | Volume 30, Issue 2, 88–100 (June 2026)
Journal homepage: http://www.dgt.uns.ac.rs/en/homepage/pannonica/

Geographic Literacy and Spatial Thinking Among Primary School Teachers in Serbia

Demir Šaćirović[A*], Elvir Muslić[B], Fadil Novalić[C]
[A]*Faculty of Teacher Education, University of Belgrade, Serbia; ORCID: 0000-0003-2625-2030*
[B]*Faculty of Sciences and Mathematics, University of Niš, Serbia; ORCID: 0009-0006-4042-6550*
[C]*Department of Computer Science, International University of Novi Pazar, Serbia; ORCID: 0000-0002-6921-0511*

Received: March 6, 2026| Revised: April 27, 2026| Accepted: May 27, 2026
doi: 10.5937/gp30-65526

ABSTRACT

Geographic literacy and spatial thinking are essential competencies for teaching Nature and Society (Priroda i društvo) in Serbian primary education, yet the level of these competencies among primary school teachers remains largely unexplored. This cross-sectional survey study investigated self-assessed geographic competencies, spatial thinking practices, and geographic knowledge among 206 primary school teachers across five regions of Serbia. Data were collected using a structured questionnaire comprising three sections: a self-assessment scale on geographic competencies (8 items, $\alpha = .645$), a spatial thinking practices scale (10 items, $\alpha = .416$), and a geographic knowledge test (8 items). Analyses included descriptive statistics, independent samples t-tests, and one-way ANOVA. Teachers reported moderate levels of geographic competency ($M = 3.66$, $SD = 0.54$). Those who had completed geography courses during their university studies scored significantly higher on all three measures ($p < .01$). Spatial thinking practices differed significantly by teaching experience ($F = 5.296$, $p = .002$), with teachers having over 25 years of experience reporting the lowest levels. Only 25.0% of respondents reported regular use of geospatial tools such as Google Earth. The knowledge test revealed uneven performance, with particularly low scores on altitude classification (17.0% correct) and map scale interpretation (56.5% correct). These results suggest that quantitative and classification-based geographic concepts may warrant greater attention in teacher preparation. However, the convenience sampling, overrepresentation of one region, and modest reliability of the spatial thinking scale limit the generalizability of the findings. Implications for teacher education and professional development are discussed.

Keywords: geographic literacy; spatial thinking, primary education; Nature and Society; Serbia; teacher competencies

*Corresponding author: Demir Šaćirović; e-mail: demirsacirovic@hotmail.com

Introduction

Geographic literacy, broadly defined as the ability to use geographic understanding and reasoning to make informed decisions about daily life and global issues (Edelson, 2012), represents a fundamental component of primary education. In Serbia, geographic content constitutes a significant portion of the Nature and Society (Priroda i društvo) curriculum taught in grades 3 and 4, as well as the World Around Us (Svet oko nas) curriculum in grades 1 and 2 (Ministarstvo prosvete, 2019). These subjects introduce young learners to key geographic concepts including spatial orientation, landscape features, climate, hydrography, and human-environment interactions.

Despite the importance of geographic content in primary education, research on the geographic literacy of primary school teachers in Serbia is notably scarce. International studies have shown that primary teachers often have limited geographic subject knowledge and low confidence in teaching geography (Catling, 2004; Catling & Morley, 2013; Preston, 2015), yet the existing body of literature in Serbia has primarily focused on secondary school geography teaching (Ivkov-Džigurski et al., 2019; Stojšić et al., 2019) and active teaching methods in geography classes (Lukić et al., 2016). Primary school teachers' geographic competencies remain an underexplored area in the Serbian context.

This gap is particularly significant because primary school teachers in Serbia are generalist educators responsible for teaching all subjects, including Nature and Society. Unlike secondary school geography teachers who hold specialized degrees, primary school teachers are trained at faculties of education (učiteljski fakulteti), where geographic content represents only a fraction of the curriculum (Šaćirović & Bratić, 2021). This raises concerns about the depth of geographic knowledge these teachers possess and their capacity to convey geographic concepts effectively.

Spatial thinking, a core component of geographic literacy, is widely recognized as a cognitive skill that supports learning across disciplines (National Research Council, 2006; Newcombe, 2010; Uttal et al., 2013). Geospatial technologies such as GIS, Google Earth, and digital mapping platforms offer promising avenues for enhancing geographic literacy in educational settings (Baker et al., 2015; Kerski, 2015; Patterson, 2007), yet the extent to which Serbian primary school teachers use these tools remains unknown.

Recent studies from the broader region have highlighted concerns about geographic literacy levels among both students and teachers. Lešćešen et al. (2024), in a study published in this journal, found significant gaps in climate change knowledge among primary school students in Serbia, suggesting potential shortcomings in how geographic content is taught. Similarly, Stojšić et al. (2019) examined the readiness of geography teachers to use mobile devices and immersive technologies, highlighting the importance of technological competencies in geographic education.

The purpose of this study is to: (1) assess the self-reported geographic competencies of primary school teachers in Serbia, (2) examine the extent to which spatial thinking practices are incorporated into Nature and Society teaching, (3) evaluate the use of geographic tools and geospatial technologies in primary education, and (4) identify factors (teaching experience, school location, geographic education background) that influence teachers' geographic literacy levels. The findings are expected to provide empirical evidence for improving teacher education curricula and professional development programs at Serbian faculties of education.

Theoretical Framework

Geographic Literacy in Primary Education

Geographic literacy encompasses three interrelated dimensions: geographic knowledge, geographic skills, and geographic dispositions (Heffron & Downs, 2012). Geographic knowledge includes factual information about places, regions, and spatial patterns. Geographic skills involve the ability to ask geographic questions, acquire geographic information, organize and analyze data, and communicate findings. Geographic dispositions reflect attitudes toward geography and a commitment to applying geographic thinking in everyday life. In the present study, geographic literacy is understood as a composite of these three dimensions and is operationalized through teachers' self-assessed competencies (Section A), their reported spatial thinking practices (Section B), and their performance on a curriculum-aligned knowledge test (Section C). This approach allows for a multi-faceted assessment that captures both perceived and demonstrated aspects of teachers' geographic literacy.

In the Serbian educational context, the Nature and Society curriculum integrates geographic content with elements of biology, ecology, history, and civic education (Ministarstvo prosvete, 2019). The geographic components include: orientation in space and time, natural characteristics of the homeland (relief, climate, hydrography), population and settlements, and human-environment relationships. Teachers are expected to facilitate students' understanding of these concepts through both theoretical instruction and practical field activities.

Spatial Thinking and the TPACK Framework

Spatial thinking refers to a set of cognitive skills that involve understanding the meaning of space, using properties of space to frame problems, and reasoning with

spatial representations such as maps, diagrams, and models (National Research Council, 2006). In an educational context, spatial thinking practices encompass the range of teaching activities through which teachers promote students' spatial reasoning — including the use of maps and atlases, orientation exercises, fieldwork, digital geospatial tools, and tasks that require students to represent spatial relationships (Gersmehl, 2014; Jo & Bednarz, 2009; Newcombe, 2010). In the present study, spatial thinking practices are operationally defined as the self-reported frequency with which teachers employ such activities in the teaching of Nature and Society content (see Section B of the instrument and Table 3).

The Technological Pedagogical Content Knowledge (TPACK) framework (Mishra & Koehler, 2006) provides a useful lens for examining how teachers integrate geographic content knowledge with pedagogical approaches and technological tools. TPACK posits that effective teaching requires the intersection of content, pedagogical, and technological knowledge — a perspective particularly relevant for primary school teachers who must make abstract geographic concepts accessible to young learners using age-appropriate methods and tools (Milson et al., 2012).

Teacher Competency and Professional Development

Research consistently demonstrates that teacher content knowledge significantly impacts student achievement (Hill et al., 2005; Shulman, 1986). In the field of geography education, studies have shown that teachers with stronger geographic content knowledge are more likely to employ inquiry-based and student-centered pedagogical approaches (Lane & Bourke, 2019). Conversely, teachers with limited geographic knowledge tend to rely heavily on textbook-based instruction and lecture methods (Preston, 2015).

The professional development of primary school teachers in geographic content has received increasing attention in the international literature. Gersmehl (2014) argued that effective geographic education requires teachers who can think spatially and model spatial reasoning for their students. This perspective aligns with the broader movement toward developing 21st-century skills in education, where spatial literacy is recognized as a core competency (Goodchild & Janelle, 2010).

Methodology

Research Design

This study employed a cross-sectional survey design to assess geographic literacy and spatial thinking practices among primary school teachers in Serbia. The quantitative approach was selected to enable statistical comparison across demographic variables and to generate generalizable findings.

Participants

The target population comprised primary school teachers (grades 1–4) currently employed in public schools in Serbia. Participants were recruited through stratified convenience sampling, with the stratification criteria being school location (urban, rural, and urban with rural branch offices) and geographic region (Belgrade, Vojvodina, Šumadija and Western Serbia, Southern and Eastern Serbia, and the Novi Pazar–Sjenica–Tutin–Prijepolje area). Within each stratum, teachers were reached through two channels: online distribution via school director networks and teacher professional associations, and paper-based distribution at professional development meetings in the Sandžak region and Belgrade. The inclusion criteria required respondents to be currently employed as primary school teachers with at least one year of teaching experience. A total of 218 responses were received. Of these, 12 were excluded: 8 due to substantial missing data (more than 20% of items left unanswered) and 4 due to failure to provide informed consent, resulting in a final analytical sample of 206 teachers. All participants provided written informed consent prior to completing the questionnaire.

Table 1. Demographic characteristics of the sample *(N = 206)*

Variable	Category	*N*	%
Gender	Male	17	8.3
	Female	189	91.7
Age	Up to 30	19	9.2
	31–40	52	25.2
	41–50	70	34.0
	Over 50	65	31.6
Education	Higher school / Vocational studies	13	6.3
	Faculty (basic academic studies)	84	40.8
	Master / Magister	106	51.5
	Doctor of Science	3	1.5
Teaching experience	Up to 5 years	21	10.2
	6–15 years	44	21.4
	16–25 years	59	28.6
	Over 25 years	82	39.8
School location	Urban	98	47.6
	Rural	55	26.7
	Urban with rural branch offices	53	25.7
Region	Belgrade	39	18.9
	Vojvodina	21	10.2
	Šumadija and Western Serbia	50	24.3
	Southern and Eastern Serbia	34	16.5
	Novi Pazar, Sjenica, Tutin, Prijepolje	62	30.1
Geography courses during studies	Yes	118	57.3
	No	60	29.1
	Do not remember	28	13.6

The sample is predominantly female (91.7%), which reflects the general gender composition of primary school teaching in Serbia. The largest proportion of respondents (39.8%) had over 25 years of teaching experience, while 10.2% were early-career teachers with up to 5 years of experience. The majority held a Master's degree (51.5%) or a basic academic degree (40.8%). Respondents were distributed across five geographic regions (Figure 1), with the largest group from the Novi Pazar, Sjenica, Tutin, and Prijepolje region (30.1%).

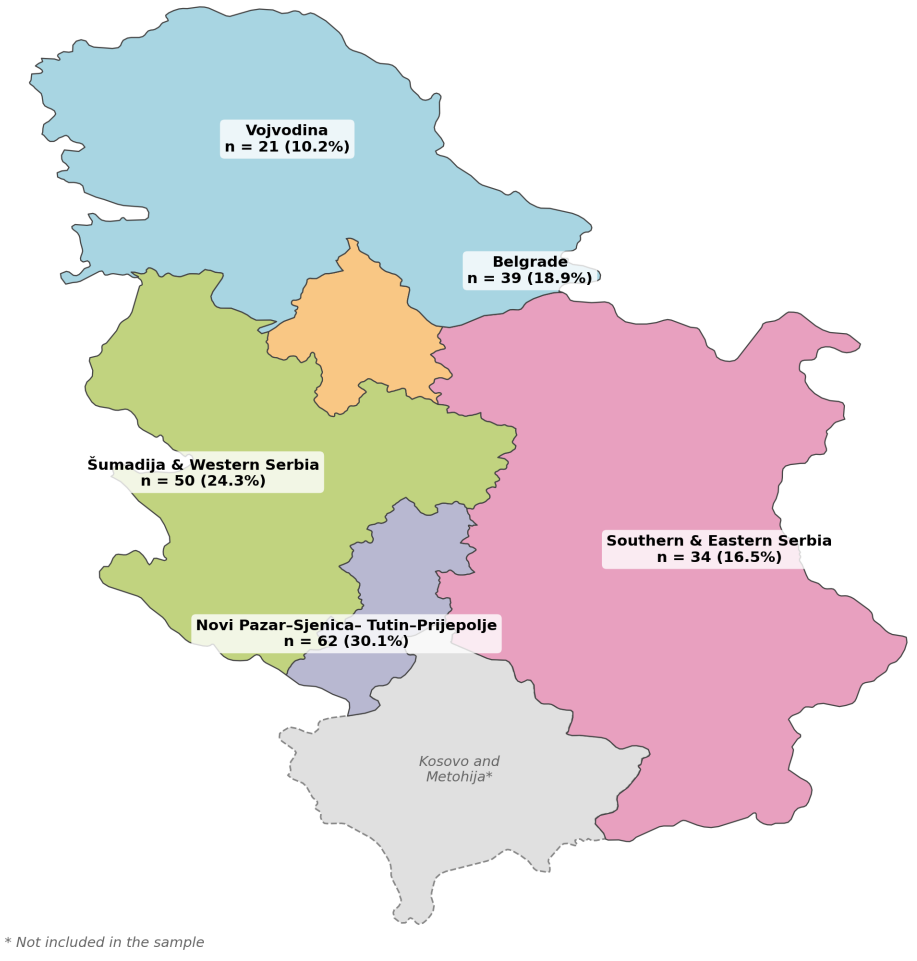

Figure 1. Geographic distribution of the sample across five regions of Serbia (N = 206)

Source: Authors' own elaboration based on Natural Earth data and survey results

Instrument

The research instrument consisted of three sections developed specifically for this study, based on the literature review and adapted to the Serbian educational context:

Section A: Self-Assessment of Geographic Competencies (8 items). This section measured teachers' perceived geographic knowledge and confidence in teaching Nature and Society content. Responses were recorded on a 5-point Likert scale (1 = strongly disagree to 5 = strongly agree). The items (listed in full in Table 2) addressed the following dimensions: perceived sufficiency of geographic knowledge for quality teaching, ability to use geographic maps effectively, confidence in explaining core concepts such as relief, climate, and hydrography, proficiency in spatial orientation and map reading, overall confidence in teaching geographic content, perceived adequacy of undergraduate geographic preparation, engagement in geography-related professional development, and perceived difficulty of geographic content relative to other curriculum areas. Items were developed drawing on the geographic literacy framework proposed by Heffron and Downs (2012) and adapted to reflect the competencies required by the Serbian Nature and Society curriculum (Ministarstvo prosvete, 2019). The scale demonstrated acceptable internal consistency (Cronbach's α = .645).

Section B: Spatial Thinking Practices (10 items). This section assessed how frequently teachers incorporate spatial thinking activities into their Nature and Society teaching. Responses were recorded on a 5-point Likert scale (1 = never to 5 = always). The items (listed in full in Table 3) captured a range of classroom practices: use of geographic maps and atlases, integration of digital geospatial tools such as Google Maps and Google Earth, organization of field activities related to geographic content, use of physical teaching aids including relief models and globes, student-led mapping exercises, development of spatial orientation skills, use of interactive digital tools, connecting geographic content to the students' local environment, comparative geographic analysis, and incorporation of geographic

observations during outdoor activities. The items were informed by research on spatial thinking in education (National Research Council, 2006; Gersmehl, 2014) and the TPACK framework (Mishra & Koehler, 2006), reflecting both traditional and technology-enhanced teaching approaches. The scale yielded a Cronbach's α of .416. This relatively low value likely reflects the conceptual breadth of the construct measured, as the items intentionally span diverse practices — from traditional map use to digital tool integration and outdoor fieldwork — rather than a single narrow behaviour. Similar challenges with internal consistency have been noted in scales measuring multidimensional teaching practices (Lane & Bourke, 2019).

Section C: Geographic Knowledge Test (8 items). This section comprised eight multiple-choice questions designed to assess factual geographic knowledge directly relevant to the Nature and Society curriculum in grades 3 and 4 (Ministarstvo prosvete, 2019). The questions (with correct response rates reported in Table 4) covered the following topics: dominant relief forms in Serbia, the outlet of the Danube River, climate classification of central Serbia, the function of a compass needle, map scale interpretation, the largest lake in the Balkans, the longest river in Serbia, and altitude classification of terrain. Each question offered four response options, with one correct answer. The items were selected to represent a range of geographic knowledge domains — physical geography, cartographic skills, and hydrography — and to vary in cognitive demand from factual recall to applied interpretation.

Prior to the main data collection, the instrument was piloted with a convenience sample of 15 primary school teachers who did not participate in the main study. The pilot aimed to evaluate item clarity, comprehensibility of instructions, and overall response burden. Based on teacher feedback, minor wording adjustments were made to several items in Section A to reduce ambiguity, and the ordering of response options in the knowledge test was reviewed to minimize potential response pattern effects. No items were added or removed following the pilot phase.

Data Collection

Data were collected during March 2026 through both online (Google Forms) and paper-based questionnaire distribution. Online questionnaires were distributed through school director networks and teacher professional associations. Paper questionnaires were administered at teacher professional development meetings in the Sandžak region and Belgrade.

Ethical Considerations

The study was conducted in accordance with the ethical guidelines of the University of Belgrade. As the research involved anonymous survey data from adult professionals and posed no risk beyond that of everyday experience, formal ethics committee approval was not required under the institutional regulations in effect at the time of data collection. All participants were informed of the purpose of the study, the voluntary nature of their participation, and their right to withdraw at any time without consequence. Informed consent was obtained from all respondents prior to their participation, either electronically (by confirming consent on the first page of the online questionnaire) or in writing (by signing the consent form attached to the paper questionnaire). No personally identifiable information was collected, and all data were stored and analysed in anonymized form.

Data Analysis

Statistical analyses were performed using IBM SPSS Statistics 26. Descriptive statistics (means, standard deviations, frequencies) were calculated for all variables. Independent samples t-tests were used to examine differences between urban and rural teachers, as well as between teachers with and without prior geographic education. One-way ANOVA with Bonferroni post-hoc correction was employed to examine differences across teaching experience groups and geographic regions. Pearson correlation coefficients were calculated to examine relationships between self-assessed competencies, spatial thinking practices, and knowledge test scores. The significance level was set at $p < .05$ for all analyses.

Results

Self-Assessment of Geographic Competencies

Table 2 presents descriptive statistics for the self-assessed geographic competencies scale. The overall scale mean was 3.66 ($SD = 0.54$), indicating a moderate level of self-assessed geographic competency among the respondents.

The highest-rated item was the ability to explain geographic concepts ($M = 3.96$), followed by confidence in using geographic maps ($M = 3.92$).

The lowest-rated item was the perception that geographic content is the most challenging part of PiD teaching ($M = 2.63$), suggesting that most teachers do not consider geography the most difficult component of the curriculum. Notably, teachers rated their undergraduate geographic preparation relatively low ($M = 3.54$), indicating a perceived gap in initial teacher education.

Table 2. Descriptive statistics for self-assessed geographic competencies *(N = 206)*

Item	*M*	*SD*
P3.1 I have sufficient geographic knowledge for quality PiD teaching	3.81	1.03
P3.2 I can effectively use geographic maps in PiD teaching	3.92	1.02
P3.3 I easily explain concepts such as relief, climate, and water bodies	3.96	0.97
P3.4 I am proficient in spatial orientation and map reading	3.83	1.04
P3.5 I feel confident teaching geographic content in PiD	3.85	1.02
P3.6 My undergraduate studies provided sufficient geographic knowledge	3.54	1.10
P3.7 I regularly update my geographic knowledge through professional development	3.71	0.92
P3.8 Geographic content is the most challenging part of PiD teaching	2.63	0.97
Overall scale mean	**3.66**	**0.54**

Note: Scale: 1 = strongly disagree, 5 = strongly agree. Cronbach's α = .645.

Table 3. Descriptive statistics for spatial thinking practices ***(N = 206)***

Item	*M*	*SD*
P4.1 I use geographic maps and atlases in PiD teaching	3.93	0.89
P4.2 I use Google Maps/Google Earth in teaching	2.88	0.97
P4.3 I organize field activities for geographic content	2.67	1.00
P4.4 I use relief models, globes, and similar teaching materials	2.93	1.04
P4.5 Students create maps/plans of their environment in my classes	3.12	0.99
P4.6 I develop students' spatial orientation skills	3.17	1.03
P4.7 I use interactive digital tools for geographic teaching	2.88	0.92
P4.8 I connect geographic content to students' local environment	3.79	0.93
P4.9 I use comparative geographic analysis in teaching	3.10	0.97
P4.10 I incorporate geographic observations in outdoor activities	2.85	0.94
Overall scale mean	**3.13**	**0.39**

Note: Scale: 1 = never, 5 = always. Cronbach's α = .416.

Spatial Thinking Practices

Table 3 presents the descriptive statistics for spatial thinking practices. The overall scale mean was 3.13 (*SD* = 0.39), indicating moderate frequency of spatial thinking practices in teaching.

The most frequently employed practice was the use of geographic maps and atlases (*M* = 3.93), followed by connecting geographic content to students' local environment (*M* = 3.79). The least frequently employed practices were organizing field activities (*M* = 2.67) and incorporating geographic observations in outdoor activities (*M* = 2.85). The use of Google Maps/Google Earth (*M* = 2.88) and interactive digital tools (*M* = 2.88) was relatively low. Only 25.0% of respondents reported regular use (often or always) of Google Maps/Google Earth in their teaching.

Geographic Knowledge Test Results

Table 4 presents the correct response rates for the geographic knowledge test. The overall mean score was 5.49 out of 8 (68.6% correct).

The compass question had the highest correct response rate (99.0%), followed by the Danube River outlet question (94.5%). The most challenging item was altitude classification (17.0% correct), followed by map scale interpretation (56.5%) and the longest river in Serbia (57.0%). These results indicate specific geographic knowledge gaps among primary school teachers, particularly in quantitative and classification-based geographic concepts.

Differences by School Location

Table 5 presents the results of independent samples t-tests comparing urban and rural school teachers.

Differences by Teaching Experience

Table 6 presents the results of one-way ANOVA comparing teachers across four teaching experience groups.

No statistically significant differences were found between urban and rural school teachers on any of the three measured variables. While urban teachers showed slightly higher self-assessed competencies and knowledge test scores, and rural teachers showed slightly higher spatial thinking practice scores, none of these differences reached statistical significance.

Table 4. Correct response rates on the geographic knowledge test ***(N = 206)***

Question	Topic	Correct (%)
P5.1	Dominant relief forms in Serbia	71.5
P5.2	Danube River outlet (Black Sea)	94.5
P5.3	Climate type of central Serbia	83.0
P5.4	Compass needle direction	99.0
P5.5	Map scale interpretation	56.5
P5.6	Largest lake in the Balkans	70.5
P5.7	Longest river in Serbia	57.0
P5.8	Altitude classification	17.0
Overall mean correct		**68.6**

Table 5. Differences in geographic competencies by school location (t-test)

Variable	Urban *M* (*SD*)	Rural *M* (*SD*)	*t*	*p*
Geographic competencies	3.71 (0.51)	3.60 (0.57)	1.201	.232
Spatial thinking practices	3.12 (0.42)	3.18 (0.36)	−0.933	.352
Knowledge test score	5.68 (1.16)	5.39 (1.11)	1.519	.131

Note: Urban N = 98, Rural N = 55. No significant differences were found at p < .05.

Table 6. Differences in geographic competencies by teaching experience (ANOVA)

Variable	≤5 yrs *M* (*SD*)	6–15 yrs *M* (*SD*)	16–25 yrs *M* (*SD*)	>25 yrs *M* (*SD*)	*F*	*p*
Geographic competencies	3.68 (0.38)	3.49 (0.66)	3.72 (0.50)	3.69 (0.52)	1.708	.167
Spatial thinking practices	3.25 (0.34)	3.25 (0.44)	3.18 (0.37)	3.01 (0.35)	5.296	.002**
Knowledge test score	5.45 (1.10)	5.49 (1.32)	5.46 (1.27)	5.53 (1.17)	0.043	.988

*Note: N (≤5 yrs) = 21, N (6–15 yrs) = 44, N (16–25 yrs) = 59, N (>25 yrs) = 82. *p < .05, **p < .01, ***p < .001.*

A statistically significant difference was found in spatial thinking practices across teaching experience groups (F = 5.296, p = .002). As illustrated in Figure 2, teachers with over 25 years of experience reported the lowest mean spatial thinking scores. Bonferroni post-hoc tests confirmed that this group differed significantly from all three other groups: compared to teachers with up to 5 years (p = .031), 6–15 years (p = .007), and 16–25 years of experience (p = .044). No significant differences were found for self-assessed geographic competencies or knowledge test scores across experience groups.

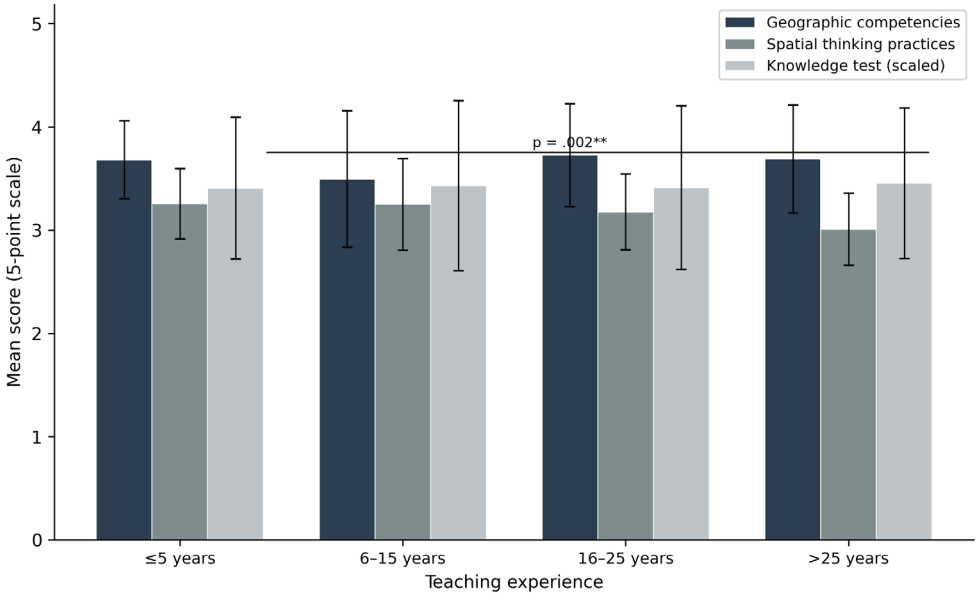

Figure 2. Mean scores on geographic competencies, spatial thinking practices, and knowledge test (scaled to 5-point) by teaching experience group. Error bars represent standard deviations. **p < .01

Source: Authors' research, based on survey data (N = 206)

Differences by Geographic Education Background

Table 7 presents the results of independent samples t-tests comparing teachers who reported having had geography courses during their university studies versus those who did not.

Teachers who had geography courses during their university studies showed significantly higher scores on all three variables: self-assessed geographic competencies (t = 3.093, p = .002), spatial thinking practices (t = 3.468, p < .001), and geographic knowledge test scores (t = 2.027, p = .044).

Differences by Region

One-way ANOVA revealed no statistically significant differences across the five geographic regions for any of the three measured variables: geographic competencies (F = 0.620, p = .649), spatial thinking practices (F = 0.462, p = .764), and knowledge test scores (F = 1.184, p = .319).

Correlation Analysis

Pearson correlation analysis revealed a moderate positive correlation between self-assessed geographic competencies and spatial thinking practices (r = .315, p < .001; Figure 3), indicating that higher self-assessed competency tends to co-occur with more frequent use of spatial thinking practices in teaching. However, as this is a cross-sectional correlation, the direction of this relationship cannot be established — it is equally pos-

Table 7. Differences by geographic education during university studies (t-test)

Variable	Yes *M* (*SD*)	No *M* (*SD*)	*t*	*p*
Geographic competencies	3.77 (0.52)	3.52 (0.52)	3.093	.002**
Spatial thinking practices	3.22 (0.39)	3.01 (0.33)	3.468	<.001***
Knowledge test score	5.63 (1.21)	5.24 (1.11)	2.027	.044*

*Note: Yes N = 118, No N = 60. *p < .05, **p < .01, ***p < .001. Teachers who selected "Do not remember" (N = 28) were excluded from this analysis.*

sible that teachers who engage more in spatial thinking activities develop greater confidence, or that a third variable, such as interest in geography, influences both. A weak but significant positive correlation was observed between spatial thinking practices and knowledge test scores (r = .164, p = .020). The correlation between self-assessed competencies and knowledge test scores was not statistically significant (r = .127, p = .073), suggesting a possible disconnect between teachers' perceived and demonstrated geographic knowledge, though the limited scope of the knowledge test (8 items) warrants caution in interpreting this finding.

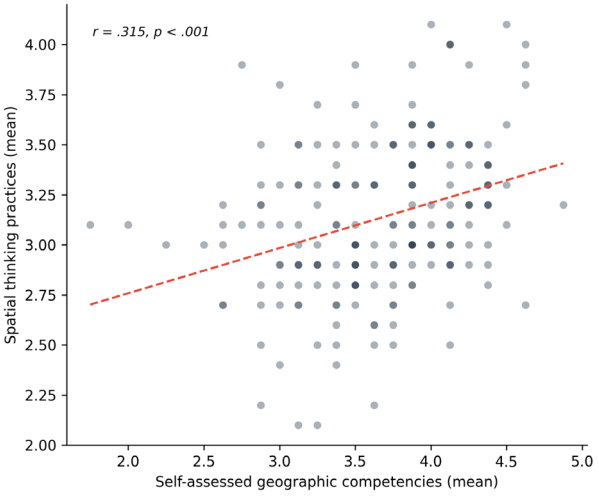

Figure 3. Scatterplot of the relationship between self-assessed geographic competencies and spatial thinking practices (N = 206). The dashed line represents the linear trend.

Source: Authors' research, based on survey data (N = 206)

Discussion

The findings of this study provide empirical insight into the geographic literacy and spatial thinking capabilities of primary school teachers in Serbia. The results reveal several important patterns that carry implications for teacher education and curriculum development.

Geographic Competency Levels

The moderate levels of self-assessed geographic competency (M = 3.66) are consistent with findings from comparable contexts. Preston (2015) reported similar patterns among primary school teachers in Australia, and Catling and Morley (2013) found that primary teachers in England often have limited and uneven geographic subject knowledge, noting that generalist educators frequently feel underprepared for geographic content delivery. In Serbia, this is particularly relevant because primary school teachers receive only limited geography-specific coursework during their undergraduate training at faculties of education — a concern reflected in the relatively low rating for undergraduate preparation (M = 3.54), which was the lowest-rated item on the competency scale apart from perceived difficulty.

What is perhaps more telling than the overall competency scores is the non-significant correlation between self-assessed competencies and actual knowledge test performance (r = .127, p = .073). This gap between perceived and demonstrated knowledge echoes the broader literature on calibration accuracy in professional self-assessment (Kruger & Dunning, 1999) and raises a practical concern: if teachers overestimate their geographic competency, they may be less likely to seek out additional training in areas where they would benefit from it. This suggests that professional development initiatives in this domain should incorporate objective diagnostic components rather than relying solely on teachers' self-identified needs.

Spatial Thinking Practices and the Experience Paradox

A particularly noteworthy finding is the significant decline in spatial thinking practices among teachers with over 25 years of experience (F = 5.296, p = .002). This "experience paradox" — where more experienced teachers employ fewer innovative pedagogical approaches — may be explained by several factors. First, veteran teachers may have been trained in an era when spatial thinking was not explicitly emphasized in teacher education curricula. Second, the rapid evolution of geospatial technologies may create a digital divide, with older teachers less comfortable incorporating these tools into their practice. Third, routinization of teaching practices over decades may reduce willingness to adopt new approaches (Day & Gu, 2010).

This finding carries implications for professional development planning. Rather than assuming that experienced teachers need less support, it may be worthwhile to consider targeted interventions aimed at helping veteran educators update their spatial thinking pedagogies and become familiar with contemporary geospatial tools. That said, these results should be interpreted in light of the modest internal consistency of the spatial thinking practices scale (α = .416). While the significant group differences are statistically robust, the heterogeneity of the scale means that the observed pattern may not apply equally to all types of spatial thinking practices captured by the instrument.

Low Adoption of Geospatial Technologies

The finding that only 25.0% of teachers regularly use Google Maps/Google Earth is concerning but consistent with international trends. Despite the demonstrated educational potential of tools such as Google Earth (Patterson, 2007), Kerski (2015) noted that their integration into primary education remains limited globally. In Serbia, potential barriers include limited ICT in-

frastructure, insufficient training during initial teacher education, and lack of curriculum-aligned resources for these technologies. The low use of field activities (M = 2.67) and outdoor observations (M = 2.85) further suggests a heavy reliance on classroom-based, textbook-oriented approaches.

Geographic Knowledge Gaps

The geographic knowledge test results (overall mean: 68.6% correct) point to uneven performance across different types of geographic knowledge. While teachers performed well on items involving commonly encountered facts — such as the outlet of the Danube River (94.5%) and compass function (99.0%) — performance was notably lower on items requiring more specialized or quantitative knowledge, particularly altitude classification (17.0%) and map scale interpretation (56.5%). The low score on altitude classification should be interpreted with caution, as it represents a single item and may partly reflect ambiguity in the question wording or unfamiliarity with the specific classification system used. Nonetheless, taken together with the relatively low performance on map scale interpretation, these results suggest that quantitative and classification-based geographic concepts may represent an area where teachers would benefit from additional support.

These patterns are broadly consistent with the findings of Lešćešen et al. (2024), who identified gaps in climate change knowledge among primary school students in Serbia. While our test comprised only eight items and cannot provide a comprehensive assessment of teachers' geographic knowledge, the results offer an initial indication that certain curriculum-relevant topics may deserve greater attention in teacher preparation and professional development.

The Role of Geographic Education During University Studies

The significant differences found between teachers who had geography courses during university studies and those who did not — across all three measured variables — provide strong empirical support for the value of geographic content in teacher preparation programs. Teachers with geographic education background demonstrated higher self-assessed competencies (p = .002), more frequent spatial thinking practices (p < .001), and better geographic knowledge (p = .044). This finding underscores the importance of maintaining and strengthening geographic coursework within faculty of education curricula, even as programs face pressure to accommodate new content areas.

Absence of Urban-Rural and Regional Differences

Contrary to expectations, no statistically significant differences were found between urban and rural teachers or across the five sampled regions on any of the three measured variables. While this absence of regional variation might suggest that the challenges identified in this study are not confined to a particular area, this interpretation should be treated with caution. The sample was not proportionally representative of the national teacher population, and the overrepresentation of respondents from the Novi Pazar–Sjenica–Tutin–Prijepolje area (30.1%) limits the extent to which regional comparisons can be generalized. Future research with more balanced regional sampling would be needed to determine whether geographic literacy challenges are indeed uniform across Serbia or whether meaningful regional differences exist that the present sample was unable to detect.

Implications for Teacher Education

The findings carry several practical implications. First, faculties of education should strengthen geographic content in teacher preparation, emphasizing quantitative concepts (scale, altitude) where gaps were most pronounced. Second, professional development should incorporate geospatial technology training. Third, special attention should be given to veteran teachers, who demonstrated significantly lower engagement with spatial thinking practices. Fourth, curriculum-aligned resources connecting geospatial technologies to Nature and Society learning outcomes could support broader adoption.

Limitations

This study has several limitations that should be considered when interpreting the findings. First, the use of convenience sampling limits the generalizability of the results to the broader population of Serbian primary school teachers. The overrepresentation of the Sandžak region (30.1%) reflects the researcher's professional networks in this area and may introduce regional bias, despite the absence of statistically significant regional differences in the data.

Second, the self-report nature of the geographic competency and spatial thinking practice scales introduces the possibility of social desirability bias, whereby teachers may overstate their competencies or the frequency of their spatial thinking practices. The non-significant correlation between self-assessed competencies and knowledge test scores (r = .127) lends some support to this concern.

Third, the modest internal consistency of the spatial thinking practices scale (α = .416) represents a methodological limitation. While we have argued that this reflects the intentional breadth of the construct, it also means that findings based on this scale — including the significant differences across experience groups — should be interpreted with appropriate caution. Future research should consider developing subscales for distinct categories of spatial thinking practices (e.g., traditional map-based activities vs. digital tool use) to improve reliability while preserving construct coverage.

Fourth, the geographic knowledge test comprised only eight items and assessed a limited range of curriculum-relevant topics. It should therefore be regarded as a screening measure rather than a comprehensive assessment of teachers' geographic knowledge. The very low performance on the altitude classification item (17.0%) may reflect item-specific factors as much as genuine knowledge gaps.

Finally, the cross-sectional design precludes causal inferences about the relationships between variables. Future studies should employ larger and more representative samples, consider longitudinal or quasi-experimental designs, incorporate classroom observation alongside self-report measures, and examine the relationship between teacher geographic literacy and student learning outcomes.

Conclusion

This study examined geographic literacy and spatial-thinking practices among 206 primary school teachers across five regions of Serbia. The results indicate moderate levels of self-assessed geographic competency, limited use of geospatial technologies, and uneven performance on a curriculum-aligned knowledge test. Among the key findings, teachers with over 25 years of experience reported significantly lower spatial thinking practices than their less experienced colleagues, and teachers who had completed geography courses during their university studies scored higher across all three measured dimensions. These patterns, while subject to the limitations of the instruments and sampling approach discussed above, point to areas that may warrant attention in teacher education and professional development — particularly the integration of quantitative geographic concepts and geospatial tools into both pre-service and in-service training. Future research with larger and more representative samples, refined measurement instruments, and classroom observation methods would help to establish a more robust evidence base for policy recommendations in this domain.

References

Baker, T. R., Battersby, S., Bednarz, S. W., Bodzin, A. M., Kolvoord, B., Moore, S., & Uttal, D. (2015). A research agenda for geospatial technologies and learning. *Journal of Geography, 114*(3), 118–130. https://doi.org/10.1080/00221341.2014.950684

Catling, S. (2004). An understanding of geography: The perspectives of English primary trainee teachers. *GeoJournal, 60*(2), 149–158. https://doi.org/10.1023/B:GEJO.0000033577.09481.87

Catling, S., & Morley, E. (2013). Enquiring into primary teachers' geographical knowledge. *Education 3–13, 41*(4), 434–442. https://doi.org/10.1080/03004279.2013.819625

Day, C., & Gu, Q. (2010). *The new lives of teachers*. Routledge.

Edelson, D. C. (2012). *Geo-literacy: Preparation for far-reaching decisions*. National GeographicEducation.https://education.nationalgeographic.org/resource/geo-literacy-preparation-far-reaching-decisions/

Gersmehl, P. (2014). *Teaching geography* (3rd ed.). Guilford Press.

Goodchild, M. F., & Janelle, D. G. (2010). Toward critical spatial thinking in the social sciences and humanities. *GeoJournal, 75*(1), 3–13. https://doi.org/10.1007/s10708-010-9340-z

Heffron, S., & Downs, R. M. (Eds.). (2012). *Geography for life: National geography standards* (2nd ed.). National Council for Geographic Education.

Hill, H. C., Rowan, B., & Ball, D. L. (2005). Effects of teachers' mathematical knowledge for teaching on student achievement. *American Educational Research Journal, 42*(2), 371–406. https://doi.org/10.3102/00028312042002371

Ivkov-Džigurski, A., Ivanović Bibić, L., Dragin, A., Miljanović, D., & Đukičin Vučković, S. (2019). The evaluation of the geography textbook quality from the students' perspective. *Geographica Pannonica, 23*(2), 121–133. https://doi.org/10.5937/gp23-22084

Jo, I., & Bednarz, S. W. (2009). Evaluating geography textbook questions from a spatial perspective: Using concepts of space, tools of representation, and cognitive processes to evaluate spatiality. *Journal of Geography, 108*(1), 4–13. https://doi.org/10.1080/00221340902758401

Kerski, J. J. (2015). Geo-awareness, geo-enablement, geotechnologies, citizen science, and storytelling: Geography on the world stage. *Geography Compass, 9*(1), 14–26. https://doi.org/10.1111/gec3.12193

Kruger, J., & Dunning, D. (1999). Unskilled and unaware of it: How difficulties in recognizing one's own incompetence lead to inflated self-assessments. *Journal of Personality and Social Psychology, 77*(6), 1121–1134. https://doi.org/10.1037/0022-3514.77.6.1121

Lane, R., & Bourke, T. (2019). Assessment in geography education: A systematic review. *International Research in Geographical and Environmental Education, 28*(1), 22–36. https://doi.org/10.1080/10382046.2017.1385340

Lešćešen, I., Basarin, B., & Vujičić, M. (2024). What do they know? Is climate change education

necessary in primary schools in Serbia? *Geographica Pannonica, 28*(2), 85–103. https://doi.org/10.5937/gp28-48045

Lukić, T., Božić, S., Sakulski, D., Babić-Kekez, S., Ivanović Bibić, L., Besermenji, S., & Dolinaj, D. (2016). Achieving competencies with grammar school students through utilisation of selected didactical principles in traditional and active teaching: Geography class case study: "Hydrography of Serbia." *Geographica Pannonica, 20*(4), 254–264. https://doi.org/10.18421/GP20.04-07

Milson, A. J., Demirci, A., & Kerski, J. J. (Eds.). (2012). *International perspectives on teaching and learning with GIS in secondary schools*. Springer. https://doi.org/10.1007/978-94-007-2120-3

Ministarstvo prosvete, nauke i tehnološkog razvoja [Ministry of Education, Science and Technological Development]. (2019). *Pravilnik o planu nastave i učenja za prvi ciklus osnovnog obrazovanja i vaspitanja i programu nastave i učenja za treći razred osnovnog obrazovanja i vaspitanja* [*Regulation on the curriculum for the first cycle of primary education and the teaching programme for the third grade of primary education*]. *Službeni glasnik Republike Srbije*.

Mishra, P., & Koehler, M. J. (2006). Technological pedagogical content knowledge: A framework for teacher knowledge. *Teachers College Record, 108*(6), 1017–1054. https://doi.org/10.1111/j.1467-9620.2006.00684.x

National Research Council. (2006). *Learning to think spatially: GIS as a support system in the K–12 curriculum*. National Academies Press. https://doi.org/10.17226/11019

Newcombe, N. S. (2010). Picture this: Increasing math and science learning by improving spatial thinking. *American Educator, 34*(2), 29–43.

Patterson, T. C. (2007). Google Earth as a (not just) geography education tool. *Journal of Geography, 106*(4), 145–152. https://doi.org/10.1080/00221340701678032

Preston, L. (2015). The place of place-based education in the Australian primary geography curriculum. *Geographical Education, 28*, 41–49.

Shulman, L. S. (1986). Those who understand: Knowledge growth in teaching. *Educational Researcher, 15*(2), 4–14. https://doi.org/10.3102/0013189X015002004

Stojšić, I., Ivkov-Džigurski, A., & Maričić, O. (2019). The readiness of geography teachers to use mobile devices in the context of immersive technologies integration into the teaching process. *Geographica Pannonica, 23*(2), 121–133. https://doi.org/10.5937/gp23-20762

Šaćirović, D., & Bratić, M. (2021). Motivational factors and satisfaction of foreign tourists visiting Belgrade as tourist destination according to their social and demographic characteristics. *Fresenius Environmental Bulletin, 30*(4A), 4085–4093.

Uttal, D. H., Meadow, N. G., Tipton, E., Hand, L. L., Alden, A. R., Warren, C., & Newcombe, N. S. (2013). The malleability of spatial skills: A meta-analysis of training studies. *Psychological Bulletin, 139*(2), 352–402. https://doi.org/10.1037/a0028446

INTERNATIONAL SCIENTIFIC JOURNAL | GEOGRAPHICA PANNONICA | Volume 30, Issue 2, 101–122 (June 2026)
Journal homepage: http://www.dgt.uns.ac.rs/en/homepage/pannonica/

Tracing Integrative Pathways: A Bibliometric Analysis of Ecosystem Services in Landscape Planning

Utkarsha Pramod Dhurve[A*], Sameer Deshkar[A]
[A]*Department of Architecture and Planning, Visvesvaraya National Institute of Technology, South Ambazari Road, Nagpur 440010, India; ORCID UPD: 0009-0001-2765-0930; SD: 0000-0002-1153-4134*

Received: December 1, 2025| Revised: April 28, 2026| Accepted: June 5, 2026
doi: 10.5937/gp30-63135

ABSTRACT

The integration of ecosystem services into landscape planning has emerged as a central paradigm for reconciling ecological integrity with socio-economic development, yet the co-evolutionary pathways through which these domains have become increasingly interdisciplinary remain poorly understood. This study employs a comprehensive bibliometric and science-mapping approach to analyze 1,930 peer-reviewed articles published between 2006 and 2025 from the Web of Science Core Collection, following a PRISMA-guided screening and selection process, utilizing timeline-based co-citation analysis, keyword co-occurrence mapping, temporal overlay analysis, and a novel Keyword–Discipline Tagging Protocol to trace the evolution of ecosystem services and landscape planning research. The study further quantifies interdisciplinary integration through a Cohesion Index (CI = 0.944) and identifies a statistically significant changepoint around 2018 marking accelerated conceptual convergence. Findings reveal three distinct phases of evolution: an early phase (2006–2015) characterized by siloed ecological and valuation-focused research; a transition phase (2016–2019) marked by the incorporation of planning and governance perspectives in response to global policy milestones such as the EU Green Infrastructure Strategy and the Sustainable Development Goals; and a post-2020 phase demonstrating hybrid convergence where boundary-spanning concepts including nature-based solutions, urban resilience, and citizen science bind ecology, planning, climate science, and governance into a shared intellectual framework. Cluster analysis identifies land use, ecology, and management as the central interdisciplinary hub with highest connectivity, while policy, equity, and public engagement emerge as the least integrated cluster, representing a critical gap despite strong overall cohesion. Persistent barriers including terminological ambiguities, data interoperability challenges, and institutional constraints continue to limit full integration, particularly regarding social and environmental justice dimensions. The study concludes that ecosystem services and landscape planning research has undergone fundamental transformation from a collection of loosely connected disciplinary inquiries to a coherent, policy-responsive, transdisciplinary knowledge system, yet the incorporation of equity and participatory dimensions remains an unfinished project requiring deliberate terminological harmonization, enhanced data infrastructures, and institutional mechanisms supporting transdisciplinary collaboration. These findings offer a replicable framework for integration science applicable to other complex socio-ecological systems.

Keywords: Ecosystem services; landscape planning; bibliometric analysis; interdisciplinary integration; nature-based solutions; policy alignment

*Corresponding author: Utkarsha Pramod Dhurve; email: updhurve@arc.vnit.ac.in; Tel.: +91-82-7503-6480

Introduction

Landscapes are dynamic systems where soil, water, vegetation, and wildlife interact, and planning determines whether these interactions are sustained or disrupted. Thus, landscape planning (LP) is fundamentally tied to ecological processes, making it essential to study how land use decisions affect biodiversity, ecosystem services (ES), and environmental resilience. Moreover, a systematic study helps identify ecological thresholds, highlight risks of degradation, and propose strategies for conservation and restoration. Without such understanding, planning risks undermining ecological integrity and long-term sustainability (Opdam, 2018; Albert et al., 2014). In addition to above landscapes are also socio-economic spaces where agriculture, forestry, urban development, and tourism coexist. Hence, studying evolution of LP can provide meaningful insights into how these activities can be harmonized to reduce conflicts and maximize synergies. It highlights trade-offs between competing land uses and helps design multifunctional landscapes that support livelihoods, employment, and food security while maintaining ecological balance (Balzan et al., 2018). The evolution of LP over the years reflects humanity's shifting relationship with the land (Etzkowitz & Leydesdorff, 2000). It has moved from a focus on aesthetics and utility to a complex, interdisciplinary field concerned with ecological resilience, social equity, and long-term sustainability (Turnhout et al., 2020; Hansen & Pauleit, 2014). This evolution can be understood through the studies that have been carried out in this context.

During the last few decades, the LP process has experienced incorporation of different approaches into it but that did not occur as a simple linear succession of methods but rather as a cumulative, often contested, layering of diverse intellectual traditions, professional practices, and societal imperatives that gradually expanded the scope, methods, and ambitions of the field. The introduction of each new approach emerged in response to perceived limitations of its predecessors, and today they coexist, interact, and are selectively applied depending on the scale, context, and objectives of a given planning effort (Kabisch, 2016; Artmann et al., 2017). Hence, understanding how these approaches entered the process reveals LP as a fundamentally hybrid discipline—one that continuously absorbs insights from ecology, design, engineering, sociology, economics, and critical theory while striving to reconcile them in practice.

The earliest foundational approach to enter LP was the aesthetic and design-based approach (Shackleton, 2022). However, a markedly different approach entered with the rise of scientific and survey-based methods in the early to mid-twentieth century, driven by the progressive era's faith in expertise and data-driven decision-making. This followed by the ecological suitability approach, which represented a transformative synthesis and methodological leap that brought ecology directly into the procedural core of LP. This approach entered the process as a direct challenge to development-driven planning that ignored environmental consequences, and it became codified in environmental legislation and review processes. The ecological suitability approach firmly established that landscape planning must be a science-based, rational, and precautionary process (Pauna et al., 2018; Cortinovis & Geneletti, 2019). The landscape ecology approach entered the process in the 1980s and 1990s as ecological theory itself evolved beyond site-specific analysis toward understanding spatial patterns, flows, and processes across entire landscapes.

The literature shows that the focus of integration of ES in LP emerged as a pathway for advancing sustainable development, especially as planners attempt to reconcile ecological integrity with socio-economic demands. In the earlier years of this century, ES became a formalized concept under the Millennium Ecosystem Assessment (Millennium Ecosystem Assessment, 2005), and received institutional support in projects like The Economics of Ecosystems and Biodiversity (TEEB, 2010) as well as the Intergovernmental Science-Policy Platform on Biodiversity and ES (IPBES, 2019). These conceptual models categorize ES into provisioning, regulatory, cultural, and supporting services and present a structured framework for the integration of ecological knowledge into land-use decision making across disciplines (Andersson et al., 2015).

However, despite robust theoretical grounding, the translation into LP practice remains limited (Díaz et al., 2015). It has been reported that around 60% of the global ES are still being eroded on account of unsustainable land-use practices and governance failures as the studies show methodological divisions: ecological studies favour biophysical measures (de Groot et al., 2010), economists take valuation approaches (Costanza et al., 1997) and planners work within regulatory or design spatial limits. Empirically, only 20% of LP projects quantitatively assess ES trade-offs (Albert et al., 2021), and fewer than 15% conduct participatory ES assessments (Baker-Médard et al., 2024), suggesting scarce application in planning practice. These limitations make it necessary to consider whether emerging transdisciplinary approaches can help bridge these divides. Participatory ES mapping and co-production methods have demonstrated advances in planning accuracy and context relevance when local knowledge is incorporated (Karrasch et al., 2014; García-Díez et al., 2020). Yet systemic constraints—such as discipline-specific funding sources, asynchronous research – policy cycles and uneven governance capacities—continue to restrict wider adoption (Brink & Wamsler, 2018; Shackleton, 2022).

In order to assess the evolutionary patterns in the context of ES and LP, previous research efforts made by Danese & Gioia (2021), and Seddon et al. (2020) who employed bibliometric approach to assess the interaction or integration of various approaches (that include but are not limited to ES, green infrastructure, landscape change, and nature-based solutions) in the LP process. However, most of the studies are topical-oriented, temporally dependent or discipline-dependent. Although these studies present trends in publication within their respective domains, they fail to show the co-evolution of the ecological and planning/governance over time. This co-evolution of ES and LP can be understood with the help of subject specific vocabulary as it appears in the various publications. In the backdrop of above information, it was imperative to review existing body of literature vis-à-vis LP and ES association or integration.

Materials and Methods

Data Collection and Search Strategy

A bibliometric analysis was performed using the Web of Science Core Collection (SCIE, SSCI, ESCI). On 29 July 2025, English peer-reviewed articles and reviews from 2006–2025 were retrieved using the Boolean query: *TS = (("Ecosystem services" OR "Integration of ecosystem services" OR "Ecosystem-based planning" OR "Urban ecosystem services" OR "Nature-based solutions") AND ("Landscape planning" OR "Landscape sustainability" OR "Rural landscape planning" OR "Green infrastructure" OR "Sustainable land-use planning"))*. After duplicate removal in R (bibliometrix v4.2), 1,930 unique records remained. A PRISMA workflow (Figure 1) ensured transparency.

Co-Citation Analysis

Using VOSviewer (v1.6.20), a timeline-based co-citation network traced the intellectual structure's evolution. A separate co-citation analysis identified foundational literature and thematic clusters.

International Collaboration Analysis

A country-level co-authorship network in VOSviewer mapped geographic productivity and collaboration patterns.

Keyword Co-Occurrence Analysis

Author keywords and Keywords Plus were cleaned and analyzed via VOSviewer to generate co-occurrence networks. Temporal overlay analysis color-coded keywords by average publication year to capture thematic evolution.

Temporal Overlay Analysis

Temporal overlay analysis was conducted as an extension of keyword co-occurrence mapping to capture the chronological evolution of research themes. Using the same keyword co-occurrence network, a temporal overlay was applied by color-coding each keyword node according to the average publication year of the articles in which it appeared.

Interdisciplinary Convergence

A multi-method approach combined: (1) a Keyword–Discipline Tagging Protocol to map keywords to fields; (2) a Cohesion Index measuring cross-cluster vs. with-

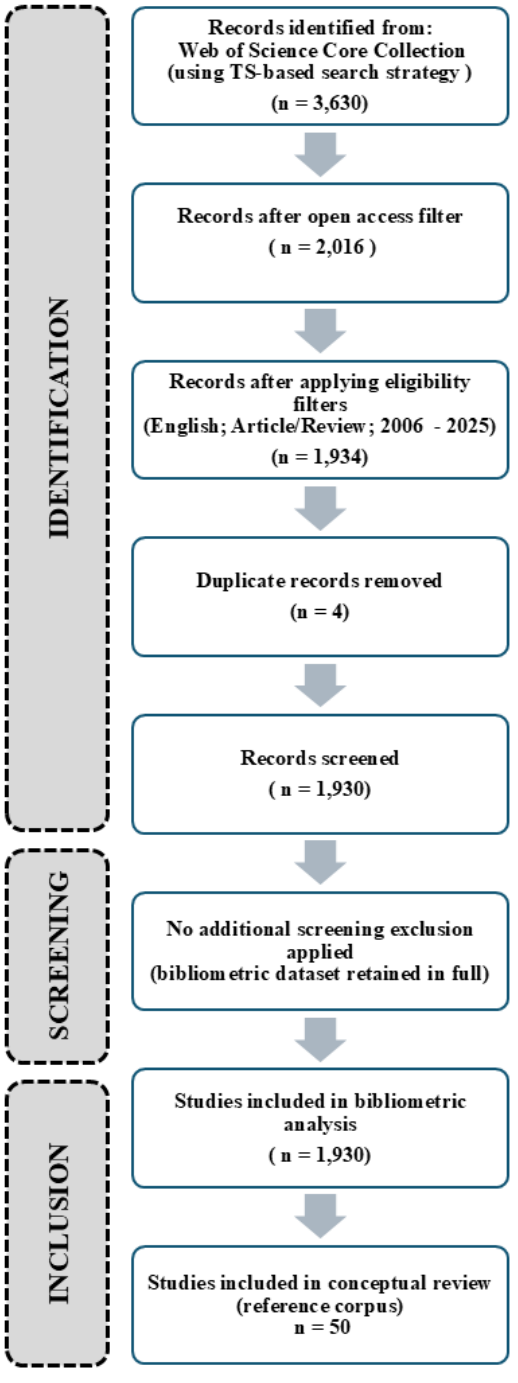

Figure 1. PRISMA flow diagram illustrating the literature search and dataset selection process.

in-cluster connectivity; (3) temporal convergence analysis using annual networks (2006–2025) with metrics including Shannon entropy; and (4) a policy-keyword alignment methodology assessing keyword usage relative to three policy milestones (EU Green Infrastructure Strategy 2013, UN SDGs 2015, IPBES, 2019), including surge magnitude and lag time calculations.

Keyword–Discipline Tagging Protocol

The Keyword–Discipline Tagging Protocol was developed to systematically map high-frequency keywords to disciplinary fields, thereby revealing the cross-domain character of the research vocabulary.

Cohesion Index

The Cohesion Index was employed as a quantitative measure of interdisciplinary integration within the field. This index compares the strength of cross-cluster keyword connections with within-cluster density, providing a single metric that captures the degree to which thematic clusters are integrated into a cohesive intellectual structure.

Temporal Convergence Analysis

Temporal convergence analysis was conducted to quantify the rate and timing of interdisciplinary integration over the study period. This analysis utilized annual keyword networks constructed for each year from 2006 to 2025. For each annual network, measures of interdisciplinary connectivity were calculated, including the proportion of cross-cluster keyword pairs, the Shannon entropy of disciplinary distribution, and the edge-share ratio representing connections between keywords from traditionally distinct domains.

Policy-Keyword Alignment Methodology

The policy-keyword alignment methodology was developed to assess the relationship between global environmental policy milestones and the adoption of policy-relevant terminology in scholarly literature. This method involved three components. First, three major international policy landmarks were selected based on their recognized influence on environmental governance and sustainability science: the European Union Green Infrastructure Strategy (2013), the adoption of the United Nations Sustainable Development Goals (2015), and the Intergovernmental Science-Policy Platform on Biodiversity and Ecosystem Services Global Assessment (2019). Second, a lexicon of policy-relevant keywords was constructed for each landmark, including terms such as nature-based solutions for the 2013 strategy, SDGs and sustainable development goals for the 2015 adoption, and urban resilience and climate adaptation for the 2019 assessment. Third, annual counts of articles containing these keywords were extracted from the dataset and normalized against total annual publication volume to account for overall growth in the field. Temporal trends in keyword usage were then plotted alongside the timing of the policy landmarks, with vertical markers indicating the years of policy adoption. The analysis examined both the magnitude of increase in keyword usage following each landmark and the lag time between policy adoption and peak scholarly uptake, which was calculated as the interval between the policy year and the year of maximum annual keyword frequency.

Phases of Knowledge Production: Temporal and Geographical Trends

The analysis of knowledge production phases combined temporal publication trends with geographic distribution patterns to characterize the evolution of research activity. Temporal analysis involved constructing a time-series of annual publication counts from 2006 to 2025, using data from the Web of Science Core Collection.

Thematic Clusters and Boundary-Spanning Keywords

The identification of thematic clusters and boundary-spanning keywords was accomplished through an integrative analysis combining the results of keyword co-occurrence mapping, temporal overlay analysis, and the Keyword–Discipline Tagging Protocol. Thematic clusters were derived from the VOSviewer cluster analysis of the keyword co-occurrence network, with each cluster interpreted based on the representative keywords with the highest occurrence frequency and centrality within the cluster. The functional role of each cluster—whether serving as a central hub, a bridging domain, a conceptual anchor, or a technical support layer—was determined by examining its connectivity level, calculated as the average co-occurrence strength between keywords within the cluster and keywords belonging to other clusters. Boundary-spanning keywords were identified through the Keyword–Discipline Tagging Protocol as those keywords assigned to three distinct disciplinary fields across primary, secondary, and tertiary categories.

Policy as a Catalyst: Milestones and Keyword Surges

For each policy landmark, keyword usage surges were quantified (percentage increase from baseline to post-policy peak), lag times calculated, and surge-period articles sampled for explicit policy references.

Persistent Divides and Untapped Synergies

A four-stage synthetic analysis diagnosed barriers: terminological ambiguities (from tagging protocol and co-citation gaps), data interoperability challenges (isolated technical vs. governance clusters), institutional constraints (policy lag, funding patterns), and untapped synergies (weak links like remote sensing–environmental justice). A framework of barriers and mitigation strategies was presented.

Results

Timeline-based co-citation analysis

Timeline-based co-citation analysis (Figure 2) shows a gradual shift in the disciplinary structure of ES–LP research. It is evident that the early studies (2006–2015) were largely rooted in ecological and environmental science, while post-2016 publications increasingly engaged with urban sustainability, climate resilience, and socio-political dimensions showing increasing conceptual convergence across ecological, planning, and governance perspectives, while some divergence remains in participatory governance and economic valuation. The present study supplements existing reviews by analyzing 50 reference ES–LP publications identified for citation importance and thematic influence to provide a conceptual foundation with which to interpret bibliometric trends. From this basis the research takes a Science-of-Science approach and uses Triple Helix as theoretical platform to consider knowledge co-evolution in academia, policy and practice contexts. In this regard, the use of keywords as markers of disciplinary stretch enabled co-occurrence and temporal trends to stand as proxies for cross-disciplinary convergence. It is on this theoretical basis that the analytical framework is developed in this section.

International collaboration analysis

The international collaboration analysis examines the geographic concentration of research productivity and co-authorship in ES–LP studies. The VOSviewer network (Figure 3) indicates that the United States and England function as dominant collaboration hubs—evidenced by their large node sizes and dense interconnections across clusters. Italy also emerges as a key European hub, facilitating strong intra-European linkages. While China represents an important and growing contributor, its network centrality remains comparatively lower than that of the USA and England.

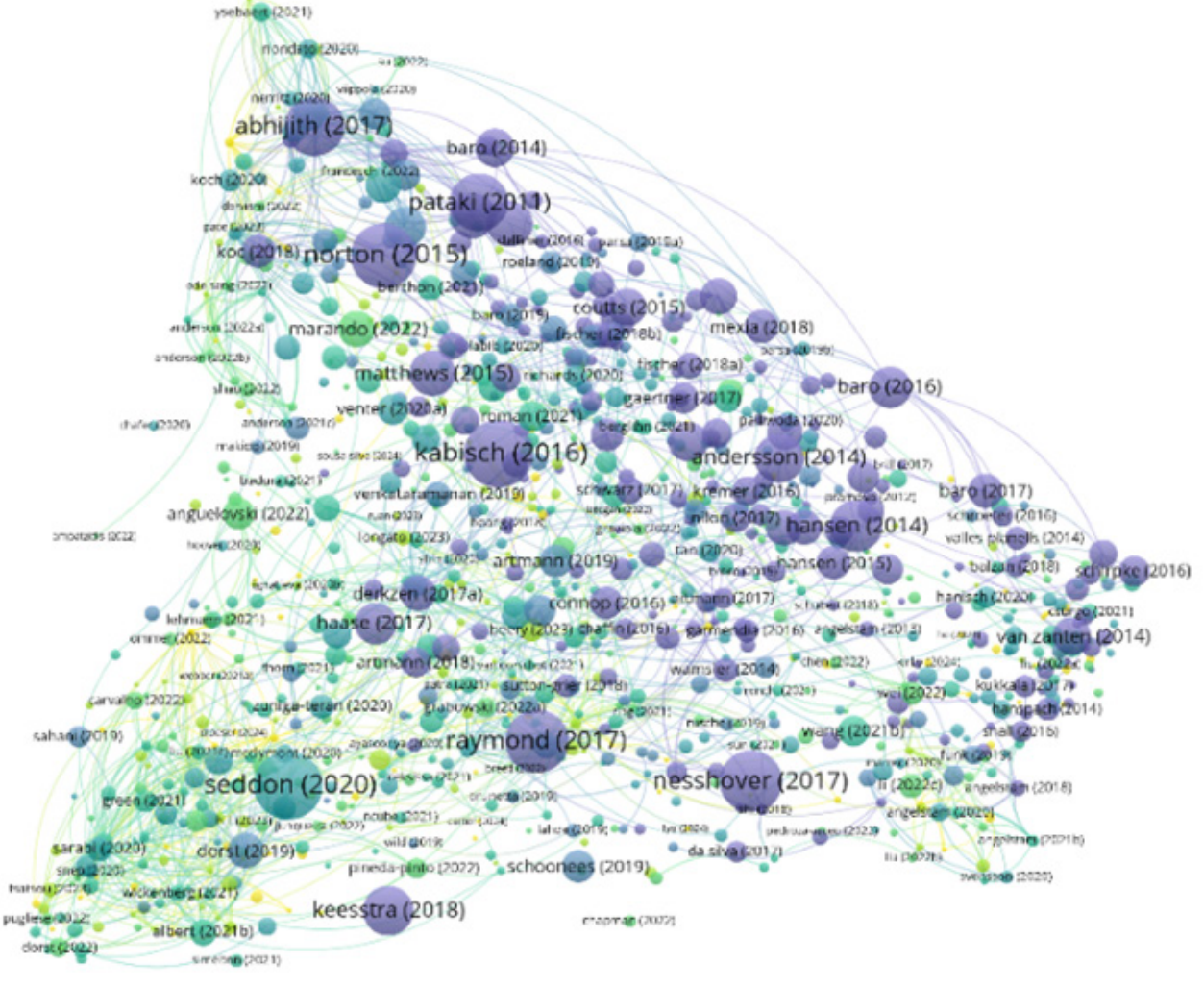

Figure 2. VOSviewer Timeline Visualization of Disciplinary Co-Citations (2006–2025), highlighting temporal and thematic evolution of interdisciplinary engagement in ES and landscape planning research.

Source: Author's analysis based on Web of Science data, visualized using VOSviewer (v1.6.20).

The keyword co-occurrence analysis

The keyword co-occurrence analysis (Figure 4; Table 1) showed the thematic system of ES–LP research, comprising 695 keywords grouped into seven clusters. The network is anchored by highly central terms such as ecosystem services, nature-based solutions, urban planning, and cities, which form the conceptual core of the field. These central nodes are strongly interconnected with clusters focusing on urban climate regulation, green infrastructure, biodiversity, and governance. While terms such as green infrastructure and landscape planning are important, they appear as embedded components within specific thematic clusters rather than dominant central nodes. Overall, the network pattern reflects an evolution towards integrative ecological–planning–governance platforms, rather than isolated disciplinary domains.

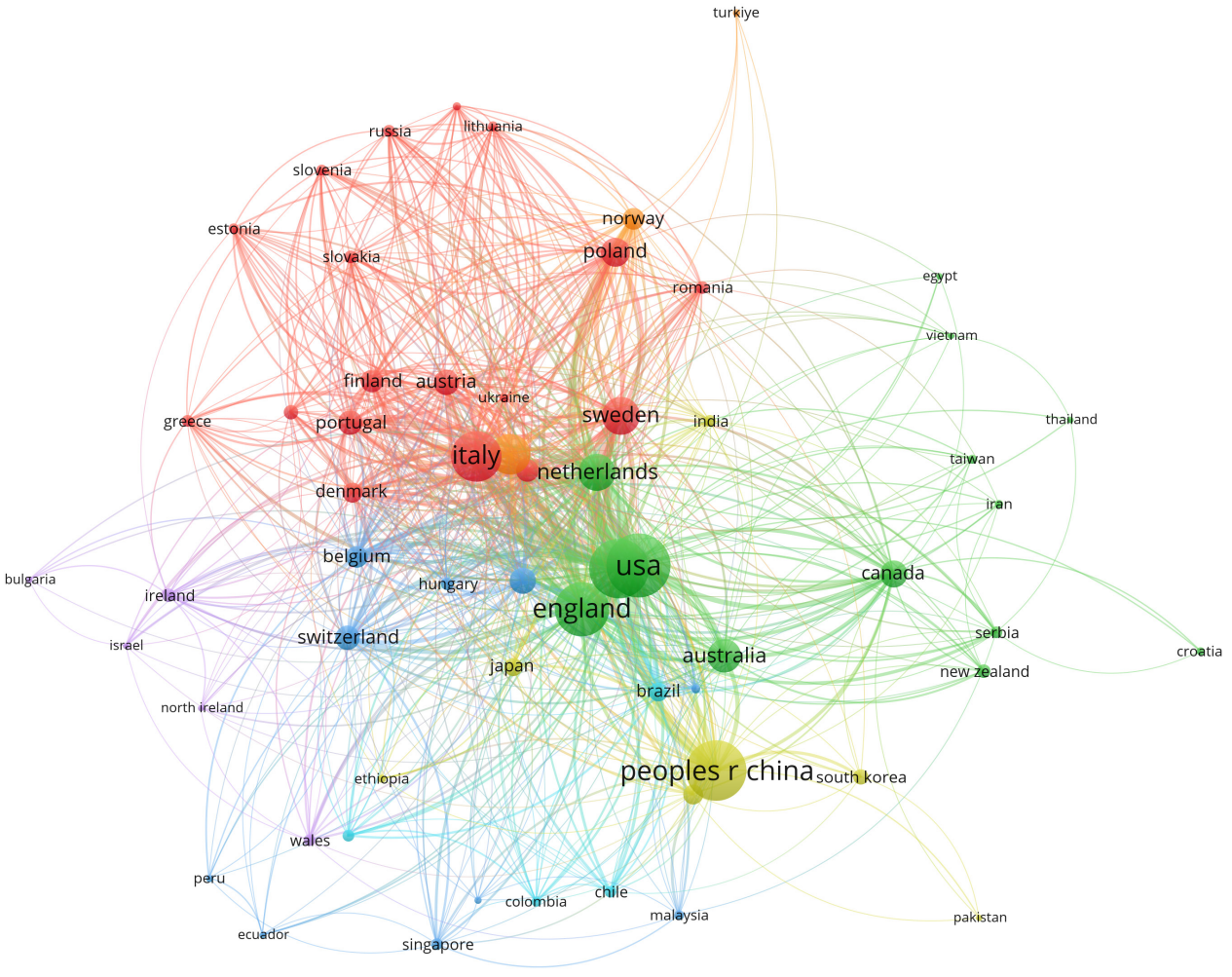

Figure 3. VOSviewer international co-authorship network by country, where circle size represents publication volume and line thickness indicates collaboration strength.

Source: Author's analysis based on Web of Science data, visualized using VOSviewer (v1.6.20).

Table 1. Keyword Co-occurrence Clusters and Thematic Structure in ES–LP Research (VOSviewer, n = 695).

Cluster	Colour	No. of Items	Cluster Theme (Interpreted)	Representative Keywords
Cluster 1	Red	149	Urban Climate, Air Quality & Thermal Environment	air pollution, air quality, urban heat island, temperature, microclimate, thermal comfort, green roofs, green walls, evapotranspiration, particulate matter (PM2.5), urban vegetation, remote sensing
Cluster 2	Green	111	Cultural Ecosystem Services & Human Perception	cultural ecosystem services, perception, public participation, landscape planning, recreation, wellbeing, aesthetics, participatory GIS, preferences, social values, tourism
Cluster 3	Blue	106	Nature-Based Solutions & Urban Water Management	green infrastructure, stormwater management, sponge city, flood mitigation, runoff, drainage systems, resilience, ecosystem-based adaptation, wetlands, sustainability
Cluster 4	Yellow	100	Landscape Ecology & Spatial Planning	land-use change, habitat fragmentation, ecological networks, connectivity, landscape patterns, biodiversity conservation, spatial analysis, ecological corridors, urban expansion
Cluster 5	Purple	100	Ecosystem Services, Biodiversity & Agriculture	biodiversity, ecosystem services, agroforestry, land management, restoration, pollination, soil, species richness, multifunctionality, conservation planning
Cluster 6	Cyan (Light Blue)	86	Social-Ecological Systems & Environmental Justice	ecosystem services, environmental justice, community, urban green space, health benefits, social vulnerability, urban agriculture, governance, equity
Cluster 7	Orange	43	Governance, Policy & Sustainability Transitions	governance, policy, climate adaptation, urban planning, sustainability transitions, decision-making, policy instruments, adaptive management, NbS implementation

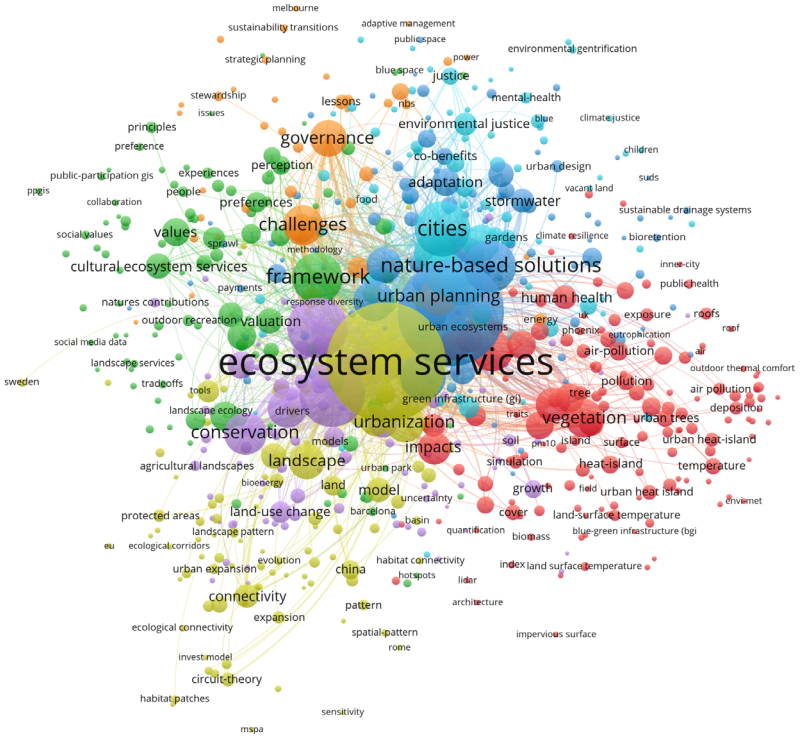

Figure 4. VOSviewer-generated keyword co-occurrence network, where node size reflects frequency and link strength indicates conceptual relatedness.

Source: Author's analysis based on Web of Science data, visualized using VOSviewer (v1.6.20).

Temporal overlay analysis

The temporal overlay analysis (Figure 5) results show development of research themes over time. Keywords are colour coded by average publication year, allowing a chronological interpretation of conceptual emergence. Foundational terms such as ecosystem services and landscape ecology appear in blue to blue-green shades, indicating their earlier emergence and continued relevance. More recent concepts (such as nature-based solutions, urban heat island, urban greening, and climate adaptation) appear in yellow shades from around 2019 onward. This pattern reflects a shift from early ecological foundations toward application-oriented, social-inclusive and climate adaptive planning approaches.

The co-citation analysis

The co-citation analysis (Figure 6) results outline the intellectual structure of ES–LP research. Conceptual networks are depicted as color-coded clusters: a green cluster around ecological economics and foundational ES theory; a red cluster related to urban ecology and environmental health; a yellow cluster that connects urban planning, green infrastructure, and spatial design; and a blue cluster on socio-ecological governance, resilience, and nature-based solutions. A smaller purple cluster emerges as a kind of transitional or bridging group, on the intersection between literature on urban ecosystem services, multifunctional landscapes and the translation of ecosystem service concepts into planning and design practice. Together, these Science Mapping analyses demonstrate the ES–LP research has transformed from ecological and economic platform to a more holistic, policy-driven, and transdisciplinary knowledge system. The convergence of biophysical, geographical and socio-political themes indicates the maturing discipline and its relevance for sustainable planning.

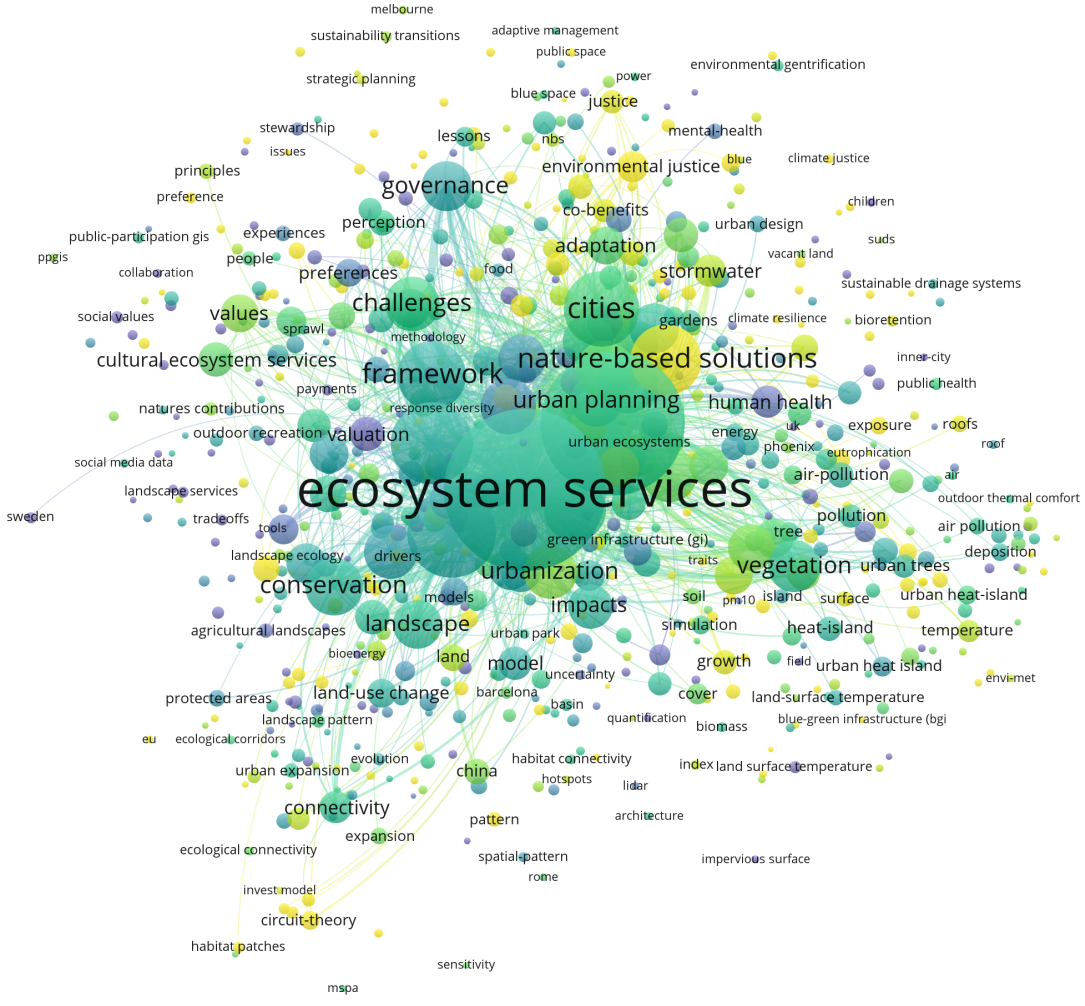

Figure 5. VOSviewer-generated temporal co-word overlay indicating chronological emergence of themes in ES–LP research (2006–2025).

Source: Author's analysis based on Web of Science data, visualized using VOSviewer (v1.6.20).

Interdisciplinary Convergence

This section evaluates the degree of interdisciplinary linkage within ES–LP research using three complementary techniques: keyword–discipline tagging, the Cohesion Index (CI), and policy–keyword temporal alignment. Together, these methods capture how ecological, planning, climate, and governance concepts intersect and evolve.

Keyword-Discipline Tagging Protocol

A Keyword–Discipline Tagging Protocol mapped high-frequency keywords to primary, secondary, and tertiary disciplinary fields based on co-occurrence patterns, clusters of cited references, and discipline taxonomies. This exposed deep cross-domain vocabulary — the words green infrastructure, urban resilience and nature-based solutions emerged repeatedly, binding ecology, planning, climate science and governance together. These associations are summarized in Table 2, which indicates that the most used keywords often cut across domains, revealing high levels of conceptual overlap within ES–LP scholarship.

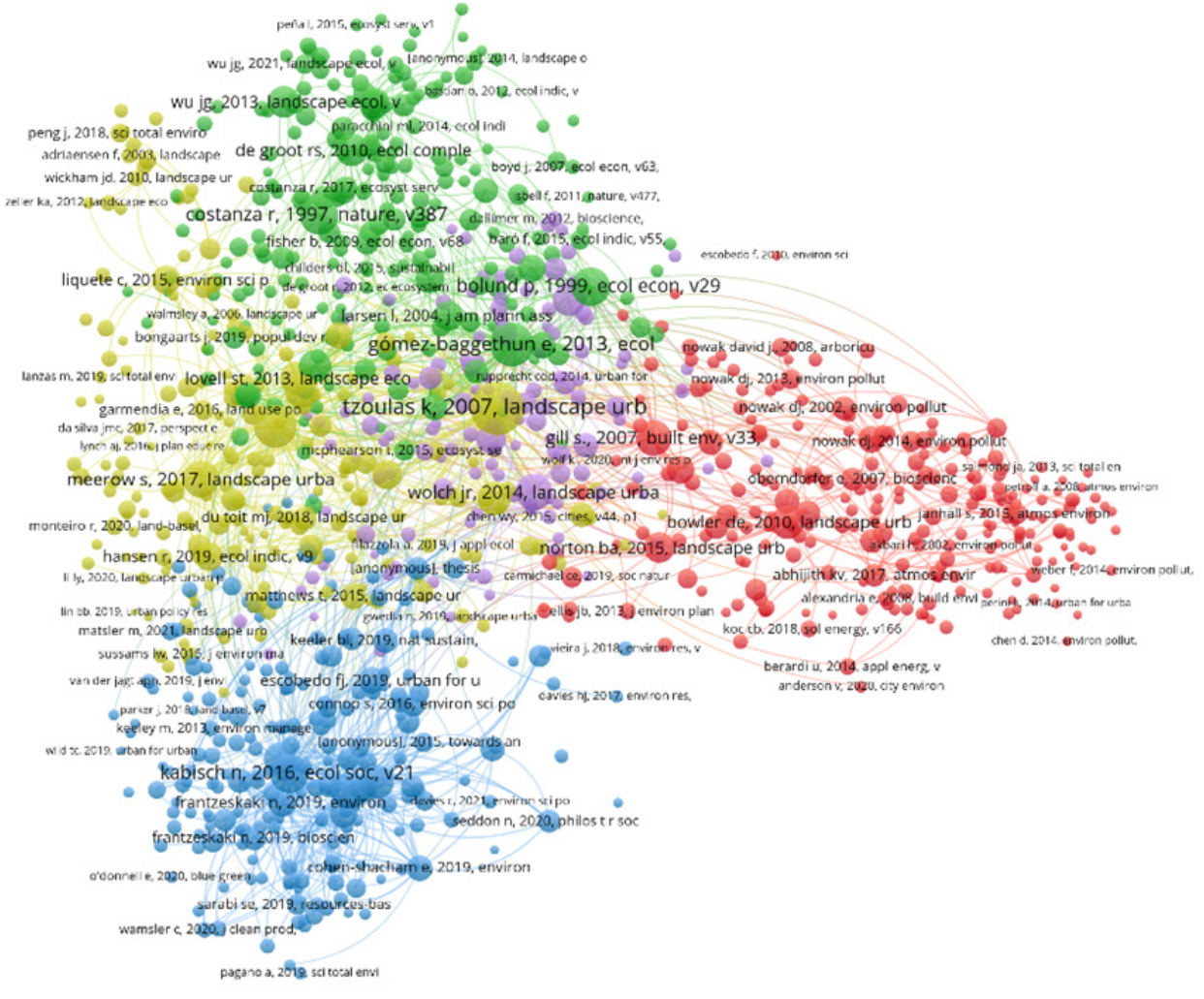

Figure 6. VOSviewer-generated co-citation network highlighting key thematic clusters in ES–LP scholarship.

Source: Author's analysis based on Web of Science data, visualized using VOSviewer (v1.6.20).

Table 2. Interdisciplinary keyword–discipline mapping based on screened and selected Web of Science records (n = 1930).

Keyword	Primary Discipline	Secondary Discipline	Tertiary Discipline	Screened and Selected References (WoS Dataset)
Green infrastructure	Urban Planning	Ecology	Civil Engineering	Norton (2015); Abhijith (2017); Cameron (2012); Haase (2017); Kumar (2019)
Ecosystem services	Ecology	Environmental Economics	Policy Studies	Nesshöver (2017); Salmond (2016); Cameron (2012); Baró (2015); Güneralp (2018)
Nature-based solutions	Environmental Planning	Climate Science	Governance	Nesshöver (2017); Keesstra (2018); Haase (2017); Dorst (2019); Berthon (2021)
Urban planning	Urban Studies	Architecture	Public Policy	Norton (2015); Baró (2015); Güneralp (2018); Geneletti (2016); McClymont (2020)
Landscape planning	Landscape Architecture	Environmental Science	Spatial Planning	Li (2022); Hessburg (2013); Gullino (2018); Bjärstig (2018); Barron (2019)
Urban resilience	Urban Planning	Climate Science	Governance	Collier (2013); Shokry (2020); Pamukcu-Albers (2021); McClymont (2020); Ochoa (2020)
Citizen science	Social Sciences	Ecology	–	Pinho (2021); Cambria (2021); Metzger (2018); Rae (2019); Abu Ali (2021)
Climate adaptation	Climate Science	Urban Resilience	Landscape Planning	Geneletti (2016); Anguelovski (2023); Sánchez (2023); Badura (2021); Knapp (2019)
Biodiversity conservation	Ecology	Conservation Biology	Environmental Policy	Güneralp (2018); Dauber (2010); Albert (2017); Fischer (2018); Berthon (2021)
Governance	Political Science	Environmental Management	Urban Studies	Dorst (2019); Kabisch (2022); Dorst (2022); Zingraff-Hamed (2020); Hersperger (2020)
Environmental justice	Sociology	Environmental Ethics	Public Health	Silva (2018); Calderón-Argelich (2021); Taguchi (2020); Kabisch (2022); Baró (2015)

The mapping summarized in Table 2 makes this cross-domain character strikingly visible. Consider green infrastructure, which is assigned primary affiliation with urban planning but immediately branches into ecology as its secondary field and civil engineering as its tertiary field—a configuration that captures the concept's dual identity as both a spatial planning strategy and a biophysical system requiring ecological understanding and engineering implementation. Similarly, nature-based solutions span environmental planning, climate science, and governance, reflecting its role as a boundary object that links climate adaptation strategies to planning practice and the institutional arrangements necessary for implementation. Even keywords that appear at first glance to belong squarely within a single discipline reveal significant multidirectionality. ES, which might be assumed to be primarily ecological, carries secondary ties to environmental economics and tertiary ties to policy studies, confirming that the concept achieved its influence precisely by providing a common language across scientific, economic, and policy communities.

The pattern holds across the Table 2. Urban planning appears not only in relation to urban studies and

architecture but also to public policy, acknowledging that planning scholarship engages with governance institutions and regulatory frameworks. Urban resilience, while primarily grounded in urban planning, draws equally from climate science and governance, reflecting the concept's emergence as a response to climate uncertainty and its reliance on institutional capacity. Even biodiversity conservation, which might seem exclusively ecological, extends into conservation biology and environmental policy, recognizing that the science of conservation operates in constant dialogue with policy mechanisms. Governance itself, mapped to political science, environmental management, and urban studies, appears as a keyword that connects institutional analysis to environmental outcomes and urban contexts. Environmental justice, assigned to sociology, environmental ethics, and public health, demonstrates that questions of equity in landscape planning have become a nexus linking social theory, normative philosophy, and health outcomes.

Cohesion Index

Interdisciplinary integration was quantified using the Cohesion Index, which compares cross-cluster keyword connections with within-cluster density. A co-occurrence matrix of the top 100 author keywords (minimum occurrence = 5) was subjected to cluster analysis following Ward's method (Murtagh and Legendre, 2014), and six thematic domains were developed (urban sustainability, ecosystem services, climate resilience, land management, measurement tools and policy/social engagement). High level of inter-cluster connectivity is visible in Figure 7, especially among ecological and planning and climate clusters, while such is not the case for socio-political concepts. Cluster roles are presented in Table 3. Sensitivity analyses, under different keyword thresholds (3 – 10) and clustering resolutions (0.8 – 1.2), generated consistent CIs (0.937 to 0.947). Bootstrap resampling (n = 1,000) showed a mean CI of 0.944 ± 0.005, representing strong and robust interdisciplinary cohesion.

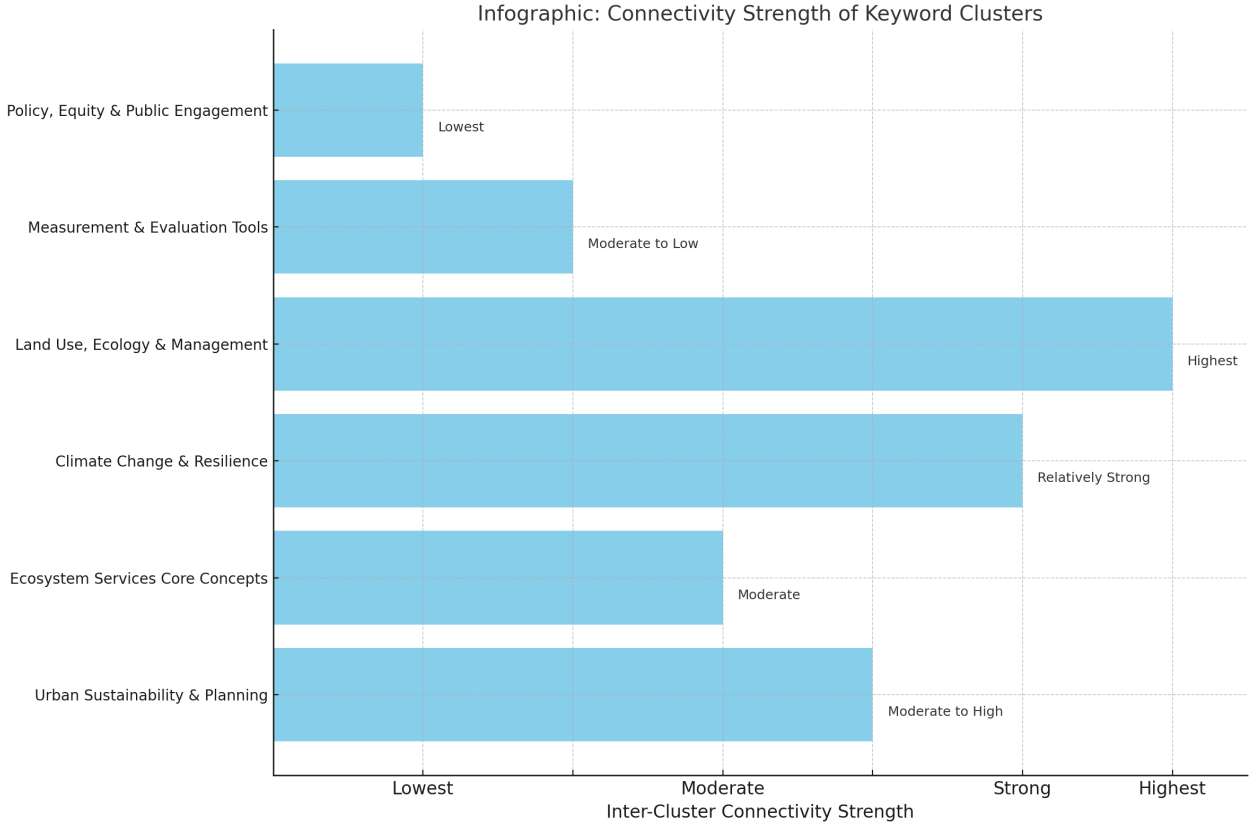

Figure 7. Inter-cluster connectivity strengths across major thematic domains in ES–LP research (2006–2025).

Source: Author's own analysis based on co-citation and cluster connectivity metrics derived from the Web of Science Core Collection (SCIE, SSCI, ESCI).

Table 3. *Integration Roles and Connectivity Levels of Thematic Clusters in ES-LP Research.*

Cluster ID	Theme / Domain	Representative Keywords	Connectivity Level	Integration Role
0	Urban Sustainability & Planning	urban green infrastructure, green roofs, urban resilience	Moderate to High	Bridges planning and ecological application
1	ES Core Concepts	ecosystem services, cultural ecosystem services, nature-based solutions	Moderate	Conceptual anchor across multiple themes
2	Climate Change & Resilience	climate adaptation, resilience, flood mitigation	Relatively Strong	Connects climate science with planning
3	Land Use, Ecology & Management	landscape connectivity, biodiversity conservation, land management	Highest	Central interdisciplinary hub
4	Measurement & Evaluation Tools	spatial analysis, remote sensing, landscape metrics	Moderate to Low	Technical support for all clusters
5	Policy, Equity & Public Engagement	environmental justice, citizen science, decision support	Lowest	Emerging social dimension; less integrated

Note: The representative keywords presented for each cluster should be viewed as indicative descriptors instead of the exclusive thematic labels. They are assigned based on relative prominence-among the mapped networks, in terms of frequency, co-occurrence strength and visual centrality. Cross-cutting terms (e.g. nature-based solutions) may conceptually relate to more than one domain but are shown within the cluster where they reflect a stronger association.

Table 3 reveals a clearly differentiated intellectual structure within ES and LP research, where six thematic clusters perform distinct yet interconnected roles in shaping the field's interdisciplinary landscape. The clusters vary considerably in their connectivity levels—ranging from highest to lowest—and in the functions they serve within the broader scholarly network. At the center of the field sits Cluster 3 (Land Use, Ecology & Management), distinguished by the highest connectivity level and described as a central interdisciplinary hub. Organized around keywords such as landscape connectivity, biodiversity conservation, and land management, this cluster functions as the intellectual core that binds together ecological science, spatial planning, and land-use decision-making.

Cluster 0 (Urban Sustainability & Planning) and Cluster 2 (Climate Change & Resilience) occupy positions of strong integrative significance, each serving as a bridge between distinct knowledge domains. Cluster 0, with its moderate to high connectivity, links urban green infrastructure, green roofs, and urban resilience—bridging planning practice with ecological application in urban contexts. Cluster 2, rated relatively strong in connectivity, connects climate science with planning through keywords such as climate adaptation, resilience, and flood mitigation, indicating that climate-related concerns have become a major conduit linking environmental science to planning interventions.

Cluster 1 (ES Core Concepts) holds a moderate connectivity level but serves a foundational role as a conceptual anchor across multiple themes. Represented by ecosystem services, cultural ecosystem services, and nature-based solutions, this cluster provides the overarching framework and shared vocabulary that enables communication across otherwise disparate research streams. Cluster 4 (Measurement & Evaluation Tools), with moderate to low connectivity, functions as a technical support layer for all clusters. Encompassing spatial analysis, remote sensing, and landscape metrics, this cluster represents the methodological infrastructure that enables empirical research across the field. Its lower connectivity may reflect that technical methods are applied across contexts but do not themselves generate high volumes of cross-cluster citation or conceptual integration—they are tools deployed within studies rather than concepts that inherently bridge diverse research communities. Cluster 5 (Policy, Equity & Public Engagement) stands apart with the lowest connectivity level, characterized as an emerging social dimension that remains less integrated into the core of the field. Its peripheral position suggests that while these social and policy dimensions are recognized as important, they have not yet achieved the same level of conceptual integration with ecological and planning themes as other clusters—representing both a gap and an opportunity for future development.

Temporal Convergence Analysis

Temporal analysis of annual keyword networks revealed a growing intermingling between ecological, planning and climate-policy terms since 2018. The segmented regression, as facilitated by the Chow test and PELT algorithm, identified a significant changepoint at about 2018 (±0.4 years). Figure 8 shows the steep slope of convergence post-2018, followed by an eventual flattening towards 2025. Similar inflection shapes were observed for Shannon entropy and edge-share ratio measures, supporting robustness.

Policy-Keyword Alignment Methodology

For policy influence, annual counts of policy-relevant terms (nature-based solutions, urban resilience, climate adaptation and SDGs) were compared against three key development landmarks – the EU Green Infrastructure Strategy (2013), the UN SDGs (2015) and the IPBES Global Assessment (2019). And keyword use surged in the years just following each milestone – NBS post 2013, SDG associated language after 2015, and resilience/adaptation terminology post-2019. Figure 9 demonstrates these alignments with distinct patterns that correlate policy adoption with keyword growth.

Phases of Knowledge Production: Temporal and Geographical Trends

A segmented analysis of annual articles (2006 – 2025) reveals three phases. The Early Stability phase (2006–2012) is characterized by a low and almost constant output of 0–4 papers/year. A Gradual Emergence phase (2013–2016) follows, with the output increasing from 12 records in 2013 to 52 records in 2016. After 2016, a substantial Resurgence is observed with nearly 300 papers by 2024, indicating renewed attention to climate-adaptive and interdisciplinary planning research.

Output remained low from 2006 to 2012, increased gradually from 2013 to 2016, and then rose sharply thereafter from 113 in 2018 to nearly 300 in 2024, with 101 recorded for partial-year 2025. This post-2016 increase aligns with expanding climate-resilience and sustainability research (UNESCO, 2022) and more general interdisciplinary policy changes (Kabisch, 2016; IPBES, 2019). Annual variations are presented in Figure 10.

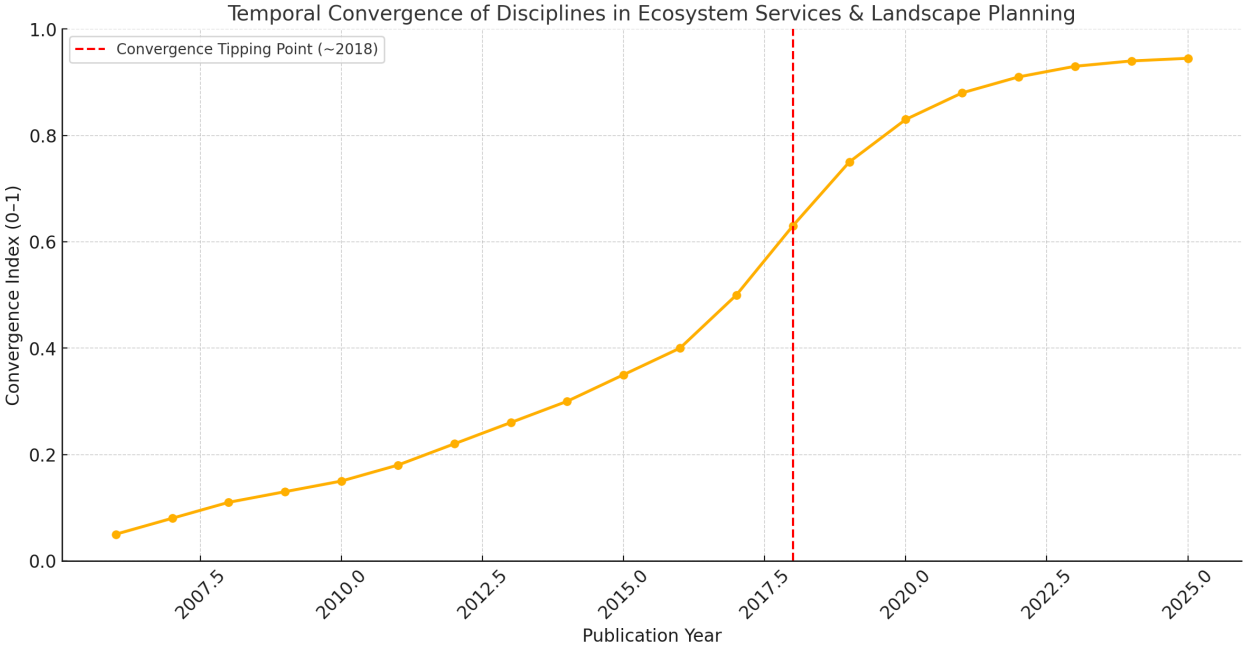

Figure 8. Temporal Convergence of Disciplinary Integration in ES and LP Research (2006–2025).

Source: Author

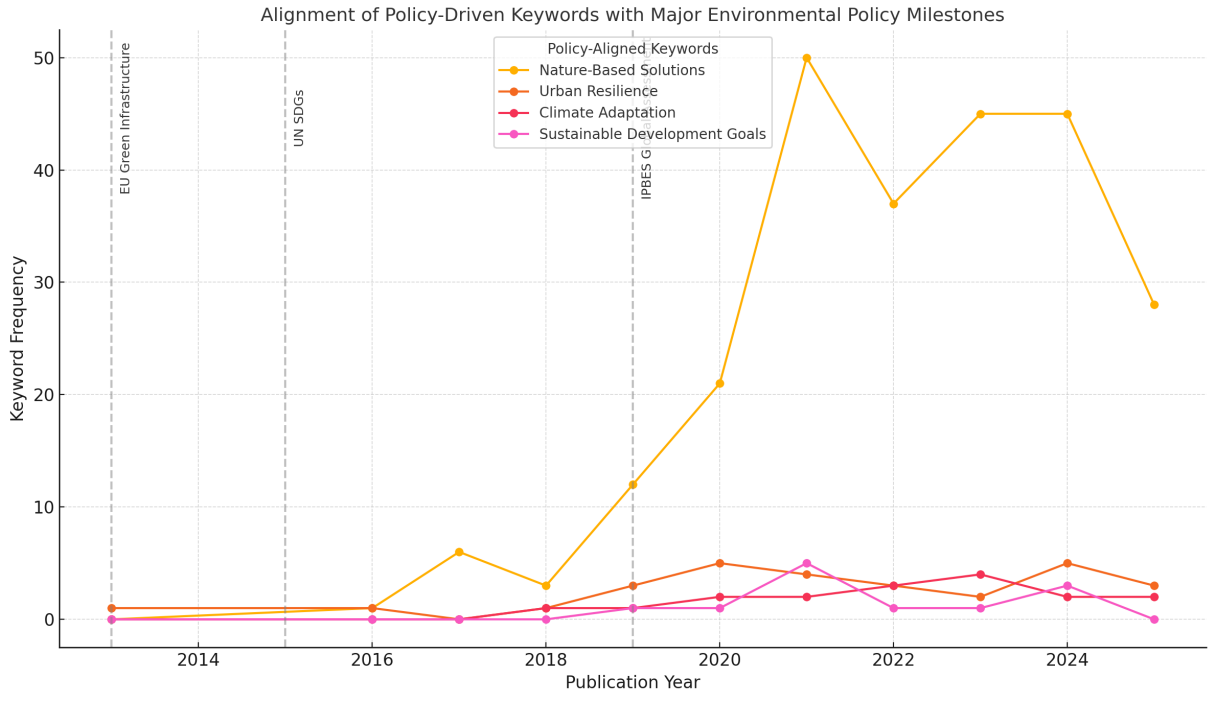

Figure 9. Policy-Driven Keyword Adoption in ES-LP Research: Alignment with Global Environmental Frameworks (2014-2024).

Source: Author

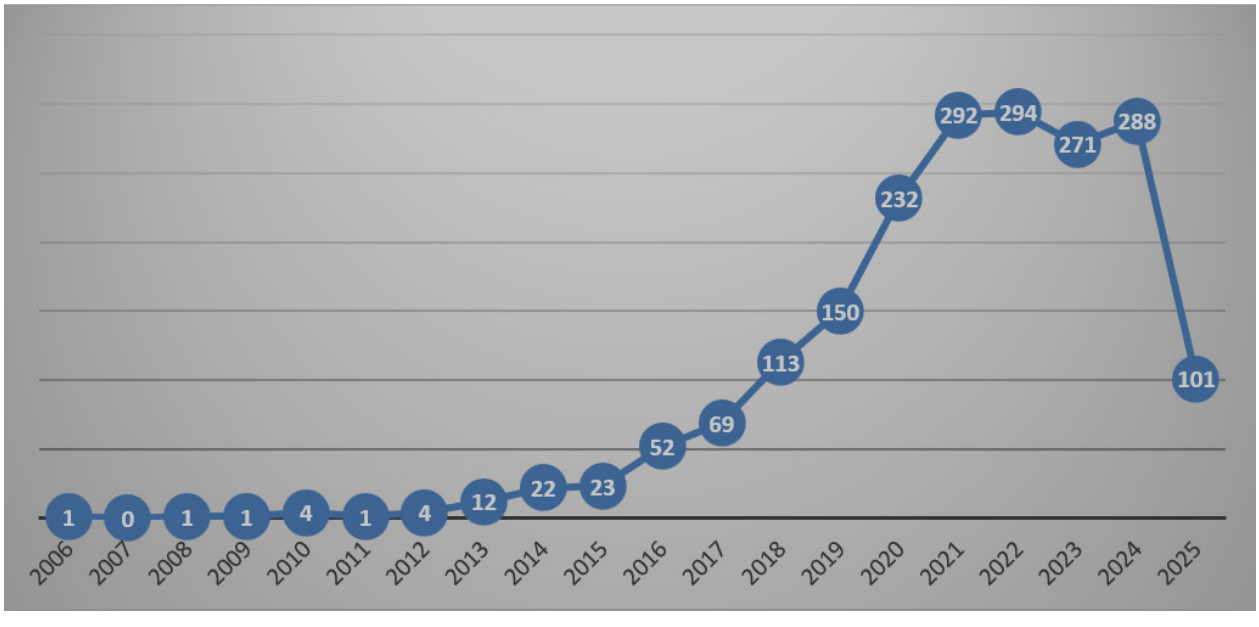

Figure 10. Annual publication trends (2006–2025) in ecosystem services and landscape planning literature. Partial-year data shown for 2025.

Source: Author's own analysis based on Web of Science (WoS) Core Collection data (SCIE, SSCI, ESCI), retrieved on 29th July 2025.

Thematic Clusters and Boundary-Spanning Keywords

Keyword co-occurrence mapping (Figure 4, 5) presents three large thematic clusters; Ecology/Environment, Urban Planning/Design and Social–Political Dimensions. These clusters are connected by core term—ES, green infrastructure, landscape planning—suggesting high level of integration in core concepts. Temporal overlays (Figure 5, 8) where there is thematic progress: ecological and value terms came to the forefront 2006–2015; climate-adaptation and planning language increased 2016–2019; and hybrid ideas (urban heat island, citizen science) are extending past 2020. The Cohesion Index (CI = 0.944) indicates that strong 'cross-cluster' connections strengthen, but participatory and equity-focused terms are less cohesive.

Policy as a Catalyst: Milestones and Keyword Surges

Policy development coincides almost precisely with changes in terminology (Figure 9). The increase in nature-based solutions is more pronounced after the 2013 EU Green Infrastructure Strategy, that of SDG-associated terms after 2015 and of urban resilience and climate adaptation following the 2019 IPBES Assessment. In general, both shifts lag 1–2 years behind policy enactment, suggesting that the academy is responding to uptake. Europe and China are the most in sync. A transient surge of health- and green-space-related terms launched in the period 2020–2022 reflects pandemic-induced shifts to environmental planning discourse.

Pathways to Interdisciplinary Maturation

Results suggest a gradual move towards ES–LP interdisciplinary convergence, which manifests into increased co-word linkages and connection strengths, together with stronger co-citations. Under this prism, the early works (2006–2015) focus on ecological and valuation themes; a shift occurred in the transition phase (2016–2019) to include planning and governance; and from 2020 onwards, hybrid concepts—nature-based solutions, citizen science, environmental justice—emphasize further social, climatic, spatial integration. These changes are influenced by policy milestones, however, the 1–2-year lag in time from when a policy is implemented to its uptake by academia may suggest researchers are largely on the back foot.

Persistent Divides and Untapped Synergies

Despite strong integration of various aspects into the LP, disciplinary gaps still persist. Terms such as sustainability and resilience still have different meanings between ecology and planning, thus undermining conceptual synchronization. Moreover, the data interoperability is poor, since ecological studies focus on biophysical variables and planning focuses on socio-economic and governance indicators. These schisms further account for the peripheral status of equity and participatory terms in keyword networks. Table 5 Main barriers and proposed solutions including terminology harmonisation, common data infrastructures, and inter-/trans-disciplinary research mechanisms.

Limitations and Future Directions

Table 6 synthesizes these limitations and identifies pathways for methodological advancement across technical, social, and governance dimensions.

Table 4. Levels of Disciplinary Integration in ES–LP Scholarship.

Integration Level	Characteristics	Examples	Drivers
Terminal (Siloed)	Keywords/clusters remain discipline-bound; minimal cross-citation.	Early-phase "biodiversity conservation" (ecology-only).	Lack of policy urgency; methodological divergences.
Bridging (Emerging)	Terms co-occur but retain primary disciplinary roots.	"Green infrastructure" (urban planning + ecology).	Policy frameworks (e.g., EU Strategy); applied research needs.
Hybrid (Converged)	Boundary-spanning terms dominate; high cross-cluster cohesion (CI = 0.944).	"Nature-based solutions" (ecology + planning + governance).	Global agendas (SDGs, IPBES); transdisciplinary co-design.
Peripheral (Underexplored)	Weak linkages despite thematic relevance.	"Remote sensing" + "environmental justice."	Institutional barriers; lack of shared methodologies.

Source: Author

Table 5. Barriers to Interdisciplinary Integration and Corresponding Mitigation Strategies.

Barrier Type	Key Findings	Proposed Solutions	Supporting Evidence
Terminological Ambiguities	- Divergent disciplinary interpretations of core concepts like "sustainability" (ecological vs. planning perspectives) - Weak conceptual bridges between ecological and policy research domains	- Develop standardized glossary of boundary-spanning terms - Conduct interdisciplinary terminology alignment workshops	- Keyword-Discipline Tagging results - Co-citation network gaps (Figure 6)
Data Interoperability	- Incompatible data types (biophysical measurements vs. socioeconomic indicators) - Isolation of technical measurement clusters from governance concepts	- Establish open-data repositories with cross-disciplinary standards - Develop unified geospatial analysis platforms	- Temporal Convergence Analysis (Figure 8) - Cluster isolation patterns (Figure 4)
Institutional Resistance	- Limited academia-policy collaboration - Policy implementation lag research adoption	- Implement funding mechanisms requiring cross-disciplinary collaboration - Create dedicated transdisciplinary research units	- Policy-Keyword Alignment findings (Figure 9) - Cohesion Index analysis

Source: Author

Table 6. Limitations and Future Research Directions for Interdisciplinary ES-LP Studies.

Category	Limitations	Future Research Directions
Database Biases	- Reliance on WoS underrepresents non-English/regional journals.	- Multi-Database Integration: Include Scopus, Dimensions, CNKI for broader geographic coverage.
	- Global South research (Africa, Latin America) is underrepresented.	- Prioritize regional databases to address Anglo-Eurocentric bias.
Tagging Subjectivity	- Manual keyword-discipline tagging introduces bias.	- NLP-Automated Classification: Use BERT/GPT models to standardize hybrid term mapping (e.g., "urban resilience").
	- Ambiguity in evolving terms (e.g., "nature-based solutions").	- Train algorithms on interdisciplinary taxonomies for consistency.
Temporal Gaps	- Dataset ends in early 2025, missing later trends.	- Longitudinal Cohesion Tracking: Apply Cohesion Index to 2025–2030 data to test convergence stability.
Policy-Research Linkages	- Policy-keyword alignment relies on retrospective correlation.	- Dynamic Policy Analysis: Use NLP to track real-time policy language (e.g., UN reports) and keyword emergence.
Technical-Social Divides	- Weak co-occurrence between technical (e.g., "remote sensing") and social terms.	- Participatory-Technical Studies: Combine geospatial tools with community-driven data to bridge gaps.

Source: Author

The development of ES–LP research indicates a clear progression toward transdisciplinary harmonization. The quick uptake of hybrid concepts – urban resilience, nature-based solutions – shows that vocabulary is converging faster than practice, and this is driven by global policy agendas. To bridge long-standing divides—between, for example, geospatial methods and environmental justice—the field will need further terminological harmonization, closer policy-research synchronization and expanded mixed method approaches. In general, ES–LP research offers a replicable approach to integration science across other complex socio-ecological systems.

Discussion

Theoretical Framework and Conceptual Approach

The analysis of collected data shows increasing conceptual convergence across ecological, planning, and governance perspectives, while some divergence remains in participatory governance and economic valuation. To fill these gaps, the present study supplements existing reviews by analyzing 50 reference ES–LP publications identified for citation importance and thematic influence to provide a conceptual foundation with which to interpret bibliometric trends. From this basis, the research takes a Science-of-Science approach and uses the Triple Helix as a theoretical platform (Etzkowitz & Leydesdorff, 2000) to consider knowledge co-evolution in academia, policy, and practice contexts. In this regard, the use of keywords as markers of disciplinary stretch enables co-occurrence and temporal trends to stand as proxies for cross-disciplinary convergence. It is on this theoretical basis that the analytical framework is developed in this section.

International Collaboration Patterns

The results of international collaboration analysis patterns align with global scientific trends where high-income countries and rapidly expanding research economies dominate environmental stewardship, probably due to stronger funding environments and extensive institutional networks (Nature Index, 2023; Wagner et al., 2017). Moreover, the strong intra-European collaboration reflects the influence of EU-funded research initiatives, particularly those supported through Horizon 2020 and related programmes (European Commission, 2020).

Keyword Co-occurrence and Intellectual Integration

The network pattern studied through keyword co-occurrence analysis reflects an evolution towards integrative ecological–planning–governance platforms, rather than isolated disciplinary domains. However, the co-citation analyses demonstrate that ES–LP research has transformed from an ecological and economic platform to a more holistic, policy-driven, and transdisciplinary knowledge system. The convergence of biophysical, geographical, and socio-political themes indicates the maturing discipline and its relevance for sustainable planning (Pataki et al., 2011; Andersson et al., 2015; Kabisch et al., 2015; Abhijith et al., 2017; Seddon et al., 2020).

Cross-Domain Conceptual Mapping

The mapping summarized in Table 2 makes the cross-domain character strikingly visible. The configuration of green infrastructure captures the concept's dual identity as both a spatial planning strategy and a biophysical system requiring ecological understanding and engineering implementation. Nature-based solutions reflect its role as a boundary object linking climate adaptation strategies to planning practice and institutional arrangements (Opdam, 2018). Ecosystem services confirms that the concept achieved its influence precisely by providing a common language across scientific, economic, and policy communities (Artmann et al., 2017). Urban planning acknowledges that planning scholarship engages with governance institutions and regulatory frameworks. Urban resilience reflects the concept's emergence as a response to climate uncertainty and its reliance on institutional capacity. Biodiversity conservation recognizes that conservation science operates in constant dialogue with policy mechanisms. Governance connects institutional analysis to environmental outcomes and urban contexts. Environmental justice demonstrates that questions of equity in landscape planning have become a nexus linking social theory, normative philosophy, and health outcomes.

Intellectual Structure: Cluster Analysis

Table 3 reveals a clearly differentiated intellectual structure. Various clusters showed that Land Use, Ecology & Management (Andersson et al., 2015) functions as the intellectual core binding together ecological science, spatial planning, and land-use decision-making. Cluster 0 (Urban Sustainability & Planning), while Climate Change & Resilience (Baker-Médard et al., 2024) serve as bridges between distinct knowledge domains. Moreover, the ES Core Concepts serves a foundational role as a conceptual anchor providing shared vocabulary and focus on Measurement & Evaluation Tools functions as a methodological infrastructure; its lower connectivity reflects that technical methods are tools deployed within studies rather than concepts that inherently bridge diverse research communities. Lastly, Policy, Equity & Public Engagement (Brink & Wamsler, 2018) stands apart as an emerging social dimension that remains less integrated—representing both a gap and an opportunity for future development.

Temporal Convergence and Policy Lag

In addition to above, the temporal convergence analysis results clearly showed that the steep post-2018 slope indicates accelerating interdisciplinary integration. However, the 1–2-year lag from policy enactment to academic uptake suggests that researchers are largely on the back foot, responding to rather than anticipating policy needs. The journey of interdisciplinary maturation suggests a gradual move towards ES–LP interdisciplinary convergence, manifested in increased co-word linkages, connection strengths, and stronger co-citations (Li et al., 2022). The evolution of concepts in ES-LP indicates that in the early stages the focus was on ecological and valuation themes, followed by planning and governance and subsequently introduction of hybrid concepts (nature-based solutions, citizen science, environmental justice) that emphasize further social, climatic, and spatial integration (Gullino, 2018). These changes are influenced by policy milestones; however, the 1–2-year lag suggests researchers are largely on the back foot.

Persistent Gaps and Obstacles to Integration

Despite strong integration, disciplinary gaps persist (Collier et al., 2013). Divergent interpretations of terms such as sustainability and resilience undermine conceptual synchronization. Poor data interoperability and institutional constraints—fragmented funding, weak academia-policy links (Hessburg et al., 2013), delays in policy uptake—exacerbate these obstacles. Table 5 presents proposed solutions including terminology harmonisation, common data infrastructures, and inter-/trans-disciplinary research mechanisms (Dorst et al., 2019).

Limitations of the Study

Although multiple disciplines are getting integrated, several limitations remain (Albert et al., 2014). For instance, the dependency on Web of Science is biased against non-English and Global South scholarship; manual keyword tagging introduces subjectivity, although at a high level of agreement between raters ($\kappa = 0.87$); the dataset extends only partially to 2025, limiting its ability to capture recent developments.

Conclusion

Based on the bibliometric, keyword-discipline, cohesion, and temporal convergence analyses, this study reveals that ecosystem services (ES) and landscape planning (LP) research has evolved from loosely connected disciplinary inquiries into an increasingly coherent and transdisciplinary knowledge system over the past two decades. This transformation occurred through distinct phases: an early phase (2006–2015) rooted in ecological and environmental science, operating within a siloed integration level; a transition phase (2016–2019) marked by the growing prominence of planning and governance perspectives, catalyzed by policy milestones such as the EU Green Infrastructure Strategy and the Sustainable Development Goals; and a post-2020 phase characterized by a hybrid, converged knowledge system dominated by boundary-spanning concepts like nature-based solutions, urban resilience, and citizen science. The quantitative evidence strongly supports this maturation: a Cohesion Index of 0.944 indicates that cross-cluster connections substantially outweigh within-cluster density; a significant change-point around 2018 accelerated the intermingling of ecological, planning, and climate-policy terms; and policy-keyword alignment shows consistent responsiveness to global governance frameworks with a one-to-two-year lag. Furthermore, keyword-discipline mapping reveals that concepts such as green infrastructure, nature-based solutions, and ecosystem services function as boundary objects, encoding interdisciplinary relationships and enabling researchers from different backgrounds to communicate with increasing fluency. Cluster analysis identifies land use, ecology, and management as the central interdisciplinary hub, while ES core concepts serve as a conceptual anchor, and policy, equity, and public engagement exhibit the lowest connectivity—representing both a critical gap and a significant opportunity.

The persistence of disciplinary divides despite strong overall integration warrants careful attention. Terminological ambiguities persist, with concepts such as sustainability and resilience carrying divergent meanings across ecological and planning communities, undermining conceptual synchronization. Data interoperability remains poor, as ecological studies prioritize biophysical measurements while planning research focuses on socioeconomic and governance indicators, creating methodological fragmentation. Institutional constraints—including fragmented funding structures, weak academia-policy linkages, and delayed policy uptake—further exacerbate these barriers. The peripheral status of equity and participatory terms in keyword networks is particularly concerning given the normative commitments of sustainability science to inclusive and just outcomes. This finding suggests that while the field has achieved remarkable integration across biophysical, spatial, and climate domains, the full incorporation of social, participatory, and environmental justice dimensions remains an unfinished project—one that will require deliberate effort to address the institutional, methodological, and terminological barriers that have thus far limited their integration.

Acknowledgements

The authors are thankful to the Department of Architecture and Planning, VNIT Nagpur for the institutional support and research-friendly environment. The authors also appreciate the support of VOSviewer, R–bibliometrix and Web of Science Core Collection for data extraction and analysis.

References

Abhijith, K. V., Kumar, P., Gallagher, J., McNabola, A., Baldauf, R., Pilla, F., Broderick, B., Di Sabatino, S., & Pulvirenti, B. (2017). Air pollution abatement performances of green infrastructure in open road and built-up street canyon environments: A review. *Atmospheric Environment, 162*, 71–86. https://doi.org/10.1016/j.atmosenv.2017.05.014

Albert, C., Aronson, J., Fürst, C., & Opdam, P. (2014). Integrating ecosystem services in landscape planning: Requirements, approaches, and impacts. *Landscape Ecology, 29*(8), 1277–1285. https://doi.org/10.1007/s10980-014-0085-0

Albert, C., Brillinger, M., Guerrero, P., Gottwald, S., Henze, J., Schmidt, S., Ott, E., & Schröter, B. (2021). Planning nature-based solutions: Principles, steps, and insights. *Ambio, 50*(8), 1446–1461. https://doi.org/10.1007/s13280-020-01430-2

Andersson, E., Tengö, M., McPhearson, T., & Kremer, P. (2015). Cultural ecosystem services as a gateway for improving urban sustainability. *Ecosystem Services, 12*, 165–168. https://doi.org/10.1016/j.ecoser.2014.08.002

Artmann, M., Bastian, O., & Grunewald, K. (2017). Using the concepts of green infrastructure and ecosystem services to specify *Leitbilder* for compact and green cities: The example of the landscape plan of Dresden (Germany). *Sustainability, 9*(2), 198. https://doi.org/10.3390/su9020198

Baker-Médard, M., Concannon, K., Gantt, C., Moen, S., & White, E. R. (2024). Socialscape ecology: Integrating social features and processes into spatially explicit marine conservation planning. *Sustainability, 16*(14), 6078. https://doi.org/10.3390/su16146078

Balzan, M. V., Caruana, J., & Zammit, A. (2018). Assessing the capacity and flow of ecosystem services in multifunctional landscapes: Evidence of a rural–urban gradient in a Mediterranean small island state. *Land Use Policy, 75*, 711–725. https://doi.org/10.1016/j.landusepol.2018.03.025

Baró, F., Haase, D., Gómez-Baggethun, E., & Frantzeskaki, N. (2015). Mismatches between ecosystem service supply and demand in urban areas: A quantitative assessment in five European cities. *Ecological Indicators, 48*, 146–156. https://doi.org/10.1016/j.ecolind.2014.08.013

Barron, S., Sheppard, S. R. J., & Condon, P. M. (2019). Planning for green infrastructure: The spatial effects of parks, forests, and trees on urban sustainability. *Sustainability, 11*(1), 241. https://doi.org/10.3390/su11010241

Berthon, K., Thomas, F., Bekessy, S., & Cernusak, L. A. (2021). Urban biodiversity and nature-based solutions: Pathways to sustainable cities. *Biological Conservation, 253*, 108923. https://doi.org/10.1016/j.biocon.2020.108923

Bjärstig, T., Sandström, C., Sténs, A., & Widmark, C. (2018). Landscape governance and planning: Perspectives from Sweden. *Land Use Policy, 72*, 315–326. https://doi.org/10.1016/j.landusepol.2017.11.011

Brink, E., & Wamsler, C. (2018). Collaborative governance for climate change adaptation: Mapping citizen–municipality interactions. *Environmental Policy and Governance, 28*(2), 82–97. https://doi.org/10.1002/eet.1795

Cameron, R. W. F., Blanuša, T., Taylor, J. E., Salisbury, A., Halstead, A. J., Henricot, B., & Thompson, K. (2012). The domestic garden – Its contribution to urban green infrastructure. *Urban Forestry & Urban Greening, 11*(2), 129–137. https://doi.org/10.1016/j.ufug.2012.01.002

Collier, M. J., Nedović-Budić, Z., Aerts, J., Connop, S., Foley, D., Foley, K., Newport, D., McQuaid, S., Slaev, A., & Verburg, P. (2013). Transitioning to resilience and sustainability in urban communities. *Cities, 32*(Suppl. 1), S21–S28. https://doi.org/10.1016/j.cities.2013.03.010

European Commission. (2020). *Horizon 2020 final report: EU framework programme for research and innovation (2014–2020)*. Publications Office of the European Union.

Cortinovis, C., & Geneletti, D. (2019). A framework to explore the effects of urban planning decisions on regulating ecosystem services in cities. *Ecosystem Services, 38*, 100946. https://doi.org/10.1016/j.ecoser.2019.100946

Costanza, R., d'Arge, R., de Groot, R., Farber, S., Grasso, M., Hannon, B., Limburg, K., Naeem, S., O'Neill, R. V., Paruelo, J., Raskin, R. G., Sutton, P., & van den Belt, M. (1997). The value of the world's ecosystem services and natural capital. *Nature, 387*(6630), 253–260. https://doi.org/10.1038/387253a0

Danese, M., & Gioia, D. (2021). Spatial analysis for landscape changes: A bibliometric review. *Applied Sciences, 11*(21), 10078. https://doi.org/10.3390/app112110078

de Groot, R. S., Alkemade, R., Braat, L., Hein, L., & Willemen, L. (2010). Challenges in integrating the concept of ecosystem services and values in landscape planning, management and decision making. *Ecological Complexity, 7*(3), 260–272. https://doi.org/10.1016/j.ecocom.2009.10.006

Díaz, S., Demissew, S., Carabias, J., Joly, C., Lonsdale, M., Ash, N., Larigauderie, A., Adhikari,

J. R., Arico, S., Báldi, A., Bartuska, A., Baste, I. A., Bilgin, A., Brondizio, E., Chan, K. M. A., Figueroa, V. E., Duraiappah, A., Fischer, M., Hill, R., ... Zlatanova, D. (2015). The IPBES conceptual framework—Connecting nature and people. *Current Opinion in Environmental Sustainability, 14*, 1–16. https://doi.org/10.1016/j.cosust.2014.11.002

Dorst, H., van der Jagt, A., Raven, R., & Runhaar, H. (2019). Transitioning towards nature-based solutions: Developing and implementing nature-based solutions in urban contexts. *Sustainability, 11*(17), 4488. https://doi.org/10.3390/su11174488

Etzkowitz, H., & Leydesdorff, L. (2000). The dynamics of innovation: From national systems and "Mode 2" to a Triple Helix of university–industry–government relations. *Research Policy, 29*(2), 109–123. https://doi.org/10.1016/S0048-7333(99)00055-4

García-Díez, V., García-Llorente, M., & González, J. A. (2020). Participatory mapping of cultural ecosystem services in Madrid: Insights for landscape planning. *Land, 9*(8), 244. https://doi.org/10.3390/land9080244

Geneletti, D., Cortinovis, C., Zardo, L., & Esmail, B. A. (2016). Ecosystem services in planning practice: Insights from a survey of spatial planners. *Environmental Impact Assessment Review, 61*, 152–160. https://doi.org/10.1016/j.eiar.2016.08.004

Gullino, P., Beccaro, G. L., & Larcher, F. (2018). Assessing and monitoring the sustainability of rural landscapes through ecosystem services. *Sustainability, 10*(11), 3920. https://doi.org/10.3390/su10113920

Güneralp, B., Huang, C. W., Seto, K. C., & Güneralp, İ. (2018). Global scenarios of urban expansion to 2030 and direct impacts on biodiversity and carbon pools. *Nature Sustainability, 1*(10), 587–595. https://doi.org/10.1038/s41893-018-0153-8

Haase, D., Kabisch, N., Haase, A., & Andersson, E. (2017). Greening cities—To be socially inclusive? About the alleged paradox of society and ecology in cities. *Landscape and Urban Planning, 165*, 1–3. https://doi.org/10.1016/j.landurbplan.2017.04.005

Hansen, R., & Pauleit, S. (2014). From multifunctionality to multiple ecosystem services? A conceptual framework for multifunctionality in green infrastructure planning for urban areas. *AMBIO, 43*(4), 516–529. https://doi.org/10.1007/s13280-014-0510-2

Hessburg, P. F., Spies, T. A., Perry, D. A., Skinner, C. N., Taylor, A. H., Brown, P. M., Stephens, S. L., Larson, A. J., Churchill, D. J., Povak, N. A., Singleton, P. H., McComb, B. C., Zielinski, W. J., Keane, R. E., Franklin, J. F., & Riegel, G. M. (2013). Managing forests for climate change adaptation: A synthesis of science, management, and policy. *Forest Ecology and Management, 310*, 1–4. https://doi.org/10.1016/j.foreco.2013.08.030

IPBES. (2019). *Global assessment report on biodiversity and ecosystem services of the Intergovernmental Science-Policy Platform on Biodiversity and Ecosystem Services*. Brondízio, E. S., Settele, J., Díaz, S., & Ngo, H. T. (Eds.). IPBES Secretariat. https://doi.org/10.5281/zenodo.3831673

Jia, R. (2025). Change-point detection in financial time series using the PELT algorithm: Simulation optimization and empirical analysis. In *Proceedings of the 2025 8th International Conference on Computer Information Science and Artificial Intelligence* (pp. 1051–1057). IEEE

Kabisch, N., Frantzeskaki, N., Pauleit, S., Naumann, S., Davis, M., Artmann, M., Haase, D., Knapp, S., Korn, H., Stadler, J., Zaunberger, K., & Bonn, A. (2016). Nature-based solutions to climate change mitigation and adaptation in urban areas: Perspectives on indicators, knowledge gaps, barriers, and opportunities for action. *Ecology and Society, 21*(2), Article 39. https://doi.org/10.5751/ES-08373-210239

Kabisch, N., Korn, H., Stadler, J., & Bonn, A. (2017a). Nature-based solutions to climate change adaptation in urban areas—Linkages between science, policy and practice. In N. Kabisch, H. Korn, J. Stadler, & A. Bonn (Eds.), *Nature-based solutions to climate change adaptation in urban areas* (pp. 1–11). Springer. https://doi.org/10.1007/978-3-319-56091-5_1

Kabisch, N., Korn, H., Stadler, J., & Bonn, A. (Eds.). (2017b). *Nature-based solutions to climate change adaptation in urban areas.* Springer. https://doi.org/10.1007/978-3-319-56091-5

Kabisch, N., Qureshi, S., & Haase, D. (2015). Human–environment interactions in urban green spaces: A systematic review of contemporary issues and prospects for future research. *Environmental Impact Assessment Review, 50*, 25–34. https://doi.org/10.1016/j.eiar.2014.08.007

Karrasch, L., Klenke, T., & Woltjer, J. (2014). Linking the ecosystem services approach to social preferences and needs in integrated coastal land use management: A planning approach. *Land Use Policy, 38*, 522–532. https://doi.org/10.1016/j.landusepol.2013.12.010

Keesstra, S., Mol, G., de Leeuw, J., Okx, J., de Cleen, M., & Visser, S. (2018). The superior effect of nature-based solutions in land management for enhancing ecosystem services. *Science of the Total Environment, 610–611*, 997–1009. https://doi.org/10.1016/j.scitotenv.2017.08.077

Kumar, P., Debele, S. E., Sahani, J., Aragão, L., Bari-

sani, F., Basu, B., ... & Di Sabatino, S. (2019). Towards an operationalisation of nature-based solutions for natural hazards. *Environment International, 133*, 105181. https://doi.org/10.1016/j.envint.2019.105181

Lennon, M. (2015). Green infrastructure and planning policy: A critical assessment. *Local Environment, 20*(8), 957–980. https://doi.org/10.1080/13549839.2014.880411

Leydesdorff, L., & Rafols, I. (2011). Indicators of the interdisciplinarity of journals: Diversity, centrality, and citations. *Journal of Informetrics, 5*(1), 87–100. https://doi.org/10.1016/j.joi.2010.09.002

Li, F., Zhang, S., Wang, R., & Li, Y. (2022). Landscape planning and sustainability transitions. *Journal of Environmental Management, 301*, 113890. https://doi.org/10.1016/j.jenvman.2021.113890

Lovell, S. T., & Taylor, J. R. (2013). Supplying urban ecosystem services through multifunctional green infrastructure in the United States. *Landscape Ecology, 28*(8), 1447–1463. https://doi.org/10.1007/s10980-013-9912-y

McClymont, K., Morrison, D., Beevers, L., & Carmen, E. (2020). Promoting ecosystem services in planning. *Land Use Policy, 97*, 104741. https://doi.org/10.1016/j.landusepol.2020.104741

Millennium Ecosystem Assessment. (2005). *Ecosystems and human well-being: Synthesis.* Island Press.

Murtagh, F., & Legendre, P. (2014). Ward's hierarchical agglomerative clustering method: Which algorithms implement Ward's criterion? *Journal of Classification, 31*(3), 274–295. https://doi.org/10.1007/s00357-014-9161-z

Nature Index. (2023). *Nature Index 2023: Science cities and institutional collaborations.* Springer Nature.

Nesshöver, C., Assmuth, T., Irvine, K. N., Rusch, G. M., Waylen, K. A., Delbaere, B., ... & Wittmer, H. (2017). The science, policy and practice of nature-based solutions: An interdisciplinary perspective. *Environmental Science & Policy, 77*, 121–134. https://doi.org/10.1016/j.envsci.2017.07.018

Norton, B. A., Coutts, A. M., Livesley, S. J., Harris, R. J., Hunter, A. M., & Williams, N. S. G. (2015). Planning for cooler cities: A framework to prioritise green infrastructure. *Landscape and Urban Planning, 134*, 127–138. https://doi.org/10.1016/j.landurbplan.2014.10.018

Nowak, D. J., Crane, D. E., & Stevens, J. C. (2006). Air pollution removal by urban trees and shrubs in the United States. *Urban Forestry & Urban Greening, 4*(3–4), 115–123. https://doi.org/10.1016/j.ufug.2006.01.007

Ochoa, V., Giampietro, M., Bukkens, S. G. F., & von Maltitz, G. (2020). Ecosystem services and resilience: A framework for integrated assessment. *Ecosystem Services, 42*, 101089. https://doi.org/10.1016/j.ecoser.2020.101089

Opdam, P., Luque, S., Nassauer, J., Verburg, P. H., & Wu, J. (2018). How can landscape ecology contribute to sustainability science? *Landscape Ecology, 33*(1), 1–7. https://doi.org/10.1007/s10980-018-0610-7

Pamukcu-Albers, P., Ugolini, F., La Rosa, D., Grădinaru, S. R., & Azevedo, J. C. (2021). Building urban resilience through nature-based solutions: How can urban planning contribute? *Urban Climate, 37*, 100855. https://doi.org/10.1016/j.uclim.2021.100855

Pataki, D. E., Carreiro, M. M., Cherrier, J., Grulke, N. E., Jennings, V., Pincetl, S., Pouyat, R. V., Whitlow, T. H., & Zipperer, W. C. (2011). Coupling biogeochemical cycles in urban environments: Ecosystem services, green solutions, and misconceptions. *Frontiers in Ecology and the Environment, 9*(1), 27–36. https://doi.org/10.1890/090220

Rafols, I., & Meyer, M. (2010). Diversity and network coherence as indicators of interdisciplinarity: Case studies in bionanoscience. *Scientometrics, 82*(2), 263–287. https://doi.org/10.1007/s11192-009-0041-y

Raymond, C. M., Frantzeskaki, N., Kabisch, N., Berry, P., Breil, M., Nita, M. R., Geneletti, D., & Calfapietra, C. (2017). A framework for assessing and implementing the co-benefits of nature-based solutions in urban areas. *Environmental Science & Policy, 77*, 15–24. https://doi.org/10.1016/j.envsci.2017.07.008

UNESCO. (2022). *UNESCO science report: The race against time for smarter development.* UNESCO Publishing.

Salmond, J. A., Tadaki, M., Vardoulakis, S., Arbuthnott, K., Coutts, A., Demuzere, M., ... & Wheeler, B. W. (2016). Health and climate related ecosystem services provided by street trees. *Environmental Health Perspectives, 124*(8), 1263–1273. https://doi.org/10.1289/EHP238

Seddon, N., Chausson, A., Berry, P., Girardin, C. A. J., Smith, A., & Turner, B. (2020). Understanding the value and limits of nature-based solutions to climate change and other global challenges. *Philosophical Transactions of the Royal Society B: Biological Sciences, 375*(1794), 20190120. https://doi.org/10.1098/rstb.2019.0120

Seddon, N., Turner, B., Berry, P., Chausson, A., & Girardin, C. A. J. (2019). Grounding nature-based climate solutions in sound biodiversity science. *Nature Climate Change, 9*(2), 84–87. https://doi.org/10.1038/s41558-019-0405-0

Shackleton, S. (2022). Transforming climate science and practice: How can co-production research improve the use of climate information in

decision-making? *Climate and Development, 14*(8), 745–758. https://doi.org/10.1080/17565529.2021.1982563

Shokry, G., Connolly, J. J. T., Anguelovski, I., & Dobbie, M. (2020). Nature-based solutions and resilience: A systematic review. *Sustainability, 12*(24), 10265. https://doi.org/10.3390/su122410265

TEEB. (2010). *The economics of ecosystems and biodiversity: Mainstreaming the economics of nature: A synthesis of the approach, conclusions and recommendations of TEEB.* Progress Press.

Turnhout, E., Metze, T., Wyborn, C., Klenk, N., & Louder, E. (2020). The politics of co-production: Participation, power, and transformation. *Current Opinion in Environmental Sustainability, 42*, 15–21. https://doi.org/10.1016/j.cosust.2019.11.009

Pauna, V. H., Picone, F., Le Guyader, G., Buonocore, E., & Franzese, P. P. (2018). The scientific research on ecosystem services: A bibliometric analysis. *Ecological Questions, 29*(3), 1–10. https://doi.org/10.12775/EQ.2018.022

Vazin, F., Chan, D. W. M., Hanaee, T., & Sarvari, H. (2024). Nature-based solutions and climate resilience: A bibliographic perspective through science mapping analysis. *Buildings, 14*(6), 1492. https://doi.org/10.3390/buildings14061492

Wagner, C. S., Whetsell, T. A., & Leydesdorff, L. (2017). Growth of international collaboration in science: Revisiting six specialties. *Scientometrics, 110*(3), 1633–1652. https://doi.org/10.1007/s11192-016-2230-9

Zhou, W. (2017). Integrating urban green infrastructure with spatial planning for sustainable cities: A review. *Landscape and Urban Planning, 158*, 62–75. https://doi.org/10.1016/j.landurbplan.2016.10.013

INTERNATIONAL SCIENTIFIC JOURNAL | GEOGRAPHICA PANNONICA | Volume 30, Issue 2, 123–135(June 2026)
Journal homepage: http://www.dgt.uns.ac.rs/en/homepage/pannonica/

Analysis of Concentration and Seasonality of Precipitation in Recife - Pernambuco, Brazil

Lidiane da Silva Araújo[A], Antonio Samuel Alves da Silva[A], Rodrigo Luiz Costa Cavalcanti[A], Thiago Matheus Paiva do Passo[A], Matheus Dias Aguiar[A], Rosendo Chagas de Albuquerque[A], Ivana Tošić[B*], Tatijana Stosic[A]

[A]*Departamento de Estatística e Informática, Universidade Federal Rural de Pernambuco, Rua Dom Manoel de Medeiros s/n, Dois Irmãos, 52171-900 Recife/PE, Brazil; ORCID LdSA: 0000-0001-7160-4379; ASAdS: 0000-0002-8759-0036; TMPdP: 0000-0002-4569-374X; MDA: 0000-0002-8146-6536; TS: 0000-0002-5691-945X*

[B]*Faculty of Physics-University of Belgrade, Institute for Meteorology; 0000-0002-7259-8828*

Received: February 6, 2026| Revised: June 24, 2026| Accepted: June 27, 2026
doi: 10.5937/gp30-64717

ABSTRACT

This study investigates the variability of precipitation distribution and rainfall seasonality regime in Recife-PE, Brazil, using the Precipitation concentration index (PCI) and Seasonality indices (SI). PCI was calculated on annual (PCI_a), seasonal (PCI_s), and supra-seasonal (PCI_{ss}) scales for the period 1962-2020. Rainfall seasonality regime classification was performed using the individual seasonality index $(\overline{SI_i})$, the general seasonality index (SI), and the replicability index (RI). The PCI_a time series revealed precipitation distribution ranging from moderate (79.66% of the years) and irregular, with mean value of $\overline{PCI_a} \approx 13.58$. Seasonality analysis indicated a mean rainfall regime classified as rather seasonal with a short drier season $(\overline{SI} \approx 0.56)$, and a high degree of replicability $(RI = 0.85)$, characterized by maximum rainfall concentrated in a few months and limited interannual variability in SI_i values. Trend analysis using the Mann-Kendall test and Sen's slope estimator showed no significant trends in the time series of PCI and SI_i, except for spring (PCI_s), which exhibited a significant negative trend. A Spearman correlation analysis between SI_i and PCI_a yielded a strong positive correlation ($\rho = 0.86$), reinforcing the link between precipitation concentration and seasonality structure.

Keywords: Seasonality index; Precipitation concentration index; Recife; Brazil

Introduction

Northeastern Brazil (NEB) exhibits pronounced spatiotemporal variability in rainfall, directly affecting agriculture, water resources, urban infrastructure, human health, and the vegetation structure of local biomes (Marengo et al., 2022; de Medeiros et al., 2022; da Silva et al., 2021; de Oliveira Souza et al., 2018). Rainfall in NEB is highly seasonal, with the peak of the rainy season typically occurring between February and April, primarily driven by the influence of the Atlantic Intertropical Convergence Zone (ITCZ) and the South American Monsoon System (SAMS). Superimposed on this seasonal cycle is pronounced interannual variability, marked by episodes of excessive rainfall and severe droughts. These fluctuations are closely linked to large-scale ocean–atmosphere phenomena, particularly the El Niño–Southern Oscillation (ENSO). Generally, the negative phase of ENSO (La Niña) is associated with above-average rainfall in NEB, while the positive

*Corresponding author: Ivana Tošić; e-mail: itosic@ff.bg.ac.rs

phase (El Niño) tends to suppress precipitation, often resulting in prolonged and severe droughts across the region (Hänsel et al., 2016).

Rainfall is highest along the coastal and forested zones (*Mata Atlântica*), making urban centers in these areas especially vulnerable to extreme precipitation events. Such events frequently result in flash floods, infrastructure disruption, increased incidence of waterborne diseases, and, in severe cases, loss of human life (Rodrigues et al., 2021).

Recife, the capital of the state of Pernambuco in Northeastern Brazil (NEB), is a coastal city that exemplifies the region's vulnerability to hydrometeorological extremes. Characterized by a humid tropical climate, Recife receives high annual rainfalls, concentrated mainly during the austral autumn and winter months (March to August), followed by a markedly drier season (Coutinho et al., 2016). This uneven distribution contributes to natural disasters such as floods and landslides (Nóbrega et al., 2023; Marengo et al., 2023), posing significant challenges for urban infrastructure, public health, and water resource management.

Several studies have addressed the impacts of rainfall variability in Recife. Pereira et al. (2025) investigated slope stability in the Nova Descoberta neighborhood using a geological-geotechnical planialtimetric model that incorporated extreme rainfall events and anthropogenic pressures. Their findings revealed that rainfall infiltration significantly compromised slope stability, while the use of plastic tarps failed to meet safety standards. Oliveira et al. (2014) analyzed water quality in the Apipucos Reservoir, located in Recife's western zone, and reported elevated concentrations of cyanobacteria during the dry season, indicating seasonal stress on aquatic ecosystems. Borges et al. (2024) examined the relationship between precipitation and confirmed dengue cases, identifying a direct correlation: the highest incidence occurred during the rainy season, with a marked decline during the dry months.

Given these diverse impacts, it is essential to investigate the temporal variability of precipitation, particularly its seasonality and concentration throughout the year. Understanding these patterns is critical for developing effective mitigation strategies and enhancing urban resilience in Recife's rapidly evolving socio-environmental landscape.

Two indices are widely recognized for their effectiveness in characterizing precipitation distribution and provide complementary insights: the Seasonality Index (SI) and the Precipitation Concentration Index (PCI). The SI quantifies the degree to which rainfall is concentrated in specific months, capturing the seasonal dynamics of precipitation regimes (Walsh & Lawler, 1981). In contrast, the PCI measures the irregularity of monthly rainfall distribution throughout the year, highlighting temporal concentration and potential extremes (Oliver, 1980). Together, these indices provide a robust framework for evaluating rainfall patterns and their implications for flood risk, drought vulnerability, and climate adaptation planning.

Both SI and PCI have been applied in diverse climatological contexts, including the assessment of rainfall concentration in river basins (Yang et al., 2020; Sa'adi et al., 2023), validation of general circulation models (Doyle, 2020), and evaluation of climate change impacts on precipitation regimes (Stosic et al., 2024).

Despite Recife's well-documented vulnerability to hydrometeorological extremes, no studies have systematically assessed rainfall seasonality and concentration using long-term datasets and standardized indices. Recently, PCI and SI were analyzed across the entire state of Pernambuco. The results showed that, compared to other regions, the Recife Metropolitan Area exhibited the lowest PCI values (indicating moderately seasonal distribution) (Silva et al., 2022) and the lowest SI values, classifying the rainfall regime as moderately seasonal, with a short dry season (da Silva Araújo et al., 2023).

The present study aims to fill a literature gap by analyzing the temporal patterns of SI and PCI in Recife using historical rainfall records. Specifically, we seek to: (i) characterize the seasonal structure of rainfall; (ii) identify trends and anomalies in rainfall concentration and seasonality; and (iii) discuss the implications for urban planning and climate adaptation in Recife.

Materials and Methods

Study area and data

Recife, the capital of Pernambuco state, is located on the eastern coast of Northeastern Brazil (NEB), near 8°S latitude and 34°W longitude (Fig. 1). It is one of the most densely populated urban centers in NEB, with over 1.5 million inhabitants. Geographically, Recife is a coastal city, about 2.5–5 m above sea level, in a region comprised of the Atlantic Rainforest Biome (Marengo et al., 2023).

The climate is humid tropical (Köppen classification: Am), characterized by high temperatures and relative humidity throughout the year, with a rainy season from March to August. Average annual precipitation is between 1,800 and 2,300 mm, with rainfall concentrated in a few months, contributing to frequent urban flooding and drainage challenges. The city's climatology is influenced by multiple atmospheric systems, including the Intertropical Convergence Zone (ITCZ), Easterly Wave Disturbances (EWD), High-Level Cyclonic Vortices (HLCV), and the South Atlantic Subtropical High (SASH), as well as ocean–atmosphere interactions such as ENSO and the Atlantic SST gradient (Borges et al., 2024).

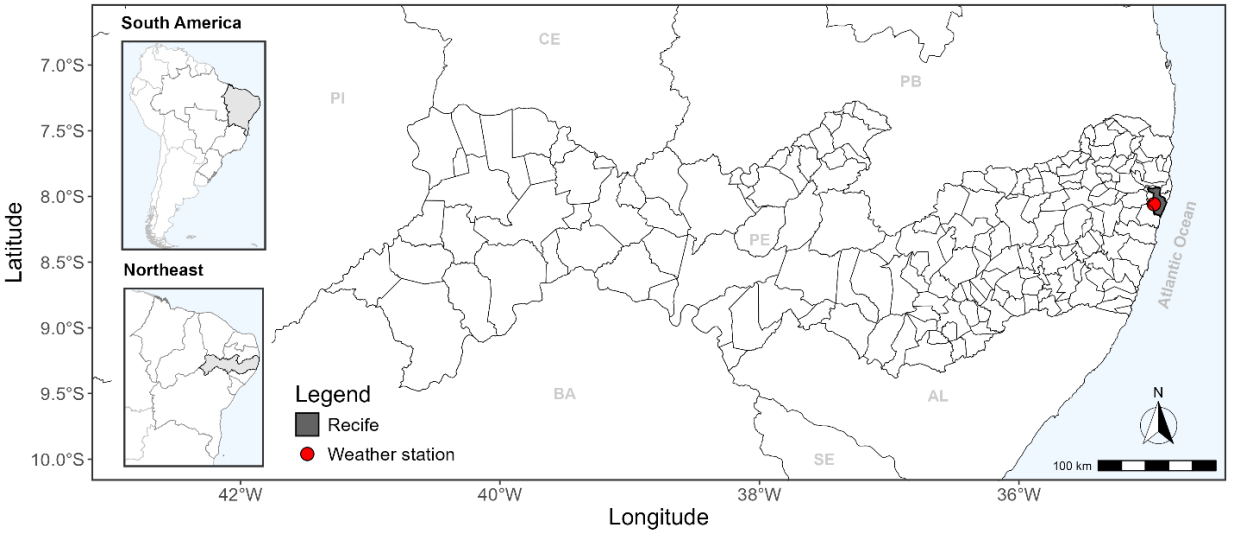

Figure 1. Map of Brazil showing the location of Pernambuco State and the Recife weather station.

The data used in this study consist of monthly accumulated precipitation records from the Curado weather station in Recife (latitude: 8.03°S, longitude: 34.55°W; altitude: 7 m), spanning the period from July 1961 to December 2020. These records were obtained from the National Water Agency (Agência Nacional de Águas – ANA, 2025).

Methods

Precipitation Concentration Index

The Precipitation Concentration Index (PCI), introduced by Oliver (1980) quantifies the degree to which annual precipitation is distributed over 12 months of the year. It is defined as:

$$PCI_a = \left[\left(\sum_{i=1}^{12} p_i^2\right) \Big/ \left(\sum_{i=1}^{12} p_i\right)^2\right] \times 100,$$

where p_i represents the monthly precipitation in month i. When applied to the full annual dataset, it results in one time series representing annual PCI values. Theoretically, PCI values range from 8.33 (indicating uniform monthly precipitation) to 100 (indicating that all annual precipitation occurs in a single month).

PCI can also be calculated for each season of year using:

$$PCI_s = \left[\left(\sum_{i=1}^{3} p_i^2\right) \Big/ \left(\sum_{i=1}^{3} p_i\right)^2\right] \times 25,$$

which produces four time series, one for each season: summer (Dec - Jan - Feb), autumn (Mar - Apr - May), winter (Jun - Jul - Aug) and spring (Sep - Oct - Nov). The theoretical range for seasonal PCI values is 8.33 to 25, with higher value indicating that total precipitation occurs within a single month of the season.

Additionally, PCI can be calculated on a supra-seasonal scale, distinguishing between wet and dry periods (De Luis et al., 2011):

$$PCI_{ss} = \left[\left(\sum_{i=1}^{6} p_i^2\right) \Big/ \left(\sum_{i=1}^{6} p_i\right)^2\right] \times 50$$

which produces two time series, one for the wet season (March to August) and another for the dry season (September to February). Theoretical values range from 8.33 to 50. The higher value is obtained when total precipitation occurs within a single month of the season.

The classification of rainfall regime based on PCI values is presented in Table 1.

Table 1. Classification of the precipitation distribution based on Precipitation Concentration Index values (Oliver, 1980).

Precipitation distribution	Class	PCI
Uniform	I	[8.33, 10]
Moderate	II	(10, 15]
Irregular	III	(15, 20]
Strongly irregular	IV	(20, PCI_{MAX}*]

*Maximum possible values of PCI are equal to 100 (for PCI_a), 25 (for PCI_s), 50 (for PCI_{ss}).

Seasonality index

To assess rainfall seasonality and its interannual variability, three complementary indices are used: the general seasonality index *(denoted as $\overline{SI}$)* , the individual seasonality index *(SI_i)*, and the replicability index *(RI)*. Their definitions and interpretations are outlined below, following the methodology of (Walsh & Lawler, 1981).

The general seasonality index $(\overline{SI})$ quantifies the average deviation of monthly precipitation from a uniform distribution over the entire study period. It is defined as:

$$\overline{SI} = \frac{1}{\overline{P}} \sum_{n=1}^{12} \left| \overline{p_n} - \frac{\overline{P}}{12} \right|,$$

where $\overline{p_n} = \frac{1}{N}\sum_{i=1}^{N} p_{in}$ is the mean precipitation in month n over N years, $\overline{P} = \frac{1}{N}\sum_{i=1}^{N} P_i$, is the mean annual precipitation, p_{in} is the precipitation in month n of year i and P_i is the total annual precipitation in year i. Theoretically $\overline{SI}$ ranges from 0 (uniform monthly distribution) to approximately 1.83 (total annual precipitation occurs in a single month). The classification of rainfall regime based on $\overline{SI}$ is presented in Table 2.

Individual seasonality index SI_i is defined as

$$SI_i = \frac{1}{P_i} \sum_{n=1}^{12} \left| p_{in} - \frac{P_i}{12} \right|,$$

where p_{in} is the precipitation amount in month n and year i and $P_i = \sum_{n=1}^{12} p_{in}$ the total precipitation in year $i = 1,...,N$ (N is the number of years of the analyzed period). This index is designed to assess the variability of the rainfall regime year-to-year. The values of SI_i vary from zero (when the same amount of monthly precipitation p_{in} occurs in each month) to 1.83 (when total annual precipitation occurs in a single month).

Mean individual seasonality index $\overline{SI_i}$ is obtained by averaging the values of SI_i over the analyzed period:

$$\overline{SI_i} = \frac{1}{N} \sum_{i=1}^{N} SI_i,$$

Table 2. Rainfall regimes classification based on $\overline{SI}$ classes (Walsh & Lawler, 1981).

Rainfall regime	Class	SI
Very equitable	I	≤ 0.19
Equitable with a definite wetter season	II	(0.19, 0.39]
Rather seasonal with a short drier season	III	(0.39, 0.59]
Seasonal	IV	(0.59, 0.79]
Markedly seasonal with a long drier season	V	(0.79, 0.99]
Most rain in a maximum 3 months or less	VI	(0.99, 1.19]
Extreme seasonality, almost all rain in 1-2 months	VII	> 1.19

where N is the number of years of the considered period and SI_i is the individual seasonality index of year i.

Replicability Index RI is defined as the ratio between the general seasonality index and the mean individual seasonality index:

$$RI = \frac{\overline{SI}}{\overline{SI_i}}$$

This index quantifies the degree of variability in rainfall regimes over time. The averages $\overline{p_n}$ and $\overline{P}$ used to calculate $\overline{SI}$, smooth out interannual fluctuations in monthly precipitation, thereby underestimating year-to-year seasonality. As a result, $\overline{SI} \leq \overline{SI_i}$, if the mean precipitation regime were identical each year, with consistent months of maximum and minimum rainfall, then $RI = 1$, indicating perfect replicability $(\overline{SI} = \overline{SI_i})$. In practice, a high RI implies that the month of maximum rainfall is concentrated within a narrow temporal window, reflecting a highly replicable rainfall regime. Conversely, a low RI suggests that the peak rainfall month varies widely across years, indicating low replicability in seasonal patterns (Walsh & Lawler, 1981; Livada & Asimakopoulos, 2005).

The modified Mann-Kendall (MMK) test

In this study we applied the Mann-Kendall test modified by effective sample size (MMK), as proposed by Yue & Wang (2004), to detect trends in serially correlated hydrological series. Compared to the classical Mann–Kendall (MK) test (Kendall, 1975; Mann, 1945), the MMK approach effectively reduces bias introduced by autocorrelations, while preserving the original MK test's robustness, non-parametric and distribution-free properties. A detailed description of the MMK procedure is provided in (Stosic et al., 2024), and all the calculations were performed using open-source software tools (Patakamuri & O'Brien, 2021; R Core Team, 2023).

Results and Discussion

Seasonal analysis

Figure 2 shows the annual precipitation values alongside the long-term mean. Periods of below-average rainfall are evident during major drought episodes in NEB, in 1979–1981, 1982–1983, 1992–1993, 1997–1998, 2010, and 2012–2016 (Marengo et al., 2017). In contrast, above-average precipitation observed in 2000 and 2011 coincides with La Niña events, which are typically associated with increased rainfall in the region (CPTEC/INPE, 2025).

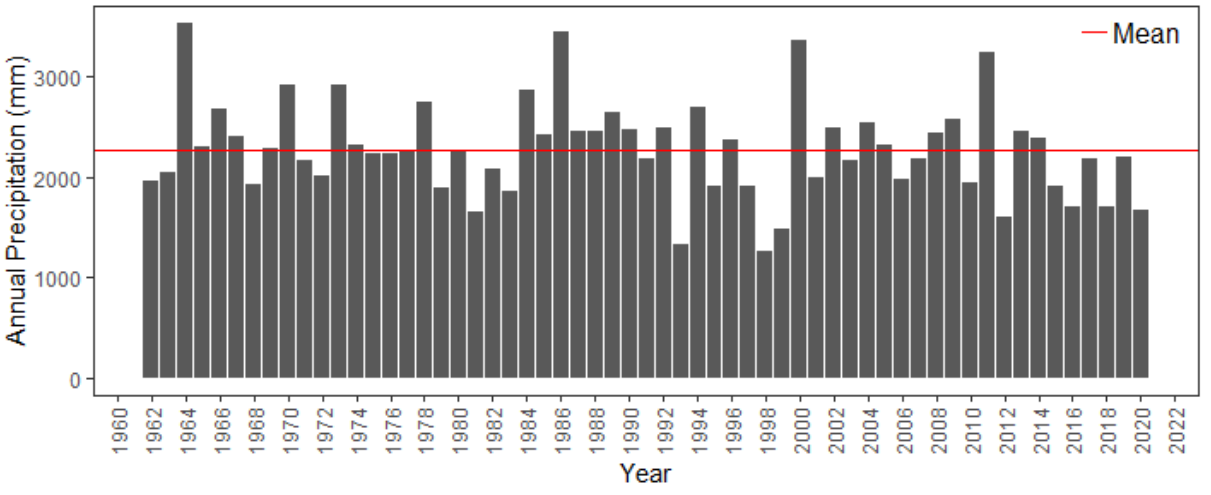

Figure 2. Annual precipitation totals for the period January 1962 to December 2020. The long-term mean of 2,270.9 mm is indicated by the red line.

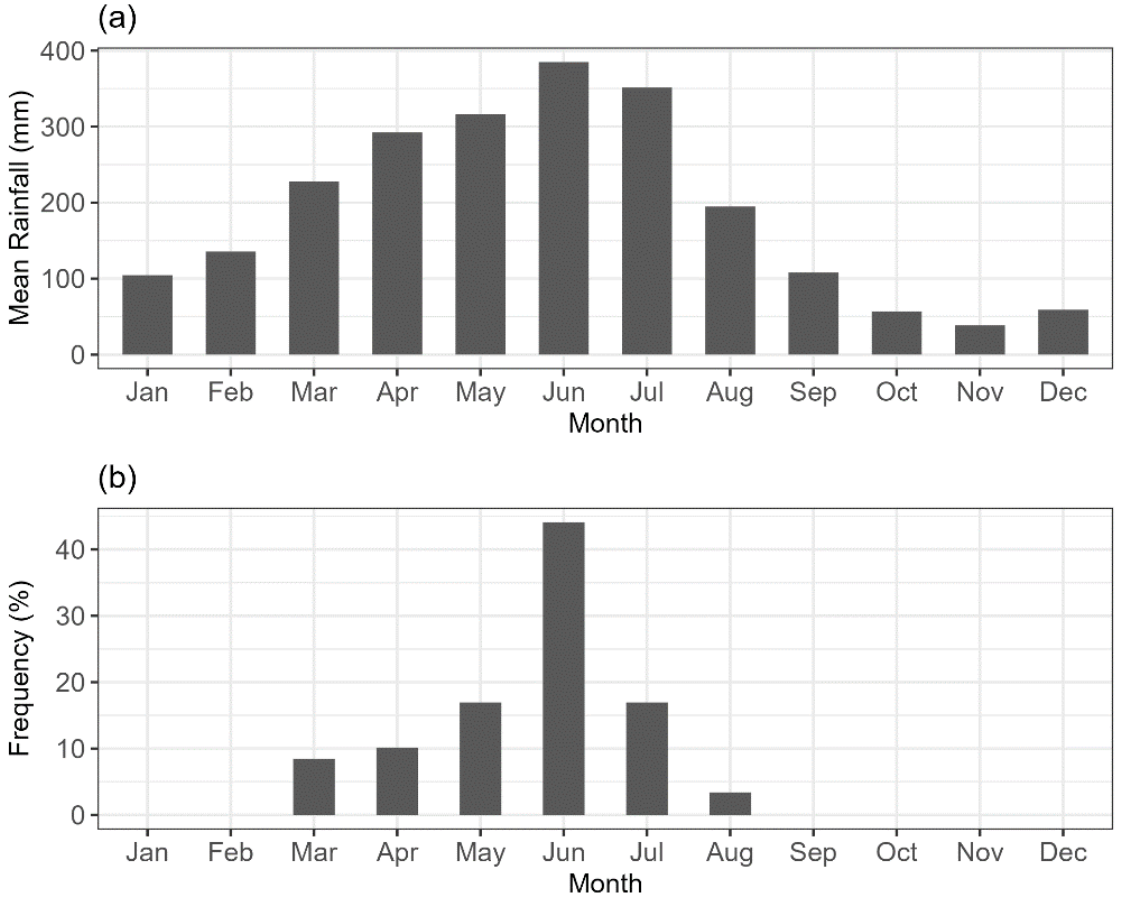

Figure 3. (a) Mean monthly precipitation for the period from 1962 to 2020, (b) Percentage frequency of the month with maximum rainfall between 1962 and 2020.

The mean monthly precipitation and the percentage frequency of the month with maximum precipitation are presented in Figure 3.

Figure 3a shows that the wet season extends from March to August, corresponding to the six months with the highest mean monthly precipitation. During this period, an average of approximately 1,769 mm is accumulated, representing about 78% of the annual mean (2,270.9 mm). The trimester October–November–December, on the other hand, exhibited the lowest mean rainfall, with only about 154 mm accumulated. The wettest period is further confirmed in Figure 3b, which indicates that, from 1962 to 2020, the months of maximum rainfall occurred exclusively between March and August, with the highest frequency in June (over 40% of all years).

Precipitation concentration index

Figures 4–6 show the time series of the Precipitation Concentration Index (PCI) at three temporal scales for 1962–2020: annual (Fig. 4), seasonal (Fig. 5), and supra-seasonal (Fig. 6). In each graph, dashed lines indicate the four PCI classification categories defined in Table 1: uniform (I), moderate (II), irregular (III), and strongly irregular (IV) precipitation distribution.

Annual scale

Figure 4 shows the results of the Precipitation Concentration Index on an annual scale *(PCI_a)* for the period 1962–2020. The precipitation distribution is predominantly classified as moderate (Class II), with a mean value of approximately $\overline{PCI_a} \approx 13.58$, although occasional irregular events are observed. The most irregular precipitation distribution, indicated by the highest annual PCI value (PCI_a= 17.78, Class III), occurred in 2005, when severe drought occurred in the Northeast region (Marengo et al., 2017). The three consecutive years 2015, 2016, and 2017, with irregular precipitation distribution, belong to the period of the multiyear drought (2011–2017) in the Northeast, which was the most extreme in decades (Cunha et al., 2019).

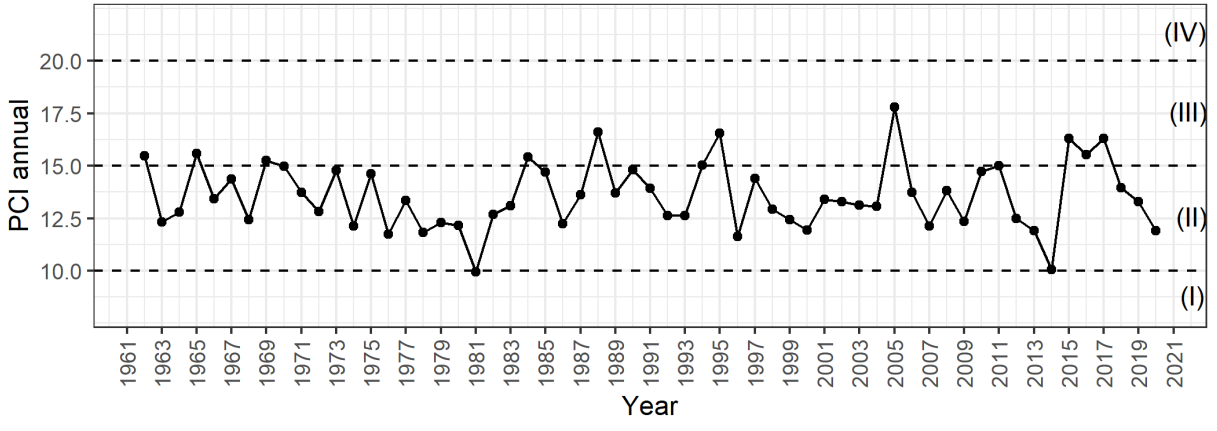

Figure 4. Time series of the precipitation concentration index on annual scale *(PCI_a)* for the period between 1962 and 2020. Dashed lines delimit the classes of the precipitation distribution (I: uniform, II: moderate, III: irregular, IV: strongly irregular) as defined in Table 1.

Seasonal scale

Figure 5 presents the seasonal time series of the Precipitation Concentration Index *(PCI_s)*. In summer (Figure 5a), for most of the period, precipitation had a moderate distribution (Class II). Irregular distribution (Class III) occurred in only five years: 1962, 1965, 1980, 2006, and 2009, with the highest PCI_s value recorded in 1965 (PCI_s = 18.3). The remaining years mainly fell into the uniform distribution category (Class I), with the lowest PCI_s value of 8.4 in 2015.

Between 2012 and 2020, the range of PCI_s values narrowed significantly, from a minimum of 8.41 in 2015 to a maximum of 10.62 in 2013, indicating a marked reduction in variability. This pattern suggests that, after 2011, the summer season maintained a relatively stable and regular precipitation regime, trending towards or remaining within the uniform distribution class.

Figures 5b and 5c show the seasonal PCI time series for autumn and winter, respectively. Both seasons exhibit similar behavior, with precipitation distributions mainly falling between uniform (Class I) and moderate (Class II). The highest PCI_s value for autumn was recorded in 2005 (PCI_s = 12.9), while for winter it occurred in 1965 (PCI_s = 12.7), both identified as drought years in NEB (Marengo et al., 2017). A notably stable period is observed in the autumn PCI_s series from 1976 to 1981, characterized by consistently uniform precipitation distribution and a narrow range of PCI_s values. These results are expected, as the period from March to August, which overlaps with the autumn and winter seasons in Recife, corresponds to the region's wet season, thereby contributing to a more evenly distributed rainfall pattern.

Figure 5d presents the PCI time series for the spring season. The values of PCI_s indicate precipitation distributions ranging between uniform (Class I) and irregular (Class III), with a predominance of years classified as moderate (Class II). Notably, clusters of similar PCI_s values are observed during 1985–1987, 1997–1999, and 2004–2006, suggesting periods of relative stability in rainfall distribution. From 2001 to 2020, the precipitation regime remained consistently within Class I and Class II, indicating a sustained trend toward uniform to moderately distributed rainfall during spring in the latter part of the study period.

Supra-seasonal scale

Figure 6 presents the time series of the Precipitation Concentration Index on a supra-seasonal scale (PCI_{ss})

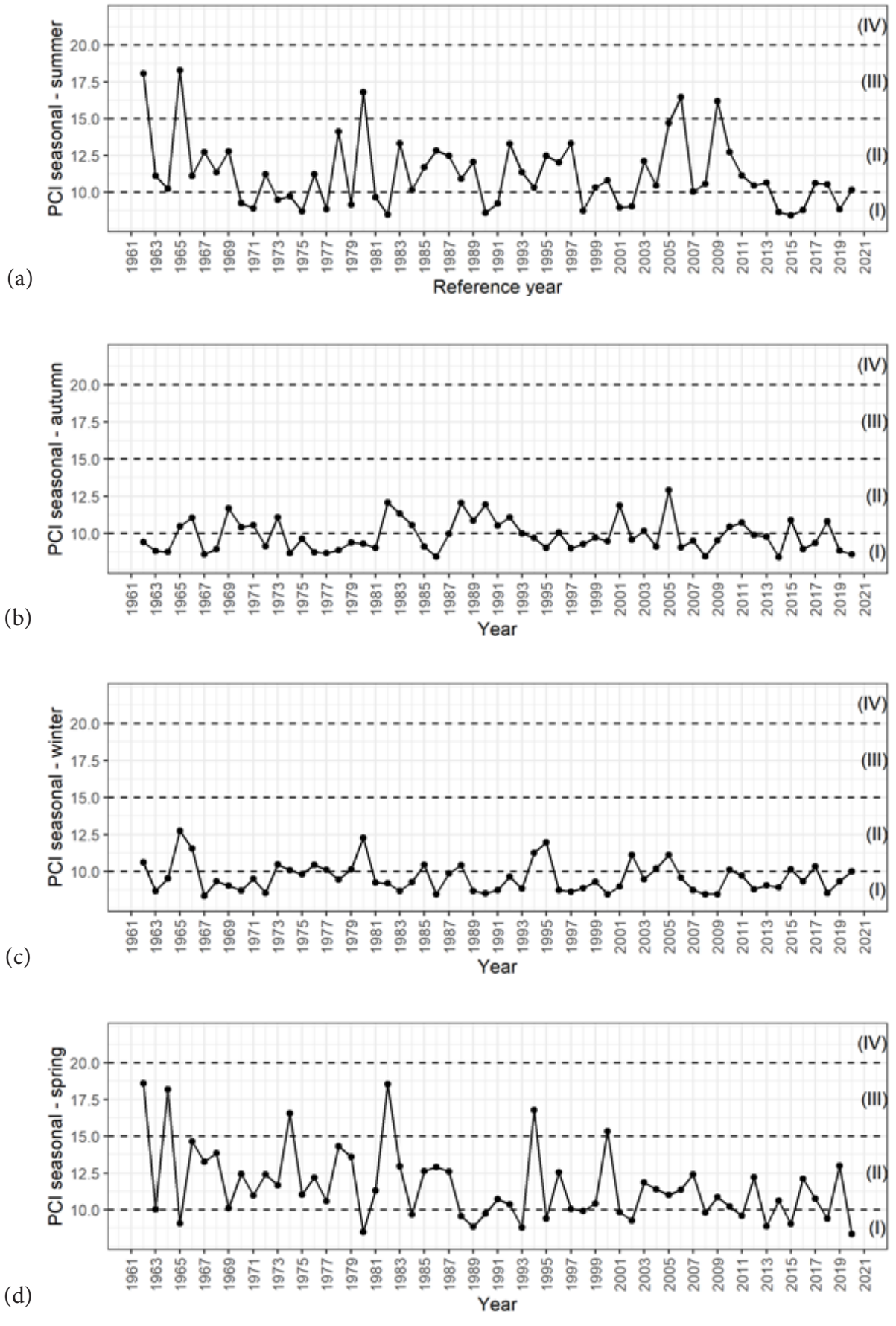

Figure 5. Time series of the precipitation concentration index on a seasonal scale (PCI_s) for the period between 1962 and 2020: (a) summer (Dec - Jan - Feb), (b) autumn (Mar - Apr - May), (c) winter (Jun - Jul - Aug), (d) spring (Sep - Oct - Nov). Dashed lines indicate the thresholds between the precipitation distribution classes (I: uniform, II: moderate, III: irregular, and IV: strongly irregular) as defined in Table 1.

for the period 1962–2020. The supra-seasonal classification distinguishes the wet season (March to August) from the dry season (September to February). The results reveal a clear separation between the two regimes, with blue dots representing the wet season and red dots the dry season.

During the wet season, precipitation concentration generally ranged between uniform (Class I) and moderate (Class II). The lowest PCI_{ss} value (8.5) was recorded in 2008, coinciding with a La Niña episode, which typically brings increased rainfall to Northeastern Brazil (NEB) (CPTEC/INPE, 2025).

In contrast, the dry season showed a more variable precipitation distribution, predominantly within the moderate category (Class II). Uniform distribution (Class I) was observed in only three years: 1981 (PCI_{ss}= 9.26), 1990 ($PCIss$ = 8.80), and 2014 (PCI_{ss} = 8.83). Notably, 2009 stands out with a strongly irregular distribution (Class IV), marked by the highest $PCIss$ value of 21.68, indicating a highly concentrated and uneven rainfall pattern during that dry season, which could be related to the El Niño episode in 2009–2010 (CPTEC/INPE, 2025).

Table 3 shows the percentage of years classified in each PCI distribution class across different temporal scales for 1962–2020. Notably, no years showed a strongly irregular precipitation distribution (Class IV), except for one year (1.69%) during the dry season. Similarly, irregular distribution (Class III) was absent in the wet season, autumn, and winter, indicating a predominance of moderate (Class II) and uniform (Class I) rainfall patterns across these scales.

The highest percentage of years with moderate precipitation distribution (Class II) was observed on the annual scale and during the dry season, both at 79.66%. In contrast, the lowest percentage of moderate distribution occurred in winter (32.20%), when precipitation was predominantly uniform (Class I) in 67.8% of the years, representing the highest frequency of uniform distribution across all scales. Conversely, the annual scale showed the lowest frequency of uniform distribution, with only one year (1.69%) classified as Class I.

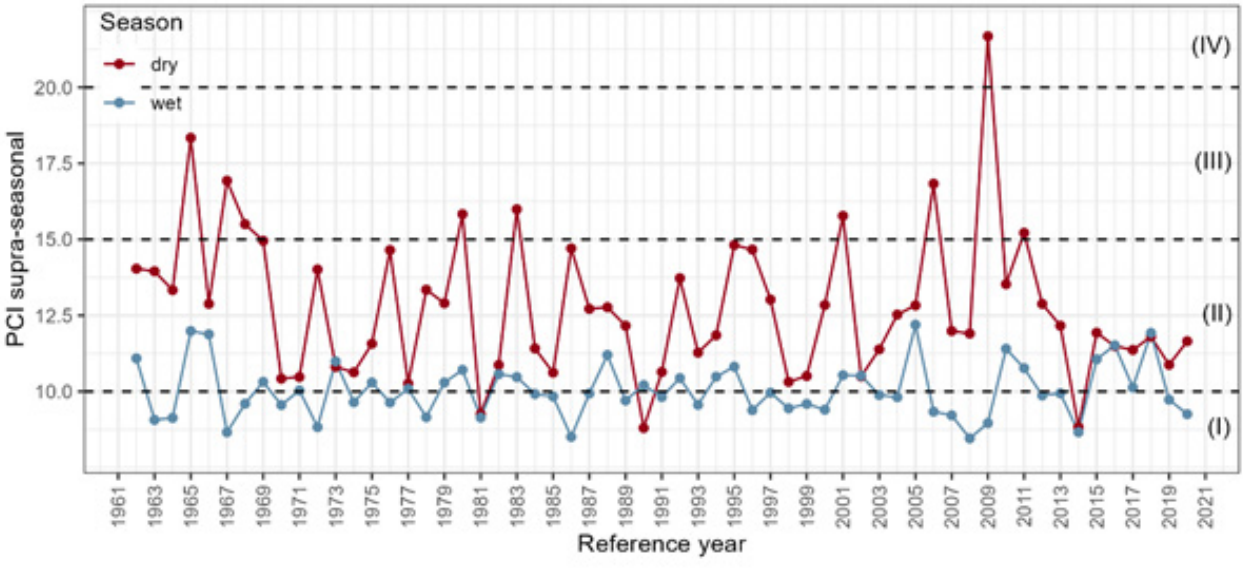

Figure 6. Time series of the Precipitation Concentration Index on a supra-seasonal scale (PCI_{ss}). Dashed lines indicate the thresholds between the precipitation distribution classes (I: uniform, II: moderate, III: irregular, and IV: strongly irregular), as defined in Table 1.

To investigate potential trends and their magnitudes in the PCI time series at annual (Fig. 4), seasonal (Fig. 5), and supra-seasonal (Fig. 6) scales, the Mann-Kendall test and Sen's slope estimator were applied. The results are summarized in Table 4. Based on the p-value (pv), no statistically significant trends were detected, except for the spring season, which exhibited a significance level below 1%. The negative sign of Q_{med} (or Z) indicates a downward trend, with a Sen's slope magnitude of $Q_{med} = 0.0466$.

Spring corresponds to the dry season in Recife, and this negative trend suggests a gradual shift towards a more uniform rainfall distribution, potentially indicating a reduced risk of drought events during this period.

Table 3. Percentage of years in each class of precipitation distribution according to the Precipitation concentration index (PCI) on annual (PCI_a, Fig.4), seasonal (PCI_s, Fig.5), and supra-seasonal (PCI_{ss}, Fig.6) scales.

Class of precipitation distribution (based on PCI)	Annual (%)	Seasonal (%)				Supra-seasonal (%)	
		Summer (Dec-Feb)	Autumn (Mar-May)	Winter (Jun-Aug)	Spring (Sep-Nov)	Dry (Sep-Feb)	Wet (Mar-Aug)
I – Uniform	1.69	30.51	61.02	67.8	28.81	5.08	55.93
II – Moderate	79.66	61.02	38.98	32.2	61.02	79.66	44.07
III – Irregular	18.64	8.47	0	0	10.17	13.56	0
IV – Strongly irregular	0	0	0	0	0	1.69	0

Table 4. Results of the Mann-Kendall test (significance level α = 5%) and Sen's slope estimator applied to the Precipitation Concentration Index (PCI) time series on annual (PCI_a; Fig. 4), seasonal (PCI_s; Fig. 5) and supra-seasonal (PCI_{ss}; Fig. 6) scales.

Timescale	Mann-Kendall test			Sen's slope
	p-value (*pv*)	*Z*	Trend test	Q_{med}
Annual PCI_a	0.9583	-0.0523	Negative non-significant	-0.001
Seasonal PCI_s				
Summer (Dec - Feb)	0.2189	-1.2294	Negative non-significant	-0.0169
Autumn (Mar - May)	0.9896	0.0131	Positive non-significant	6.83E-05
Winter (Jun - Aug)	0.4403	-0.7717	Negative non-significant	-0.0057
Spring (Sep - Nov)	0.0042	-2.8643	Negative significant	-0.0466
Supra-seasonal PCI_{ss}				
Dry season (Sep - Feb)	0.1779	-1.3471	Negative non-significant	-0.0255
Wet season (Mar - Aug)	0.824	0.2223	Positive non-significant	0.0021

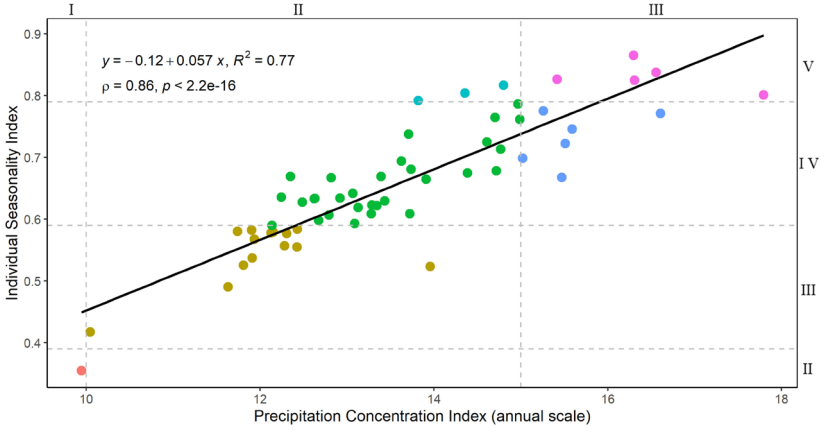

Figure 8. Scatter diagram of the individual seasonality index (SI_i) plotted against the annual Precipitation Concentration Index (PCI_a), including the linear regression line (black). Each color represents a distinct pair of corresponding rainfall regime classes (based on SI_i) and precipitation distribution classes (based on PCI_a) that occurred simultaneously in the same year.

Seasonality index

Figure 7 presents the time series of the individual seasonality index SI_i with dashed lines marking the thresholds between rainfall regime classes as defined in Table 2. The results indicate year-to-year variability mainly between Class III (rather seasonal with a short drier season) and Class V (markedly seasonal with a long drier season). Of the 59 years analyzed, 36 years (61.02%) fell into Class IV (seasonal), 14 years (23.73%) into Class III, and 8 years (13.56%) into Class V, resulting in an average $\overline{SI_i} \approx 0.66$, which corresponds to Class IV. An exception occurred in 1981, when the SI_i value of 0.35 placed the year in Class II, indicating a more equable rainfall regime with a definite wetter season.

The general seasonality index ($\overline{SI} \approx 0.56$) indicates that the mean rainfall regime in Recife over the entire period (1962–2020) was fairly seasonal with a short dry season, corresponding to Class III, but close to the threshold between Classes III and IV. As previously noted, it is expected that $\overline{SI_i} > \overline{SI}$, since the formulation of the general index tends to smooth interannual variability, thereby underestimating year-to-year seasonality.

The Mann-Kendall test applied to the SI_i time series (Fig. 7) revealed no statistically significant trend *(pv ~ 0.92)* at the α = 5% significance level. This result indicates that the annual rainfall regime in Recife continues to oscillate between Class III (rather seasonal with a short drier season) and Class V (markedly seasonal with a long drier season), with the mean $\overline{SI_i}$ falling within Class IV (seasonal).

The replicability index (*RI*), calculated as the ratio $\overline{SI}/\overline{SI_i}$ yielded *RI* = 0.85, suggesting a highly replicable rainfall regime (Livada & Asimakopoulos, 2005). This interpretation is supported by two key observations: i) the percentage frequency of the month with maximum rainfall (Fig. 3b) shows that, on average, peak precipitation is concentrated in a few months, most notably in June; ii) the year-to-year variability in SI_i values is relatively narrow, with fluctuations primarily between Classes III and IV.

Together, these findings, along with the high RI value, indicate that the mean rainfall regime in Recife shows a high degree of replicability, characterized by consistent seasonal patterns and limited interannual variability.

Figure 8 shows the scatter diagram of the individual seasonality index (SI_i) as a function of the annual Precipitation Concentration Index (PCI_a). Dashed lines delineate the classes of annual rainfall regimes (based on SI_i values, shown on the right) and precipitation distribution classes (based on PCI_a values, shown at the top). Color coding distinguishes between the different classes.

The diagram reveals a clear linear relationship between SI_i and PCI_a indicating that SI_i increases proportionally with PCI_a. This implies that a uniform precipitation distribution (low PCI_a) corresponds to a very equable rainfall regime (Class I), while a strongly irregular precipitation distribution (high PCI_a) is associated with extreme seasonality (Class VII), where most rainfall is concentrated in only one or two months. The Spearman correlation analysis confirms this relationship, yielding a correlation coefficient of ρ = 0.86, which indicates a strong positive association between the two indices.

Implications for urban planning and climate adaptation

The results of this study provide new information about the precipitation regime of Recife and have direct implications for urban resilience and climate adaptation strategies. The rainfall regime was characterized as rather seasonal with a short dry season and exhibited a high degree of replicability (RI = 0.85), indicating that the temporal distribution of precipitation is relatively stable from year to year. This behavior is consistent with the climatological characteristics of the eastern coast of northeastern Brazil (ENEB) where rainfall is strongly influenced by large-scale atmospheric systems and ocean–atmosphere interactions. Among the main atmospheric systems related to rainfall seasonality in ENEB are the Upper-Tropospheric Cyclonic Vortices – UTCV, Intertropical Convergence Zone - ITCZ), Cold Fronts and Easterly Wave Disturbances – EWD (Lyra et al., 2024).

The predominance of moderate precipitation concentration at the annual scale and the lower concentration of rainfall during autumn and winter agree with previous studies which have reported a marked wet season from March to August (Coutinho et al., 2016). The absence of significant long-term trends in most PCI and SI series suggests that the overall rainfall regime in Recife remained relatively stable during the study period. However, the significant negative trend detected in spring PCI indicates a gradual reduction in precipitation concentration during this season, which may reflect subtle changes in intra-annual rainfall distribution. The absence of statistically significant trend in annual PCI and SI in Recife was also found in recent studies (Silva et al., 2022; da Silva Araújo et al., 2023).

From a practical perspective, these findings support several adaptation measures. First, stormwater drainage systems and urban flood-control infrastructure should be designed and maintained considering the concentration of rainfall during peak months, particularly June, when flood risks are greatest. Second, water storage and supply systems can be designed according to replicable and relatively predictable seasonal rainfall regime, ensuring water capture during wet months and adequate reserves during drier periods. Third, the observed changes in spring precipitation concentration suggest the need for adaptive planning in sectors de-

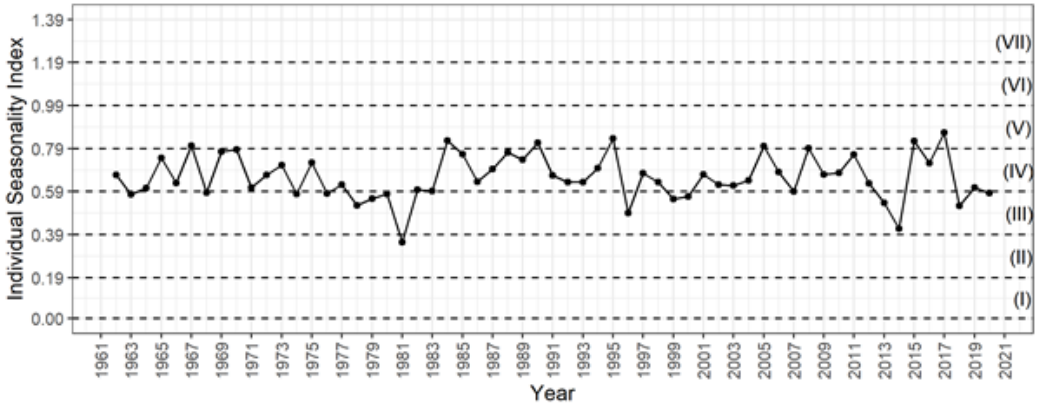

Figure 7. Time series of the individual seasonality index SI_i. Dashed lines represent the thresholds separating rainfall regime classes (I – VII), as defined in Table 2.

pendent on seasonal rainfall, including agriculture and water-resource management.

The methodology adopted in this study offers several advantages. The combined use of PCI, SI, and RI provides a comprehensive assessment of precipitation distribution, seasonality, and temporal consistency. In addition, the Mann–Kendall test and Sen's slope estimator are robust non-parametric techniques that are widely used for detecting climatic trends because they are less sensitive to outliers and do not require normally distributed data. The application of these complementary indices enabled a detailed characterization of Recife's rainfall regime across multiple temporal scales.

Nevertheless, some limitations should be acknowledged. The analysis was based on precipitation records from a single location, which may not fully capture spatial variability across the metropolitan region of Recife. Future studies could integrate spatial datasets, climate-model projections, and the influence of large-scale climate drivers such as the El Niño–Southern Oscillation (ENSO) and Atlantic sea-surface temperature variability.

Overall, the results demonstrate that while Recife's precipitation regime remains relatively stable, ongoing monitoring is necessary to detect emerging changes in rainfall seasonality and concentration that could affect urban infrastructure, water security, and climate adaptation planning.

Conclusions

This study investigated precipitation variability in Recife, Pernambuco, Brazil, from July 1961 to December 2020, focusing on precipitation distribution and seasonality. Monthly precipitation data were analyzed using the Precipitation Concentration Index (PCI) at annual, seasonal, and supra-seasonal scales, together with the Seasonality Index (SI) and the Replicability Index (RI). Temporal trends were assessed using the Mann–Kendall test and Sen's slope estimator, while the relationship between precipitation concentration and seasonality was evaluated through Spearman correlation analysis.

The results showed that precipitation distribution at the annual scale was predominantly moderate (79.66% of the years) with a mean annual PCI of approximately 13.58. Rainfall regime ranged from rather seasonal with a short dry season to markedly seasonal with a long dry season, with seasonal conditions prevailing in 61.02% of the years. The high RI value (0.85) indicated strong interannual consistency in rainfall seasonality, demonstrating that Recife's precipitation regime is relatively predictable. The highest variability in precipitation concentration was observed during the dry season and in summer and spring, whereas autumn and winter generally exhibited more uniform precipitation distribution. Trend analysis revealed no significant changes in both precipitation indices, except for a significant negative trend in spring PCI, suggesting a gradual decrease in precipitation concentration during that season. The strong positive correlation between annual PCI and SI confirmed the close relationship between rainfall concentration and seasonality.

The methodology employed in this study proved effective for characterizing rainfall variability and seasonality across multiple temporal scales. The combined application of PCI, SI, RI, and non-parametric trend analysis provided a robust framework for understanding precipitation dynamics and identifying potential changes in rainfall behavior relevant to climate adaptation and water-resource management.

The findings contribute directly to several United Nations Sustainable Development Goals (SDGs) (United Nations, 2015). In particular, they support SDG 6 (Clean water and sanitation) by providing information that can improve water-resource planning, storage strategies, and sustainable water management. The results also contribute to SDG 11 (Sustainable cities and communities) by supporting the design of resilient urban drainage systems and flood-risk reduction measures. Furthermore, the study contributes to SDG 13 (Climate action) by enhancing the understanding of rainfall variability and seasonality, thereby supporting

evidence-based climate adaptation and resilience planning. Consequently, the research provides valuable scientific information for policymakers, urban planners, and water managers seeking to strengthen climate resilience and sustainable development in Recife and other tropical coastal cities.

Acknowledgments: A.S.A.S. and T.S acknowledge support of Brazilian agency CNPq (grants No 306590/2024-7 and 309499/2022-4). I.T. acknowledge support of the Ministry of Science, Technological Development and Innovation of the Republic of Serbia, grant No. 451-03-34/2026-03/200162.

References

Borges, I. V. G., Musah, A., Dutra, L. M. M., Tunali, M., Lima, C. L., Tunali, M. M., . . . Ambrizzi, T. (2024). Analysis of the interrelationship between precipitation and confirmed dengue cases in the city of Recife (Brazil) covering climate and public health information. *Frontiers in Public Health, 12*, 1456043. https://doi.org/10.3389/fpubh.2024.1456043

Centro de previsão de tempo e Estudos Climaticos – CPTEC/INPE http://enos.cptec.inpe.br/ Last access: September 2025

Coutinho, A. P., Lassabatere, L., Montenegro, S., Antonino, A. C. D., Angulo-Jaramillo, R., & Cabral, J. J. (2016). Hydraulic characterization and hydrological behaviour of a pilot permeable pavement in an urban centre, Brazil. *Hydrological Processes, 30*(23), 4242–4254. https://ui.adsabs.harvard.edu/abs/2016HyPr...30.4242C

Cunha, A. P. M., Zeri, M., Deusdará Leal, K., Costa, L., Cuartas, L. A., Marengo, J. A., . . . Ribeiro-Neto, G. (2019). Extreme drought events over Brazil from 2011 to 2019. *Atmosphere, 10*(11), 642. https://doi.org/10.3390/atmos10110642

da Silva, M. V., Pandorfi, H., Jardim, A. M. D. R. F., de Oliveira-Júnior, J. F., da Divincula, J. S., Giongo, P. R., ... & Lopes, P. M. O. (2021). Spatial modeling of rainfall patterns and groundwater on the coast of northeastern Brazil. *Urban Climate*, *38*, 100911. https://doi.org/10.1016/j.uclim.2021.100911

da Silva Araújo, L., da Silva, A. S. A., Menezes, R. S. C., Stosic, B., & Stosic, T. (2023). Analysis of rainfall seasonality in Pernambuco, Brazil. *Theoretical and Applied Climatology*, *153*(1), 137–154. https://doi.org/10.1007/s00704-023-04462-9

De Luis, M., González-Hidalgo, J. C., Brunetti, M., & Longares, L. A. (2011). Precipitation concentration changes in Spain 1946–2005. *Natural Hazards and Earth System Sciences, 11*(5), 1259–1265. https://doi.org/10.5194/nhess-11-1259-2011

de Medeiros, F. J., Gomes, R. D. S., Coutinho, M. D. L., & Lima, K. C. (2022). Meteorological droughts and water resources: Historical and future perspectives for Rio Grande do Norte state, Northeast Brazil. *International Journal of Climatology, 42*(13), 6976–6995. https://doi.org/10.1002/joc.7624

de Oliveira Souza, T. C., Delgado, R. C., Magistrali, I. C., Dos Santos, G. L., de Carvalho, D. C., Teodoro, P. E., & Caúla, R. H. (2018). Spectral trend of vegetation with rainfall in events of El Niño-Southern Oscillation for Atlantic Forest biome, Brazil. *Environmental Monitoring and Assessment, 190*(11), Article 688. https://doi.org/10.1007/s10661-018-7060-1

Doyle, M. E. (2020). Observed and simulated changes in precipitation seasonality in Argentina. *International Journal of Climatology, 40*(3), 1716–1737. https://doi.org/10.1002/joc.6297

Hänsel, S., Medeiros, D. M., Matschullat, J., Petta, R. A., & de Mendonça Silva, I. (2016). Assessing homogeneity and climate variability of temperature and precipitation series in the capitals of North-Eastern Brazil. *Frontiers in Earth Science, 4*, Article 29. https://doi.org/10.3389/feart.2016.00029

Kendall, M. G. (1975). *Rank correlation methods*. Charles Griffin: London, UK.

Livada, I., & Asimakopoulos, D. N. (2005). Individual seasonality index of rainfall regimes in Greece. *Climate Research, 28*, 155–161. https://doi.org/10.3354/cr028155

Lyra, M. J. A., Gomes, H. B., Herdies, D. L., Ramirez, E., Cavalcante, L. C. V., de Freitas, I. G. F., & Beneti, C. A. A. (2024). Extreme precipitation events over the east coast of northeast Brazil: Synoptic study and MPAS simulation. *Weather and Climate Extremes, 45*, Article 100711. https://doi.org/10.1016/j.wace.2024.100711

Mann, H. B. (1945). Nonparametric tests against trend. *Econometrica, 13*(3), 245–259. https://doi.org/10.2307/1907187

Marengo, J. A., Torres, R. R., & Alves, L. M. (2017). Drought in Northeast Brazil—past, present, and future. *Theoretical and Applied Climatology, 129*(3), 1189–1200. https://doi.org/10.1007/s00704-016-1840-8

Marengo, J. A., Galdos, M. V., Challinor, A., Cunha, A. P., Marin, F. R., Vianna, M. D. S., Alvala, R. C. S., Alves, L. M., Moraes, O. L., & Bender, F. (2022). Drought in Northeast Brazil: A review of agricultural and policy adaptation options for food security. *Climate Resilience and Sustainability, 1*(1), e17. https://doi.org/10.1002/cli2.17

Marengo, J. A., Alcantara, E., Cunha, A. P., Seluchi, M., Nobre, C. A., Dolif, G., Goncalves, D., Assis Dias, M. C., Cuartas, L. A., Bender, F., Ramos, A. M., Mantovani, J. R., Alvalá, R. C. S., & Moraes, O. L. (2023). Flash floods and landslides in the city of Recife, Northeast Brazil after heavy rain on May 25–28, 2022: Causes, impacts, and disaster preparedness. *Weather and Climate Extremes, 39*, 100545. https://doi.org/10.1016/j.wace.2022.100545

National Water Agency (Agência Nacional de Águas - ANA) https://www.gov.br/ana/pt-br, Last access September 2025.

Nóbrega, R. S., Coutinho, C. D., Lino, A. P., & de Albuquerque Wanderley, L. S. (2023). Flood events in the city of Recife, Northeastern Brazil: History and contemporary risks. In J. A. Nóbrega & R. S. Nóbrega (Eds.), *Urban flooding in Brazil* (pp. 171–192). Springer. https://doi.org/10.1007/978-3-031-20898-0_9

Oliveira, F. H. D., Ara, A. L. C. E., Moreira, C. H., Lira, O. O., Padilha, M., Do Rosário, F., & Shinohara, N. K. (2014). Seasonal changes of water quality in a tropical shallow and eutrophic reservoir in the metropolitan region of Recife (Pernambuco-Brazil). *Anais da Academia Brasileira de Ciências, 86*(4), 1863–1872. https://doi.org/10.1590/0001-3765201420140128

Oliver, J. E. (1980). Monthly precipitation distribution: A comparative index. *The Professional Geographer, 32*(3), 300–309. https://doi.org/10.1111/j.0033-0124.1980.00300.x

Patakamuri, S., & O'Brien, N. (2021). *Modifiedmk: Modified versions of Mann Kendall and Spearman's Rho trend tests* (R package version 1.6). CRAN. https://CRAN.R-project.org/package=modifiedmk

Pereira, P. G. D. S., Coutinho, R. Q., de Souza Neto, D. P., & Gomes, I. F. (2025). Stability analysis of an urban slope under human activities and critical rainfall: Case study of Recife, Brazil. *Geotechnical and Geological Engineering, 43*(2), Article 68. https://doi.org/10.1007/s10706-024-03011-z

R Core Team (2023). *A Language and Environment for Statistical Computing*. R Foundation for Statistical Computing, Vienna, Austria. https://www.R-project.org/

Rodrigues, D. T., Gonçalves, W. A., Spyrides, M. H. C., Andrade, L. D. M. B., de Souza, D. O., de Araujo, P. A. A., ... & e Silva, C. M. S. (2021). Probability of occurrence of extreme precipitation events and natural disasters in the city of Natal, Brazil. *Urban Climate*, *35*, Article 100753. https://doi.org/10.1016/j.uclim.2020.100753

Sa'adi, Z., Yusop, Z., & Alias, N. E. (2023). Long-term homogeneity and trend analysis of seasonality and extreme rainfall under the influence of climate change in Johor River basin, Malaysia. *Natural Hazards*, *117*(2), 1813–1845. https://doi.org/10.1007/s11069-023-05930-1

Silva, T. R. B. F., Santos, C. A. C. D., Silva, D. J. F., Santos, C. A. G., da Silva, R. M., & de Brito, J. I. B. (2022). Climate indices-based analysis of rainfall spatiotemporal variability in Pernambuco State, Brazil. *Water*, *14*(14), Article 2190. https://doi.org/10.3390/w14142190

Stosic, T., Tošić, M., Lazić, I., da Silva Araújo, L., Alves da Silva, A. S., Putniković, S., Djurdjević, V., Tošić, I., & Stosic, B. (2024). Changes in rainfall seasonality in Serbia from 1961 to 2020. *Theoretical and Applied Climatology, 155*, 4123–4138. https://doi.org/10.1007/s00704-024-04871-4

United Nations. (2015). *Transforming our world: The 2030 Agenda for Sustainable Development*. United Nations. https://sdgs.un.org/2030agenda

Walsh, R. P. D., & Lawler, D. M. (1981). Rainfall seasonality: description, spatial patterns and change through time. *Weather*, *36*(7), 201–208. https://doi.org/10.1002/j.1477-8696.1981.tb05400.x

Yang, P., Zhang, Y., Xia, J., & Sun, S. (2020). Investigation of precipitation concentration and trends and their potential drivers in the major river basins of Central Asia. *Atmospheric Research*, *245*, Article 105128. https://doi.org/10.1016/j.atmosres.2020.105128

Yue, S., & Wang, C. (2004). The Mann-Kendall test modified by effective sample size to detect trend in serially correlated hydrological series. *Water Resources Management*, *18*(3), 201–218. https://doi.org/10.1023/B:WARM.0000043140.61082.60

INTERNATIONAL SCIENTIFIC JOURNAL | GEOGRAPHICA PANNONICA | Volume 30, Issue 2, 136–152 (June 2026)
Journal homepage: http://www.dgt.uns.ac.rs/en/homepage/pannonica/

Decoding Landscape Evolution: A Geomorphometric Approach to the Lebanese Terrain

Jean A. Doumit[A*]

[A]*Lebanese University, Faculty of Letters and Human Sciences, Department of Geography, Geospatial Lab, Fanar, Beirut, Lebanon; ORCID: 0000-0002-7472-8139*

Received: February 12, 2026| Revised: June 17, 2026| Accepted: July 3, 2026
doi: 10.5937/gp30-64913

ABSTRACT

Theories of landscape evolution by Davis, Penck, and King describe the development of terrain through successive stages, but the choice of the most suitable model for a particular region needs to be supported by quantitative geomorphometric evidence. This study addresses two questions: which descriptive model best explains the topographic evolution of Lebanon, and at what stage of its development the present terrain is. Strahler stream orders 3 to 11 were used to construct nine isobase surfaces using GIS-based hydrological analysis with ALOS digital elevation models at 12.5 m resolution. The hypsometric integral, hypsometric curves, fractal dimensions, profile curvature, relative relief, and a modified surface index were used to characterize each surface. Results show a proportional decrease in slope and elevation with increasing number of isobases. Isobases 5-7 are indicative of equilibrium landscape development, while isobases 8-9 represent an older, disequilibrium stage. Of the three competing theories, Penck's model of simultaneous uplift and erosion best explains Lebanon's terrain, given its tectonic history along the Dead Sea Transform Fault System. The results are used to create a predictive landscape evolution map of Lebanon, defining five spatial zones of progressive terrain dissection. Besides the Lebanese context, the proposed isobase-based geomorphometric framework provides a reproducible methodology for other tectonically active regions and a physiographic baseline for future geological mapping, tectonic analysis, and natural hazard assessment.

Keywords: Geomorphometry; DEM; Isobase; terrain evolution; Davis; Penck

Introduction

Geomorphologists have reconstructed landscape history using methods that map sedimentary features, terrain configurations, and geological structures. Their approach depends on identifying present-day manifestations of geomorphological processes to understand landscape evolution.

Geomorphology is the study of the origin and evolution of landforms and landscapes shaped by the ongoing interaction of internal forces within the Earth and surface processes. Landscape development begins with endogenous processes such as tectonic uplift, faulting, and crustal deformation. These processes create topographic relief and provide a framework for the Earth's surface. When rocks are exposed, they are weathered into loose material ready for transport. Gravity-driven slope processes such as landslides, rockfalls, and soil creep then move this material downslope. Erosional agents such as rivers, glaciers, wind, and waves continue to erode, transport, and redistribute sediment across the landscape. Finally, as the energy of the transport

*Corresponding author: Jean A. Doumit; email: jeandoumit@ul.edu.lb, jeandoumit@gmail.com

agents diminishes, sediment accumulates, contributing to the formation of new landforms. All these processes are interconnected and together constitute a dynamic system. Tectonic forces produce topography; weathering and slope processes supply and transport sediment; and erosion, transport, and deposition modify Earth's surface over time. These processes result in changes to drainage patterns, slope configurations, and overall landscape transformation (Burt et al., 2008).

Throughout history, scientists have used various terms to describe landscape evolution, including erosion cycles, slope evolution, and geographic cycles, as articulated by early scholars such as Davis (1899), Penck (1953), King (1953), Hack (1960), and Crickmay (1974).

William Morris Davis, an influential figure in the field, introduced a seminal model for the sequence of landscape evolution. According to his framework, the process begins with rapid uplift, which provides the fluvial system with the potential energy needed to erode the landscape. This erosion progresses through juvenile, mature, and old-age stages, typically characterized by tectonic stability (Davis, 1889, 1899, 1909). The terrain's slope gradually decreases, forming a low-relief plain near the riverbed (Figure 1).

In continental Europe, Davis's theory found less resonance, as geomorphologists adopted the modifications to landscape evolution theory by Walther Penck and Lester C. King, leading to divergent approaches across regions.

In his theory, Davis classified landscape development into youth, maturity, and old age (see Figure 1a).

Penck introduced a different terminology for his model, using the phrases "increasing or accelerating rate of development," "uniform rate of development," and "decreasing or decelerating rate of development" instead of the three traditional stages (see Figure 1b) (Von Engeln, 1960).

Alongside Davis's consideration of uplift and crustal stability in his erosion cycle, King's framework divided the stages of land development into young, mature, and old phases (see Figure 1c).

King's geomorphic systems, including landscape, pediplanation, and hillslope models, were primarily shaped by South Africa's characteristics, particularly its arid and savanna regions. King argued that Davis's dry-erosion cycle was relevant to the South African landscape (King, 1953).

According to Davis, the erosion cycle in wet temperate countries primarily manifests in fluvial landscapes, featuring an increase during the juvenile phase followed by a decrease with age (Davis, 1905).

King (1953) describes pediplanation as a process of relief reduction by the parallel retreat of slopes, leading to the formation of extensive pediplains. He claimed that landform evolution is a phased process rather than staged as proposed by Davis and that climate is an important factor in controlling the geomorphic cycle (King, 1953; Summerfield, 1991).

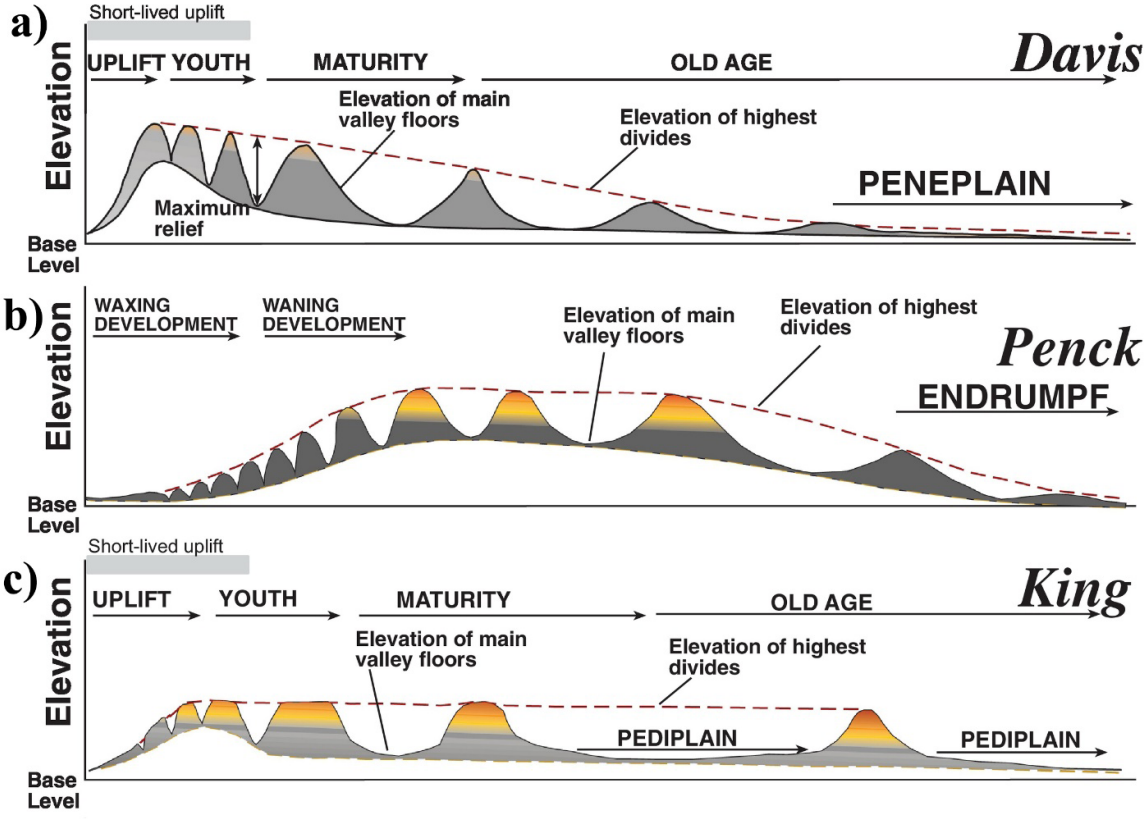

Figure 1. Landscape Evolution Profiles: (a) Davis' Landscape Evolution Theory, (b) Penck's Theory, (c) King's Theory (Adapted from Vasconcelos & Carmo, 2018).

Table 1. A summary of Davis, Penck, and King's theories.

Davis' theory (Davis, 1899)	Penck's theory (Penck, 1953)	King's theory (King, 1953)
Sudden Upliftment.	The long process of Upliftment.	Sudden process of mountain Upliftment.
Erosion starts after the uplift stops.	Upliftment and erosion are simultaneous.	The erosion process begins after uplift ceases.
Landform refers to the process of weathering, which is carried out by agents such as wind, air, groundwater, and sea waves. Landforms are classified into three stages: youth, maturity, and old age.	Landforms reflect the combined effects of endogenic and exogenic forces. Landform development is classified in phases rather than stages.	Landforms are in equilibrium with the climate and do not affect their development cycle. Landscape development is a cyclical process and is classified into three stages: youth, maturity, and old age.

Table 1 compares the theories proposed by Davis, Penck, and King. It also presents hypotheses about which theory may apply to the landscape evolution of Lebanon, leading us to pose the following questions:

As Philip G. Worcester postulated, the landscape evolution (or erosion) cycle is the time it takes for rivers to reduce newly formed landmasses to their original levels (Worcester, 1958).

Water and rivers are the primary agents of erosion, while water-related processes significantly shape much of Earth's surface (Hamood, 2009).

The drainage network and its sensitivity to factors such as lithology and climate act as reliable indicators of tectonic activity. Flows of similar orders are frequently associated with comparable geologic events and ages (Horton, 1945; Golts & Rosenthal, 1993; Strahler, 1952).

Numerous scientists, including Gravelius (1914), Horton (1945), Dury (1952), Strahler (1957), Filosofov (1960), Pannekoek (1967), Golts and Rosenthal (1993), and Florinsky (2012), have studied landscape evolution based on stream networks, where erosion networks assign relative geologic ages to various stream orders.

Isobase plains represent hypothetical plains formed by connecting stream profiles of similar stream orders. They serve as indicators of basalt plain erosion, are associated with comparable erosional phases, and potentially represent erosion-tectonic events (Filosofov, 1960).

The analysis of isobase areas can yield valuable insights, including 1) the identification of young tectonic processes; 2) the creation of morphotectonic maps; and 3) the delineation of tectonic areas and their movement directions (Gary et al., 1973).

This paper reports the construction of isobase maps of Lebanon based on stream-order hierarchies to evaluate landscape evolution patterns and assess the applicability of established geomorphological models. The isobases concept used in this research is based on the methodological approach of Filosofov (1975) and Golts and Rosenthal (1993) and is conceptually associated with the sub-envelope surface approaches developed by Hack (1960) and subsequently extended in geomorphometric studies such as Gomez et al. (2006). These methods are often used to define geomorphic surfaces at the regional scale and to identify possible tectonic influences on landscape development.

Recent advances in Geographic Information Systems (GIS) and high-resolution Digital Elevation Models (DEMs) have considerably improved the capacity to quantitatively analyze topography and landscape evolution. These technologies are now widely used in tectonically active areas, such as mountain belts in the Himalayas, the Andes, and the Mediterranean, to determine morphometric indices, quantify uplift and erosion patterns, and characterize the organization of the drainage network. In particular, the application of isobase mapping, hypsometric analysis, and other related geomorphic metrics has been successfully used to differentiate spatial variations in geomorphic maturity and to identify areas affected by neotectonics activity, even in the presence of complex lithological variations.

However, integrated regional-scale studies that apply isobase-based geomorphometric analysis, combined with multiple morphometric indices, to reconstruct landscape evolution are still lacking in Lebanon. Previous studies in the region have largely been limited to localized basin-scale studies or structural geological interpretations, with few applications of comprehensive DEM-derived quantitative frameworks at the national scale.

This study is intended to fill this gap by integrating isobase mapping with a variety of morphometric techniques, including stream-order statistics, bifurcation ratio, hypsometric curves, hypsometric integrals, relative and anomalous relief, fractal dimension analysis, profile curvature, and surface roughness indices. These parameters are determined using GIS- and DEM-based algorithms to assess spatial variations in landscape form and evolutionary stage across Lebanon.

The scientific contribution of this research is the first systematic, region-wide application of isobase surface analysis, integrated with multi-parameter morphometric evaluation, in Lebanon. Results are ex-

pected to provide a quantitative framework for interpreting landscape evolution, identify spatial patterns of uplift and erosion, and evaluate potential tectonic controls on drainage development. In addition to the geomorphological implications, the study has practical implications for tectonic geomorphology, watershed management, environmental planning, and studies of landform evolution in structurally complex mountainous regions.

In this experimental study, we will use morphometric indices of isobase surfaces, such as the hypsometric curve, relative and anomalous relief, fractal dimensions, profile curvature, hypsometric integral, surface roughness, and surface index, to address these questions:

1. Which of the proposed theories is best suited to explain the landscape evolution of the Lebanese terrain?
2. What is the latest evolutionary stage, as shown in Figure 1?

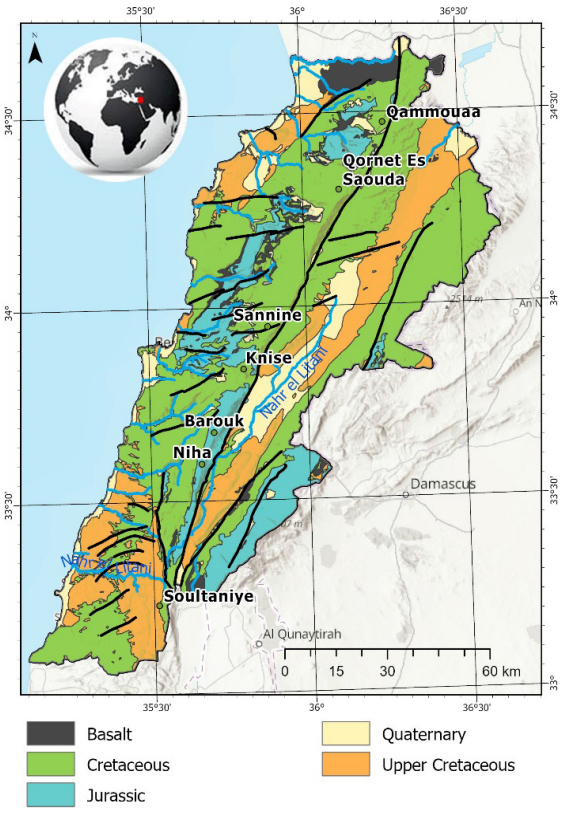

Figure 2. Lithology map of the study area highlighting landscape structures.

Material and Methods

a) Study area and datasets

The Lebanese landscape comprises three primary geomorphological structures: the Western Lebanon Mountains, culminating at Cornet Es Sawda at 3083 meters above sea level; the Bekaa Valley; and the Eastern Anti-Lebanon Mountains, dominated by Mount Hermon, which rises to 2814 meters above sea level.

Lebanon's river network can be categorized into two groups. The first group comprises 12 major rivers that drain the Lebanese mountain range and flow through steep gorges. The second group includes the two major rivers, Litani and Al Assi (Orontes).

The geological evolution of Lebanon unfolds in five distinct episodes:

1) Late Permian to Late Triassic, marked by initial rifting.

2) The Early to Late Jurassic was marked by stability and warm, clear seas, with the oldest rocks in Lebanon dating back to the Lower Jurassic.

3) The period from the Late Jurassic to the Middle Cretaceous is marked by uplift, volcanic activity, and the development of deltas linked to the pre-Chouf sandstone uplift.

4) From the Late Cretaceous to the early Eocene, characterized by high seas and gentle folding.

5) From the Middle Eocene to present times, tectonic uplift and climatic cooling have taken place, particularly emphasized by significant uplift during the late Eocene and Oligocene (Walley, 1998).

The study area was significantly influenced by the initial movements of the Dead Sea Transform Fault System, resulting in tilting, uplifting, and disruption of drainage patterns.

Throughout various geological episodes, persistent uplifts and significant disruptions in water flow occurred as different blocks slid past one another along strike-slip faults. A noteworthy example of this phenomenon is the Litani River, which likely once flowed southward into the Jordan Valley but was redirected eastward toward the Mediterranean by uplift (Dubertret, 1934, 1947; Walley, 1998).

Leveraging Penck's theory, which accounts for the geological episodes in Lebanese geology, we can construct isobase surfaces and compare their geomorphic indices to understand the landscape's evolutionary processes.

The accuracy of surface modeling and morphometric analysis hinges on the quality of digital elevation models (DEMs) and sample size. The Advanced Land Observing Satellite (ALOS) DEM, available on the Alaska Satellite Facility website, provides elevation data with a spatial resolution of 12.5 meters (Logan et al., 2014).

b) Drainage System Extraction

Before generating stream networks from the DEM, it is essential to fill the model's nested wells to ensure proper flow direction and to prevent artifacts that could

obstruct the flow path. Using ArcGIS Pro's hydrologic analysis tools, we generated and classified streams by Strahler order.

The drainage system was extracted using GIS hydrologic methods, including drainage direction, flow accumulation, and stream order calculations for each pixel. Then, the extracted flows were ordered according to Strahler's (1957) hierarchy (Doumit, 2017).

c) Isobase Surface Construction

The spatial translation of stream elevations into isobase surfaces provides significant value for structural, geological, and tectonic studies (Dury, 1952; Filosofov, 1960; Golts & Rosenthal, 1993; Grohmann et al., 2007, 2011).

According to Golts and Rosenthal (1993), streams of similar order indicate similar geologic events and belong to comparable geologic ages. Interpolating elevations of these streams generates isobasic surfaces that represent the same erosional events. Variations in topography within an isobasic surface can help identify potential structures or elevated blocks associated with structural landscape evolution (Golts & Rosenthal, 1993; Grohmann et al., 2007; Domínguez-González et al., 2015).

Preparing isobasic maps begins with an initial sketch of valley orders, excluding all valleys except those of the last order from the second-order base contour. The third-order base outline includes all valleys except those of the first and second orders, and so on (Dury, 1952; Filosofov, 1960; 1970; Pannekoek, 1967).

Isobase areas for orders 1 and 2 were excluded, while higher-order terms were applied to alluvial modeling. Subtracting the older order (n) base area from the younger (n-1) results in a residual map of order n-1. This map illustrates the extent of erosional dissection in the area over the time elapsed between the formation of these two basal surfaces.

The recent hilltops in Lebanon exhibit Pliocene-Quaternary uplift. An envelope surface tangential to the interfluves was determined by interpolating ridge-network elevations derived from the DEM. The last isobase surface of order nine serves as an under-envelope. Surface (end hull or peneplain).

Geomorphometry involves the quantitative measurement of landscapes, facilitating the characterization of landforms by their geometric shape and size. These measurements enable geomorphologists to objectively compare landforms and calculate parameters essential for identifying specific regional features, such as the degree of tectonic activity (Keller & Pinter, 1996).

To quantitatively analyze the landscape represented by the generated isobase surfaces, we calculated geomorphometric indices such as:

1. Hypsometric curve (*Hc*)

The hypsometric curve represents the distribution of elevations over a land area (Strahler, 1952). It provides insights into elevation variation across the landscape. Hypsometric curves have helped decipher the evolution of drainage networks and can serve as valuable tools in distinguishing between active and inactive tectonic areas (Keller & Pinter, 1996). The curve is constructed by plotting cumulative elevation against total area (see Figure 8). Convex hypsometric curves typically characterize youthful, recently eroded areas, while S-shaped curves indicate regions with moderate erosion. Concave curve shapes are associated with eroded, older areas (Strahler, 1957).

2. Relative relief (*Rr*)

Relative relief (Rr) is the difference between the highest and lowest elevations in an area. Rr emphasizes the complexity and patterns of elevation variation (Doumit & Kiselev, 2019).

$$Rr = Z_{max} - Z_{min} \qquad (1)$$

Relative relief in a relative velocity index of landscape evolution and vertical tectonic movements (Florinsky, 2012); high Rr values indicate elevated surfaces (Scotti et al., 2014).

3. Fractal dimensions (*FD*)

Mandelbrot (1982) introduced the fractal dimension to measure texture and evaluate complex forms. The experiment investigated the fractal dimensions of isobase surfaces to understand how they evolve with changes in the landscape. The formula for fractal dimensions is based on calculated slopes and seeks a linear relationship between precision and length in a log/log plot:

$$\mathrm{FD} = \frac{\log(2)}{\log(2) + \log(\sin(\frac{180 - \mathrm{slope}}{2}))} \qquad (2)$$

Fractal dimension values of a surface range from 2 to 3, indicating surface heterogeneity; low values correspond to flat, smooth areas, while high values correspond to complex areas (Doumit, 2017).

4. Profile curvature (*Pc*)

Generally, curvature is calculated from a surface representation using a partial quadratic equation (Zevenbergen & Thorne, 1987).

Profile curvature or vertical plane curvature, *Pc,* is parallel to the slope direction and defined as

$$Pc = \frac{-2(DH^2 + EG^2 - FGH)}{(G^2 + H^2)} \qquad (3)$$

Where:

$$D = \frac{\frac{z_4 + z_6}{2} - z_5}{d^2};$$

$$E = \frac{\frac{z_2+z_8}{2}-z_5}{d^2};$$

$$F = \frac{-z_1+z_3+z_7-z_9}{4d^2};$$

$$G = \frac{-z_4+z_6}{2d};$$

$$H = \frac{z_2+z_8}{2d}$$

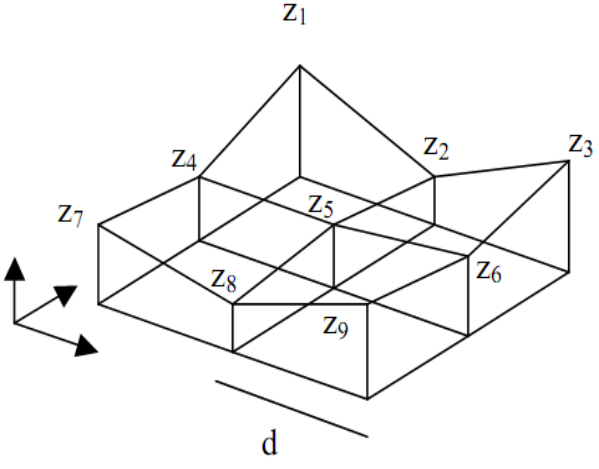

Figure 3. DEM 3×3 Matrix of profile curvature calculation (Doumit, 2017).

Profile curvature is a measure of the rate at which water drains across the surface, influenced by changes in slope. It plays a pivotal role in erosion and deposition processes. It is typically positive in convex areas, indicating a tendency toward erosion, and negative in concave areas, indicating a propensity for deposition. These characteristics describe the second accumulation mechanism (Zevenbergen & Thorne, 1987).

In areas with convex curvature, erosion predominates, whereas areas with concave curvature are more prone to deposition (Evans, 1980; Doumit, 2017).

5. Hypsometric integral (*HI*)

The hypsometric integral is the distribution of surface area with respect to elevation, evaluating the landscape response to active tectonics (Strahler, 1952; Mahmood & Gloaguen, 2012; Domínguez-González et al., 2015).

Pike and Wilson (1971) calculated the Hypsometric Integral with this equation:

$$HI = \frac{Z_{mean}-Z_{min}}{Z_{max}-Z_{mean}} \qquad (4)$$

Where Z_{mean}, Z_{min}, and Z_{max} are the mean, minimum, and maximum elevations of the study area.

6. Surface index (*SI*)

The surface index, like the hypsometric integral, measures erosion and determines a landscape's maturity. In line with research by Andreani et al. (2014) and Domínguez-González et al. (2015), combining DEM elevations with the hypsometric integral and surface roughness enables classification of landscapes based on their state of dynamic equilibrium. This approach allows discrimination between areas with low local relief and those with rugged terrain (Andreani et al., 2014).

To calculate the surface index (*SI*), it is essential to normalize the DEM, hypsometric integral, and surface roughness values so that pixel values range from 0 to 1.

$$SI = (N_h \times N_{HI}) - N_{SR} \qquad (5)$$

where N_h, N_{HI}, and N_{SR} represent the normalized DEM, hypsometric integral, and surface roughness values.

In their study, Lee et al. (1990) tested fractal dimension-based surface roughness under both field and laboratory conditions. The results revealed a strong correlation between surface roughness and fractal dimensions, with higher fractal dimensions corresponding to rougher terrains.

Our research conducted a correlation analysis between surface roughness and the fractal dimensions of the selected isobase surfaces. Following normalization of the fractal dimension rasters, we modified formula (5) by substitution.

$$SI_M = (N_h \times N_{HI}) - N_{FD} \qquad (6)$$

Positive *SI* values indicate elevated surfaces with low local relief, whereas negative SI values indicate rugged landscapes (Domínguez-González et al., 2015).

The hypsometric integral (*HI*) effectively highlights topographic scarps, while the surface index (*SI*) emphasizes elevated low-relief landscapes (Andreani & Gloaguen, 2016).

Results and Discussion

After applying the hydrologic GIS algorithm to the ALOS DEM to extract stream orders, we generated 11 stream orders. Excluding the first two orders, we interpolated the elevation vertices of the remaining nine stream orders to create nine distinct isobase areas (refer to Figure 4).

Isobase number 9 was omitted from the analysis due to spatial limitations at the elevation vertices of the 11th-order grid, particularly along the Litani River. These spatial constraints made surface interpolation unfeasible.

Figure 4 displays successive isobase plots depicting the terrain surface derived from the ALOS DEM. Figure 4a spans an elevation range from 0 to 3113, representing the highest points on Lebanon's Qornet Es Sawda Mountain; figures 4b, 4c, and 4d exhibit similar elevation intervals. However, isobases 4, 5, 6, 7, and 8, which show decreasing elevation intervals, effectively illustrate the landscape evolution as presented in Table 2, showcasing the various landforms and their corresponding elevation values.

The successive isobase surfaces illustrate a notable transition from rugged to smoother terrain in a visual analysis. This transformation begins with isobase five and culminates with isobase eight. It reflects significant terrain evolution characterized by the gradual disappearance of the Lebanese western mountain range. This change is accompanied by a pronounced reduction in relative relief, as evidenced by the height-interval differences between isobases five and eight.

Table 2 presents summary statistics of elevations for each isobase area. It is important to note that surface interpolations affect the minimum elevation values across all isobase areas and do not indicate sea-level rise. The mean elevation values show a clear decrease from isobase 1 to isobase 8, effectively illustrating the landscape's evolution and the differences in elevation between these surfaces.

Isobases 1, 2, and 3 have the same minimum and maximum elevation values, though there are some differences in the mean elevation. These areas show relatively minor landscape evolution.

Conversely, a significant elevation range of 1391 meters between isobase 4 and isobase 8 indicates a substantial landscape evolution.

Although dating and correlating geological episodes that explain variation in landscape evolution across isobases is challenging, these episodes can be compared to the stages of Davis and Penck through geomorphometric analysis.

The visual analysis of the isobases in Figure 4, combined with the elevation data in Table 1, suggests similar isobase surfaces and notable landscape evolution. To distinguish isobase areas, we used a Pearson correlation matrix to compare landscapes with low versus high evolutionary rates, gaining deeper insights into landscape evolution.

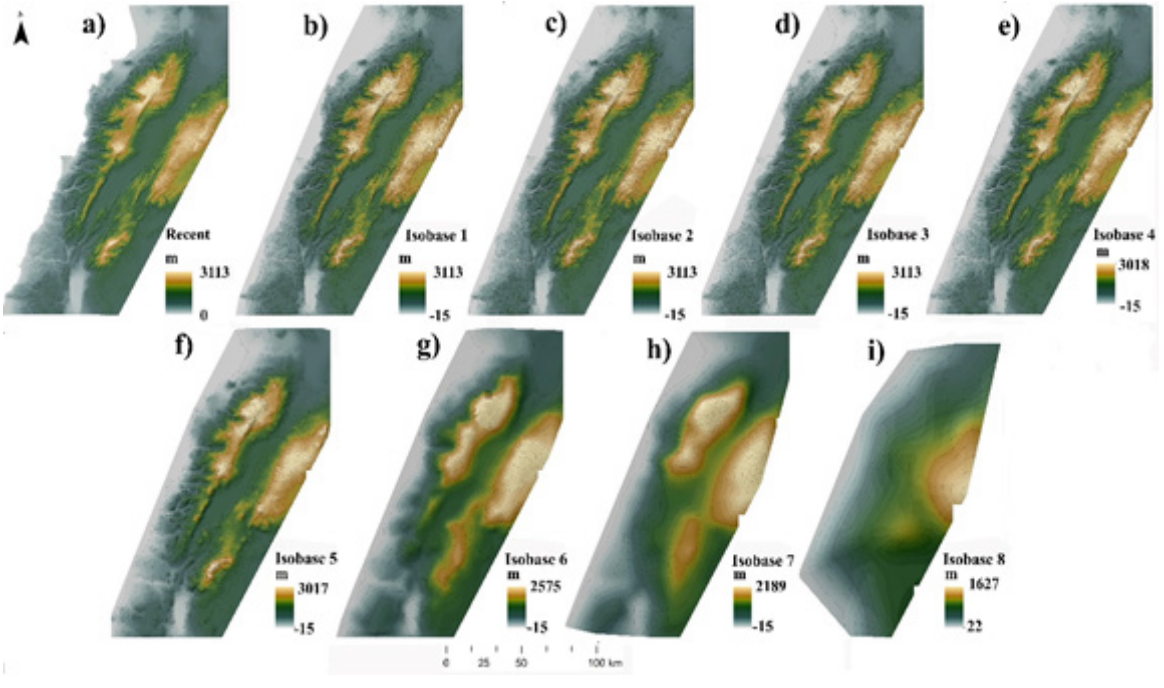

Figure 4. Landscape evolution of Lebanon's surfaces: a) recent surface, b) Isobase 1 surface, c) Isobase 2, d) Isobase 3, e) Isobase 4, f) Isobase 5, g) Isobase 6, h) Isobase 7, i) Isobase 8.

Table 2. Elevation statistics of the generated isobase surfaces, minimum, mean, maximum, and standard deviation.

	Elevations, m			
Surfaces	Minimum	Mean	Maximum	Std
Recent	0	999	3113	617
Isobase 1	-15	935	3113	643
Isobase 2	-15	936	3113	642
Isobase 3	-15	935	3113	642
Isobase 4	-15	929	3018	639
Isobase 5	-15	887	3017	619
Isobase 6	-15	818	2575	567
Isobase 7	-15	730	2189	508
Isobase 8	22	622	1627	373

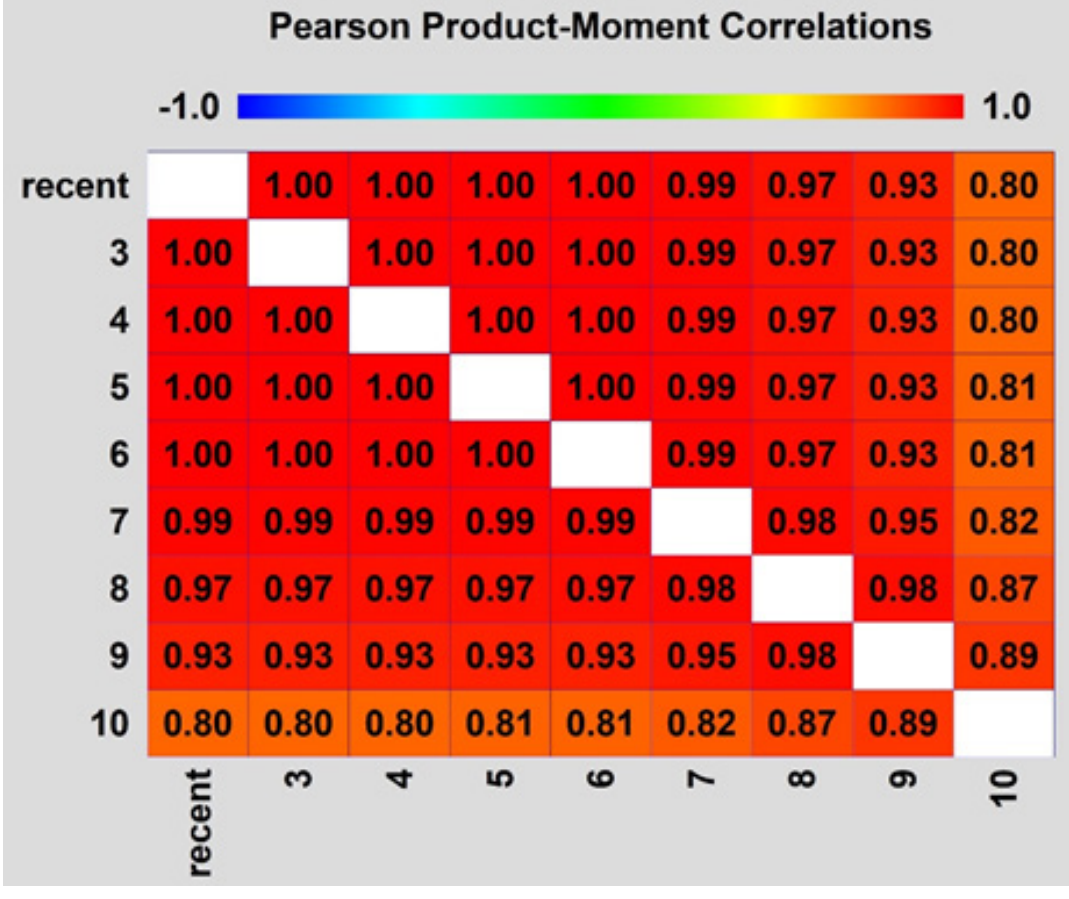

Figure 5. Pearson correlation matrix of isobase surfaces.

Figure 5 shows the Pearson product-moment correlations between each pair of isobase surfaces. These correlation values assess the strength of the linear relationship between the plots and demonstrate a high correlation among isobase plots 1, 2, 3, and 4, indicating low landscape development. In contrast, the correlation values decreased from 0.99 for isobase 5 to 0.8 for isobase 8, indicating high landscape development.

The youngest area (DEM) shows a strong correlation with isobases 1, 2, 3, and 4, while the correlation diminishes for isobases 5, 6, 7, and 8.

Based on the visual analysis results in Figure 4, the elevation statistics in Table 2, and our correlation findings, we have excluded isobases 1, 2, 3, and 4 because they are highly similar and not relevant to landscape evolution.

Isobase plots 5, 6, 7, and 8 illustrate spatial variations in topographic and fundamental morphometric

indices, including surface profile, hypsometry, relative relief, hypsometric integral, profile curvature, fractal dimensions, and surface index, thereby enabling a comprehensive analysis of landscape evolution.

Isobase surfaces 5, 6, 7, and 8 represent hypothetical surfaces eroded to the level of the main valley floors. Contour lines (interfluves) were generated from the DEM to construct an envelope surface connecting the highest-elevation watersheds (see Figure 6). The crests of stream order 11 were interpolated to form an under-envelope surface that links the main valley bottoms.

The Anti-Lebanon mountain range drains into the Bekaa Valley, while Mount Lebanon drains into the sea (Figure 6b). It is reasonable to expect that the equivalent uplift of the two mountain ranges would result in lower relief in the Anti-Lebanon (Gomez et al., 2006).

As shown in Figures 6a (longitudinal) and 6b (transverse), two profiles illustrate the topographical, isobase, envelope, and sub-envelope surfaces, highlighting the differences in topography and landscape evolution between Mount Lebanon and the Anti-Lebanon.

The longitudinal and transverse profiles in Figures 6a and b indicate low relief and high elevation, suggesting late Cenozoic uplift (Gomez et al., 2006). These revisions aim to improve the paragraph's clarity and coherence while preserving the accuracy of the information.

Figure 6a shows a longitudinal profile traversing the western mountainous chain of Lebanon. Conversely, Figure 6b depicts a transverse profile that crosses the western mountainous chain of Lebanon, the Bekaa Valley, and the eastern mountainous chain, showing the changes in elevation between isobases.

The longitudinal profile of the Lebanese mountain range (Figure 6a) illustrates significant landscape evolution, particularly at the summits of Qammouaa, Qornet Es Sawda, and Sannine mountains. This evolution is expressed as substantial elevation differences between the envelope and sub-envelope surfaces, referred to as relief energy (Doumit & Kiselev, 2019). The Knisse, Barrouk, Niha, and Soultaniye mountains exhibit lower relief energy.

Both the Lebanon and Anti-Lebanon mountain ranges exhibit significant topographic residuals (Figure 6), but the relief energies are more pronounced in the Lebanon Mountains compared to the Anti-Lebanon.

These disparities in relief can be attributed to differences in climate between the wetter Mount Lebanon region (with an average annual precipitation of approximately 800 mm) and the drier Anti-Lebanon region (with a mean annual precipitation of around 400 mm). Variations in base levels contribute to these differences.

While establishing precise geological ages for the generated isobase surfaces is challenging, they remain important for understanding geological history. It can be classified based on the Davis stages. Specifically, the interval from the recent surface to isobase 5 can be considered the youth stage; isobases 6 and 7 represent maturity; isobase 8 signifies old terrain; and the sub-envelope complements this classification.

The isobase surfaces can be linked to Penck's stages: the envelope corresponds to isobase 5, which indicates the waxing or acceleration stage, while isobases 6 and 7 indicate uniform development. Additionally, isobase 8 and the sub-envelope surfaces characterize the waning or development stage.

To quantify landscape evolution and gain insights into maturity and differences between mature and less mature terrain, we developed these isobase surfaces, which provide a comprehensive comparison of geomorphological indices across the evolving landscape.

In our study, we utilized surface analysis (slope and elevation), surface hypsometry (hypsometric curves and hypsometric integrals), and terrain derivatives (profile curvature and surface index).

When discussing landscape evolution, we refer to the evolution of slopes. Davis's theory is often referred to as the slope-slope theory, and Penck's theory uses the same terminology (Davis, 1899).

The scatter plots in Figure 7 show the average slopes across eight adjacent cells along the x-axis, plotted against height above sea level on the y-axis. As indicated by ALOS DEM, the highest recorded average slope on the recent surface reaches 18 degrees, while the maximum elevation above sea level is 3113 meters. Figure 7a depicts elevated slope values within the 2400 to 2800 meters elevation range, with lower slope values at lower elevations.

Moving on to Figure 7b, which corresponds to Isobase 5, we observe a maximum elevation of 3017 meters and a maximum average slope of 13.5 degrees. Here, the youngest surface shows higher slopes at higher elevations. Figure 7c shows a decrease in slope to 0-5 degrees, alongside a reduction in elevation to 2500 meters, indicating the formation of a steeper slope. This trend continues in Isobase 7, as illustrated in Figure 7d, with an average slope of 4 degrees and an elevation of 2200 meters. Ultimately, low slope values of less than 2 degrees are reached on the surface of Isobase 8, as depicted in Figure 7e.

The scatter plots in Figure 7 clearly illustrate a proportional decrease in slope and elevation, with close similarities in their shapes. These observations, with a dynamic difference in scale, highlight the proportional nature of landscape evolution among the isobase surfaces.

To gain a more comprehensive understanding of elevation evolution, we divided all surfaces into eight intervals, as outlined in Table 3, which shows surface hypsometry and the areas corresponding to elevation intervals across the landscape-evolution surfaces.

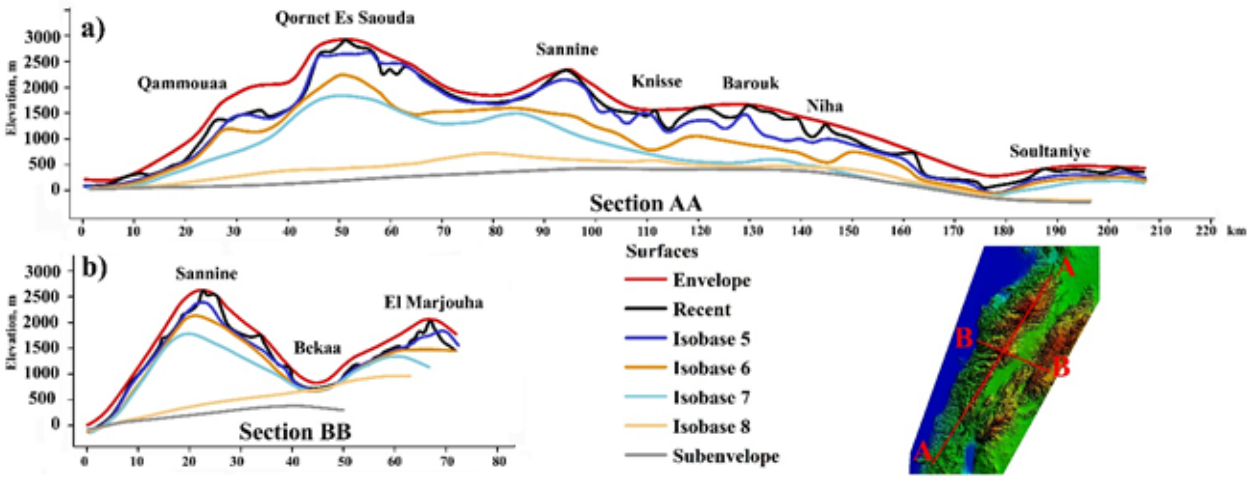

Figure 6. Illustrates the profiles of the topographic, envelope, and isobase surfaces.

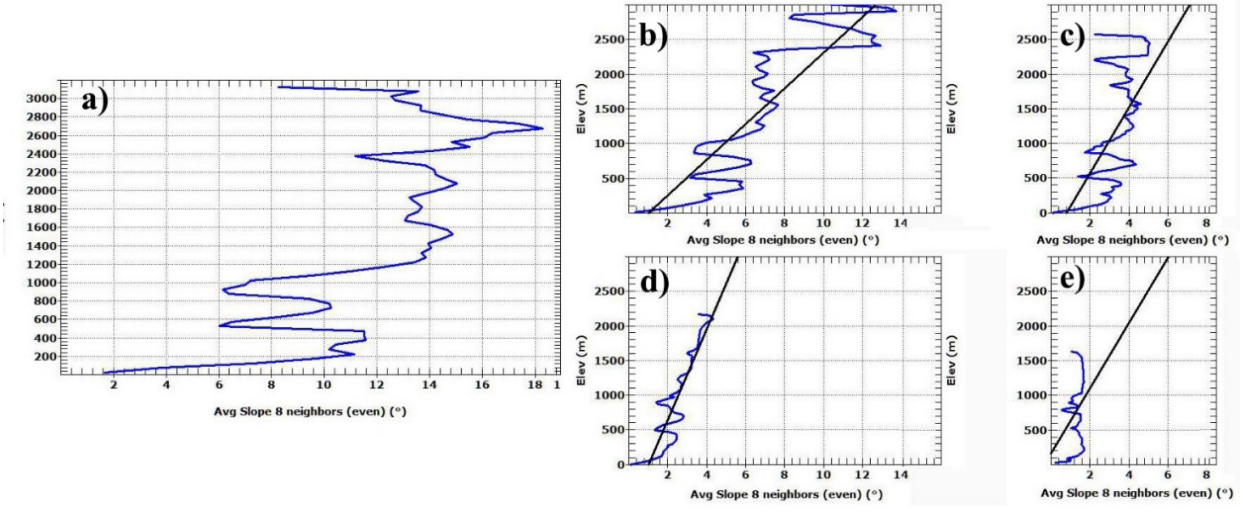

Figure 7. Scatter plot of slopes and average elevations: a) recent surface, b) isobase 5, c) isobase 6, d) isobase 7, and e) isobase 8.

Table 3. Percentage of areas corresponding to elevation intervals.

Elevation intervals, area percentages								
Surfaces	0-100	100-250	250-500	500-750	750-1000	1000-1500	1500-2000	> 2000
Recent	20	22	4	6	6	9	5	29
Isobase 5	8	9	14	20	19	3	17	11
Isobase 6	12	13	20	22	3	4	20	6
Isobase 7	9	12	16	15	17	3	13	15
Isobase 8	15	20	29	3	5	3	24	0

On the younger surface, the percentage of elevations is highest in the interval above 2000 meters, indicating that 29 percent of the Lebanese territory experienced significant uplift. The decrease in the percentage of surface area above 2000 meters for isobases 5 and 6 is attributed to pronounced erosion, while the rapid increase in surface area for isobase 7 suggests potential for uplift or sedimentary movement.

During the old stage or the declining development of isobase 8, Table 3 shows a low percentage of areas within the 500–1500-meter interval due to extensive erosion. This results in a high percentage of areas within the 100–500-meter interval, indicating substantial sedimentation movements.

The considerable variation in surface percentages across all elevation intervals underscores the simultaneous occurrence of tectonic movements and erosional processes of varying magnitudes.

The hypsometric curve in Figure 8 shows a continuous relationship between relative elevation and the percentage of the hypsometric curve.

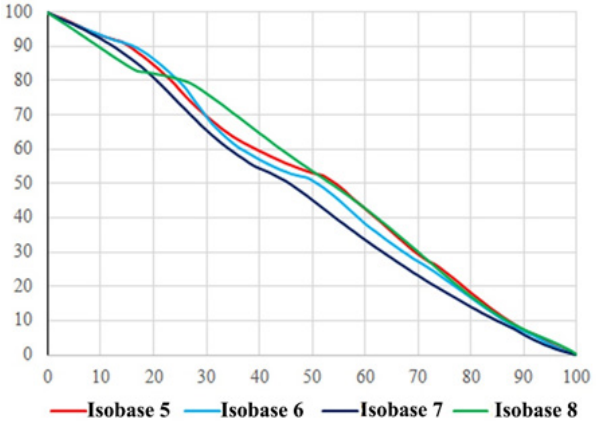

Figure 8. The hypsometric curve of Isobase surfaces.

On isobases 5, 6, and 7, the curve shape varies approximately in proportion to relative relief and area, indicating equilibrium landscape development. However, the curved shape of isobase 8, characterized by an inflection point, signifies a state of disequilibrium associated with an older stage. Relative relief was computed using Equation 1 within a 3 x 3 matrix, utilizing data from the ALOS DEM for the recent area and from the generated isobase areas 5, 6, 7, and 8.

Table 4. Minimum, mean, maximum, and standard deviation of relative relief for the recent and isobase surfaces.

Surfaces	Minimum	Mean	Maximum	Std
Recent	0	104	599	79
Isobase 5	0	46	273	39
Isobase 6	0	29	152	20
Isobase 7	0	21	100	15
Isobase 8	0	11	23	5

The theories proposed by Davis and Penck analyze the development of absolute and relative relief at various stages of landscape evolution. According to Davis, absolute relief remains relatively constant in the juvenile stage, reflecting the erosion process following uplift. However, Penck suggests that absolute relief increases during this stage, attributed to the simultaneous processes of erosion and uplift (Penck, 1953). This stage can be unpredictable because the terrain model for the surface before the youngest one is poorly documented.

Both theories agree that the juvenile stage is characterized by increased relative relief, as shown in Table 4, which reports a wide elevation range of 0 to 599 meters on the recent surface.

Moving to the mature stage, Davis asserts that absolute relief decreases, leading to valley deepening and uplift, a pattern consistent across isobases 4, 5, 6, 7, and 8 in Table 2. Penck suggests that relative relief remains stable during this stage, while absolute relief stays nearly constant.

Table 2 also shows constant absolute relief (maximum elevation) for isobases 1, 2, and 3, indicating constant relative relief, as predicted by Davis' theory. However, according to Penck's theory, the declining phase of development begins in the youngest area and extends to isobases 1, 2, and 3.

Regarding the old stage, both Davis and Penck agree that absolute and relative relief decrease directly (Davis, 1899; Penck, 1953). Relative relief values diminished with isobases 5, 6, 7, and 8.

Fractal dimension values of a surface can range from 2 for flat, smooth surfaces to 3 for very complex, rugged surfaces. The fractal dimensions of the recent and isobase surfaces were calculated using Equation 2.

Figure 9 presents a map of the fractal dimensions of the isolated surfaces, highlighting regions of extreme slope and terrain complexity. In Figure 9a, the recent surface is highly complex in areas with significant relative relief, such as the Yammouneh fault and deep river valleys, with fractal dimensions ranging from 2.02 to 2.04. These areas are elevated and heavily eroded due to substantial topographic differences.

The lowest fractal dimension values (2) are found in the isobase regions 5 and 6 in the Beqaa Valley, particularly in the Amiq area (i.e., low-amplitude landscapes).

Figure 9b of isobase 5 shows a stretched interval of values ranging from 2 flat-surface amplitudes to 2.4 high-elevation amplitudes along the Yammouneh fault, the Ibrahim River, and the Qadisha River valleys.

As the landscape evolves from Isobase 6 to Isobase 8, the fractal dimension decreases, and the terrain becomes smoother rather than flat.

During this period, landform inversion may occur; that is, slopes may initially have convex profiles (Figure 6), then become concave, and, at a later stage, become convex again, particularly if depositional material is involved (Moss, 1977).

Profile curvature measures the curvature of each isobase surface to better illustrate slope development.

Table 5. Profile curvature types and the percentage of the area

Profile Curvature (PC) area%			
Surface	Concave	Straight	Convex
Recent	16	51	32
Isobase 5	28	31	41
Isobase 6	45	20	35
Isobase 7	11	37	52
Isobase 8	10	58	32

Table 5 summarizes the percentages of areas with concave, straight, and convex profile curvature on the isobase surfaces. In isobase 5, the hillside displays a convex slope before significant water-related development, indicating a high percentage of convex areas influenced by gravitational processes.

As water's influence increases, the slope gradually becomes concave. In isobase 6, the concave shape balances convex and concave slopes, resulting in a gravitational wash effect. The deep weathering of isobase 7 surfaces creates a convex slope, with a significant 52% of the area occupied by convex features.

The slope dynamics are at play in isobase 8, characterized by high landscape evolution and rapid forces of change (Coates, 1984). Penck (1953) mentions in his theory that during the decreasing or developmental phase, gravity processes dominate in the upper range (in our case, isobase 6) while washing tendencies prevail in the lower range (isobase 7).

The hypsometric integral, calculated using equation 4, provides insights into the erosion stage and the factors influencing it, such as tectonic, climatic, and lithologic factors. Low hypsometric integral values, close to 0, indicate older, highly dissected areas. In contrast, high values near 1 indicate regions with high relative relief, such as smooth upland surfaces intersected by deep rivers, as in the valleys of the Ibrahim and Abou Ali rivers, which are indicative of younger, less-eroded areas (Sarp et al., 2011).

The hypsometric integral maps of the isobase surfaces (Figure 10) predominantly reflect tectonic features. The highest values are concentrated along the Lebanon and Anti-Lebanon mountain ranges, while the lowest values are observed in depressions and inareas of the Beqaa Valley.

The Hypsometric Integral (HI) values range from 0 to 0.99, with lower values typically observed in depressions and higher values at the crests of uplifted regions. Specifically, in the recent isobase 5 and 6 surfaces, the high and low HI values fall within the intervals of 0.58-0.99 and 0-0.42, respectively.

However, on isobase surfaces 7 and 8, as shown in Figures 10d and 10e, the high-value interval vanishes, indicating the disappearance of young, less eroded areas. The older and more eroded regions now fall within the HI range of 0-0.42.

This outcome suggests that young, less-eroded areas become increasingly scarce during the waning or developmental stage.

To discriminate low terrain based on elevations, we employed the modified Surface Index (SI) as defined in equation 6. The calculated SI for the recent surface ranges from -0.92 to 0.68, with a few negative values observed in the V-shaped river valleys.

The disparities in landscape evolution are likely attributable to factors such as tectonic processes, erodibility, weathering, and landscape aging resulting from fluvial erosion, hillslope diffusion, and uplift.

- Penck (1953), in his theory, mentions that in the waning or development stage, the gravity produced is in the upper region, in our case, and based on profile curvature, results in the gravity produced in isobase 6 and the wash slope of the lower region in isobase 7.
- From the Hypsometric integral result, in the waning or development stage, young and less eroded areas disappeared.
- The Surface Index in the evolution stage of isobases 8 and 9 highlights the appearance of three zones: a high dissected low-elevation zone, a moderately dissected hilly zone, and a third low dissected high-elevation zone. These zones may be associated with the End Rumpf stage.
- Prediction of the landscape evolution map of Lebanon-based isobase surfaces.

SI maps (Figure 11) highlight areas of low terrain amplitude, surrounded by more dissected complex landforms with high roughness, as indicated by fractal dimensions. Figure 11 illustrates the dual-terrain distribution, with positive values indicating elevated relief and negative values denoting dissected low relief.

SI is a measure of erosion: areas with low fractal dimensions yield positive SI values, whereas highly dissected terrain with high fractal dimension yields negative SI values. In recent surface, SI values range from -0.92 to 0.68, with negative values associated with highly dissected areas, such as V-shaped valleys.

Both the Lebanon and Anti-Lebanon mountainous chains exhibit positive surface indices, with higher values observed on their crests. Figure 11a delineates a transition belt from negative to positive SI values, dividing Lebanon into two regions: Eastern tectonic uplifted areas and Western erosion-prone areas. This transition belt becomes more complex in isobases 5 and 6 (Figures 11b and 11c), and the lower SI interval (-0.92 to 0.05) widens across the Ibrahim River valley and the higher lands of the Abou Ali River basin.

On the isobase surface 7, the transition belt assumes a smoother form, connecting Lebanon and the Anti-Lebanon Mountains and encircling the Beqaa Valley. In the western part, dissection intensifies in the Ibrahim and Abou Ali watersheds (Figure 11d).

In the landscape evolution stage of isobase 8 (Figure 11e), three zones emerge: a highly dissected low-elevation zone (the coastal area), a moderately dissected hilly zone in the middle and south of the study area, and a third low-dissected high-elevation zone to the east. This result allows us to relate isobase 8 and isobase 9 to the End Rumpf landscape evolution stage (slopes backwashing) of Penck, which depends on uplift and erosion.

Landscape assessment involves mapping the residual topography of the recent surface by subtracting isobase 5 from isobase 6 to form topographic surface A, subtracting isobase 6 from isobase 7 to form surface B, and subtracting isobase 7 from isobase 8 to create topographic surface C (Filosofov, 1975). These three topographic residual surfaces depict terrain fluvial incision, influenced by factors such as tectonic activity, isobase surface variations, lithology, vegetation, and climate (Gomez et al., 2006). These factors collectively

contribute to the Landscape evolution map of Lebanon in Figure 12.

The predicted landscape evolution map of Lebanon (Figure 12) aligns with the profiles in Figure 6, highlighting areas of high- to low-evolution during the erosion cycle and categorized into five stages. Stage one represents the initial development episode, encompassing the evolution of the Lebanon mountainous chain, including Qornet Es Sawda, Sannine, Barouk, Knise, and some isolated hills. The final stage of the evolution map corresponds to older river terraces, formed by vertical erosion of streams into their depositional floodplains. This stage exhibits terraces at different heights, indicative of former riverbed levels, particularly along the Abou Ali and Ibrahim rivers.

The results of morphometrical analysis of the isobase surfaces reveal several key findings:

- The decrease in slope and elevation is proportional to landscape evolution between isobase surfaces.

- The variation in isobase surfaces' elevation intervals confirms varying degrees of simultaneous tectonic movements and erosion processes.

Hypsometric curves indicate equilibrium in landscape evolution on isobase surfaces 5 and 6, but an imbalance in the evolution of the older stage isobase surfaces 8 and 9.

- Relative relief results suggest that, according to Davis's theory, the mature stage begins with isobase surface 4, whereas, following Penck's theory, waning development initiates with the recent surface and continues in Isobases 1, 2, and 3.

- For the old stage, both Davis's and Planck's theories concur that absolute and relative relief decrease directly, with relative relief values declining in isobases 5, 6, 7, and 8.

- Fractal dimensions decrease, and the terrain becomes smoother, though not flat, as landscape evolution progresses from isobase 6 to isobase 8.

Based on the experimental results, Penck's theory is better suited to the landscape evolution of the Lebanese terrain. The recent evolution stage is the waning or development stage, with no further uplift, gravity, or wash slopes.

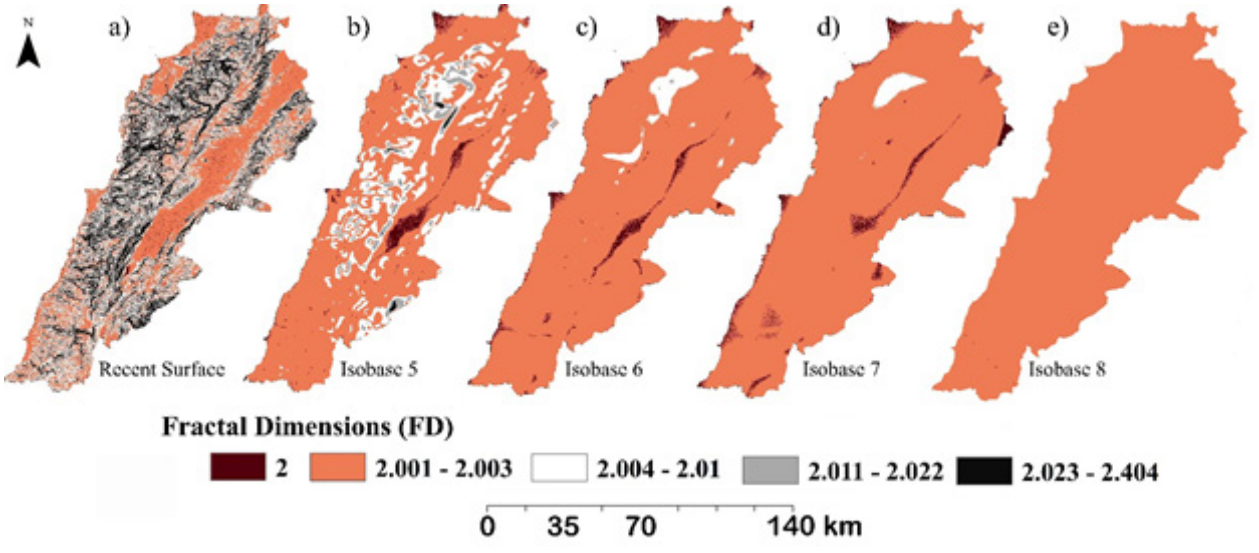

Figure 9. Fractal dimensions maps: a) recent surface, b) isobase 5, c) isobase 6, d) isobase 7, and e) isobase 8.

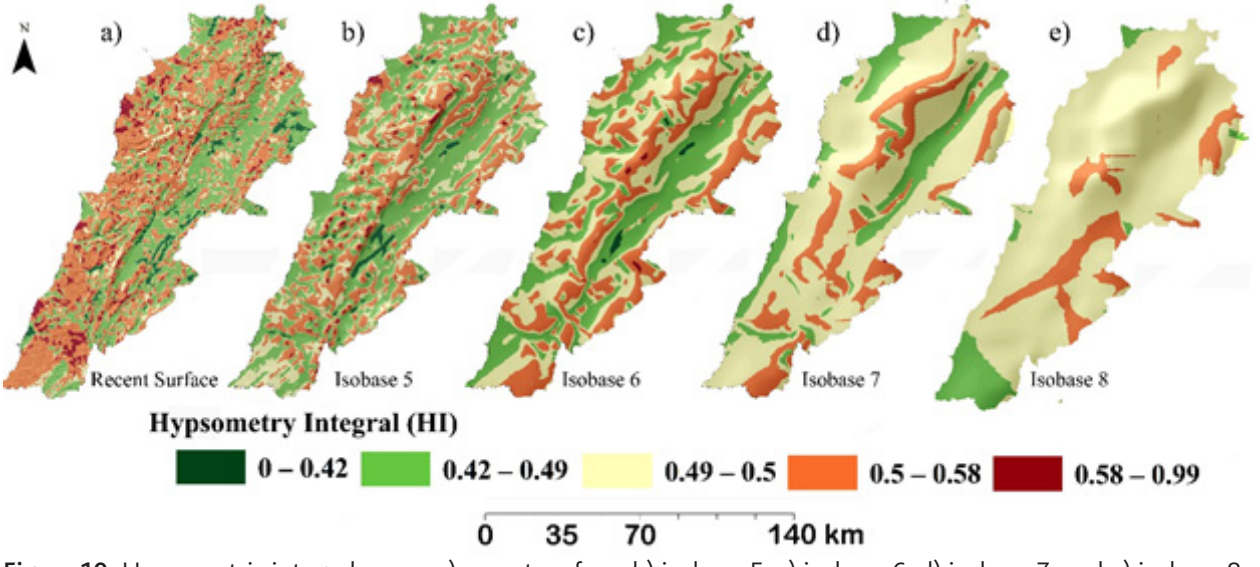

Figure 10. Hypsometric integral maps: a) recent surface, b) isobase 5, c) isobase 6, d) isobase 7, and e) isobase 8.

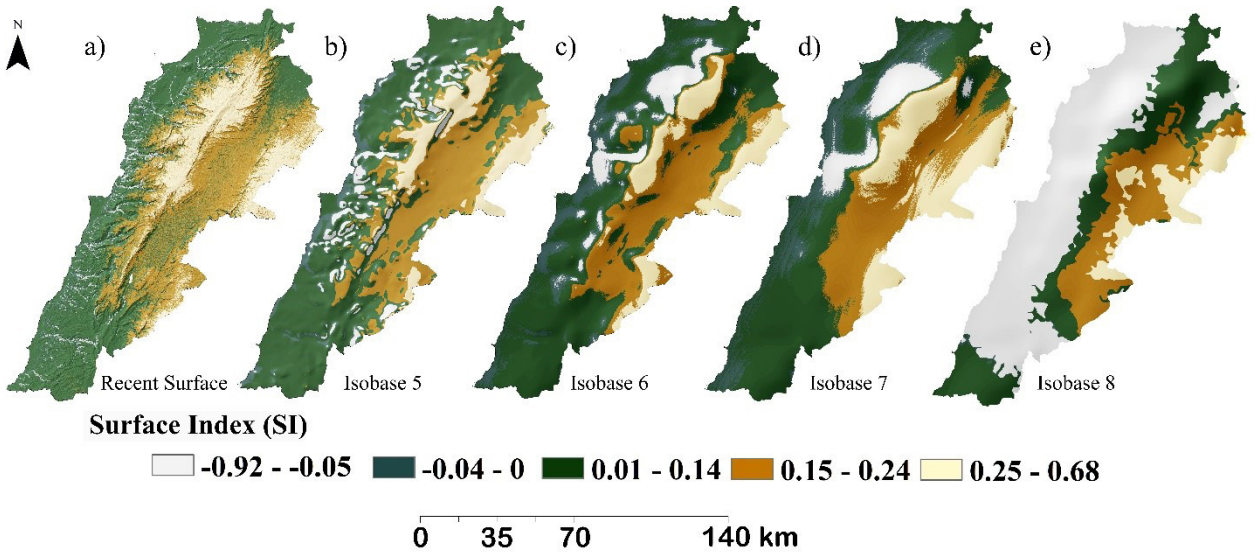

Figure 11. Surface index maps: a) recent surface, b) isobase 5, c) isobase 6, d) isobase 7, and e) isobase 8.

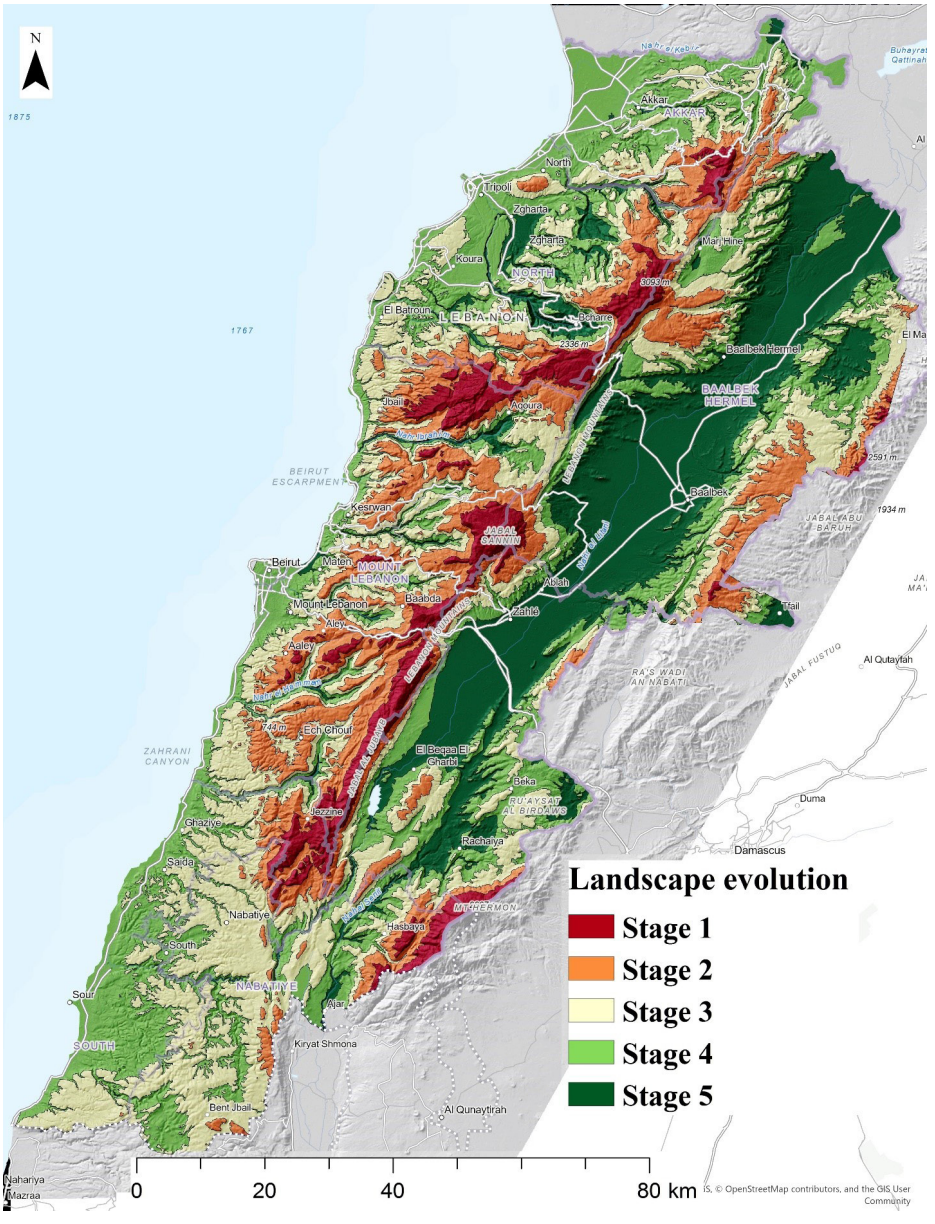

Figure 12. Landscape evolution map of Lebanon.

Conclusion

In our experiment, we aimed to comprehensively analyze landscape evolution. We used DEM and GIS tools to generate stream-order networks, construct isobase surfaces, and calculate geomorphometric indices. The analysis delineated distinct terrain patterns, shedding light on various tectonic and erosional stages.

We employed methods including topographic profiles, hypsometric curves, and morphometric maps applied to isobase surfaces of stream orders to gain insights into the spatial distribution of landscape evolution. The results of our geomorphometric analysis provided valuable insights, enabling us to link landscape evolution in Lebanon to Penck's theory.

It is important to note that our analysis focused exclusively on physiographic landscape forms to predict landscape evolution and was not directly linked to geological or tectonic studies. Instead, it introduced a novel approach that could complement future geological and tectonic analyses of the study area.

Based on our findings and applying Penck's theory, we propose a new hypothesis: both the waxing (accelerating) and uniform development stages have occurred, and we are currently in the waning (development) stage. The recent Lebanese terrain and isobases 1, 2, 3, and 4 are at the peak of the waning (mature) stage. Successive isobases 5, 6, and 7 mark the end of the waning development stage and the beginning of the old age stage. Isobases 8 and 9 represent the End Rumpf stage.

This experiment enhances our understanding of landscape evolution in Lebanon and underscores the potential of geomorphometric analysis to offer valuable insights into complex geological processes.

References

Andreani, L., Stanek, K. P., Gloaguen, R., Krentz, O., & Domínguez-González, L. (2014). DEM-based analysis of interactions between tectonics and landscapes in the Ore Mountains and Eger Rift (East Germany and NW Czech Republic). *Remote Sensing, 6*(9), 7971–8001.

Andreani, L., & Gloaguen, R. (2016). Geomorphic analysis of transient landscapes in the Sierra Madre de Chiapas and Maya Mountains (northern Central America): Implications for the North American–Caribbean–Cocos plate boundary. *Earth Surface Dynamics, 4*, 71–102. https://doi.org/10.5194/esurf-4-71-2016

Burt, T. P., Chorley, R. J., Brunsden, D., Cox, N. J., & Goudie, A. S. (Eds.). (2008). *The history of the study of landforms* (Vol. 4). The Geological Society.

Coates, D. R. (1984). Landforms and landscapes as measures of relative time. In *Quaternary dating methods* (pp. 247–267). https://doi.org/10.1016/S0920-5446(08)70075-X

Crickmay, C. H. (1974). *The work of the river: A critical study of the central aspects of geomorphology*. American Elsevier Publishing Company.

Davis, W. M. (1889). The rivers and valleys of Pennsylvania. *National Geographic Magazine, 1*, 183–253.

Davis, W. M. (1899). The geographical cycle. *The Geographical Journal, 14*(5), 481–504. https://doi.org/10.2307/1774538

Davis, W. M. (1905). Complications of the geographical cycle. In *Eighth International Geographical Congress, Washington, 1904* (pp. 150–163).

Davis, W. M. (1909). *Geographical essays* (D. W. John son, Ed.). Ginn and Company.

Domínguez-González, L., Andreani, L., Stanek, K. P., & Gloaguen, R. (2015). Geomorphotectonic evolution of the Jamaican restraining bend. *Geomorphology, 228*, 320–334. https://doi.org/10.1016/j.geomorph.2014.09.019

Doumit, J. A. (2017). *Digital terrain analysis of Lebanon: A study of geomorphometry*. Scientific Edition Polygraph Center, Kuban State University.

Doumit, J. A., & Kiselev, E. N. (2019). The quantitative approach of relative height and microrelief: Three case studies from Lebanon. In *Science and practice solutions: Strategic and tactical tasks of sustainable development of Russia* (pp. 16–19).

Dubertret, L. (1934). Présentation d'une carte géologique générale au 1:1 000 000 de la Syrie et du Liban. *Revue de Géographie Physique et de Géologie Dynamique, 6*(4), 269–318.

Dubertret, L. (1947). Aperçu de géographie physique sur le Liban, l'Anti-Liban et la Damascène. *Notes et Mémoires, 4*, 191–226.

Dury, G. H. (1952). *Map interpretation*. Edward Arnold.

Evans, I. S. (1980). An integrated system of terrain analysis and slope mapping. *Zeitschrift für Geomorphologie, Neue Folge, Supplementband, 36*, 274–295.

Filosofov, V. P. (1960). *A brief guide to morphometric methods in search of tectonic structures*. Saratov University Publishing House. [In Russian]

Filosofov, V. P. (1970). Maps of isobases and residual relief. In *Application of geomorphic methods in structural investigations* (pp. 43–52). NEDRA. [In Russian]

Filosofov, V. P. (1975). *The basis of the morphometric method in search of tectonic structures*. Saratov University Publishing House. [In Russian]

Florinsky, I. V. (2012). Digital elevation models. In *Digital terrain analysis in soil science and geology* (pp. 1–25). Academic Press. https://doi.org/10.1016/B978-0-12-385036-2.00003-1

Gary, M., McAfee, R., Jr., & Wolf, C. L. (Eds.). (1973). *Glossary of geology* (2nd ed.). American Geological Institute.

Golts, S., & Rosenthal, E. (1993). A morphotectonic map of the northern Arava in Israel, derived from isobase lines. *Geomorphology, 7*, 305–315. https://doi.org/10.1016/0169-555X(93)90060-F

Gomez, F., Khawlie, M., Tabet, C., Darkal, A. N., Khair, K., & Barazangi, M. (2006). Late Cenozoic uplift along the northern Dead Sea Transform in Lebanon and Syria. *Earth and Planetary Science Letters, 241*, 913–931. https://doi.org/10.1016/j.epsl.2005.10.029

Gravelius, H. (1914). *Flusskunde*. G. J. Göschen'sche Verlagshandlung.

Grohmann, C. H., Riccomini, C., & Alves, F. M. (2007). SRTM-based morphotectonic analysis of the Poços de Caldas Alkaline Massif, southeastern Brazil. *Computers & Geosciences, 33*(1).

Grohmann, C. H., Riccomini, C., & Chamani, M. A. C. (2011). Regional-scale analysis of landform configuration with base-level (isobase) maps. *Hydrology and Earth System Sciences, 15*, 1493–1504. https://doi.org/10.5194/hess-15-1493-2011

Hack, J. T. (1960). Interpretation of erosional topography in humid temperate regions. *American Journal of Science, 258-A*, 80–97.

Hamood, R. R. (2009). The cycle of erosion was proposed in Davis and Penck's comparative study. *Al-Fatih Journal, 5*(38), 65–79.

Horton, R. E. (1945). Erosional development of streams and their drainage basins: Hydrophysical approach to quantitative morphology. *Geological Society of America Bulletin, 56*(3), 275–370. https://doi.org/10.1130/0016-7606(1945)56%5B275:EDOSAT%5D2.0.CO;2

Keller, E. A., & Pinter, N. (1996). *Active tectonics: Earthquakes, uplift, and landscape*. Prentice Hall.

King, L. C. (1953). Canons of landscape evolution. *Geological Society of America Bulletin, 64*(7), 721–752. https://doi.org/10.1130/0016-7606(1953)64%5B721:COLE%5D2.0.CO;2

Lee, Y. H., Carr, J. R., Barr, D. J., & Haas, C. J. (1990). The fractal dimension as a measure of the roughness of rock discontinuity profiles. *International Journal of Rock Mechanics and Mining Sciences & Geomechanics Abstracts, 27*(6), 453–464. https://doi.org/10.1016/0148-9062(90)90998-H

Logan, T. A., Nicoll, J., Laurencelle, J., Hogenson, K., Gens, R., Buechler, B., Barton, B., Shreve, W., Stern, T., Drew, L., & Guritz, R. (2014, December). Radiometrically terrain-corrected ALOS PALSAR data available from the Alaska Satellite Facility [Conference presentation abstract]. *American Geophysical Union Fall Meeting 2014*.

Mahmood, S. A., & Gloaguen, R. (2012). Appraisal of active tectonics in Hindu Kush: Insights from DEM-derived geomorphic indices and drainage analysis. *Geoscience Frontiers, 3*, 407–428. https://doi.org/10.1016/j.gsf.2011.12.002

Mandelbrot, B. B. (1982). *The fractal geometry of nature*. W. H. Freeman.

Moss, J. H. (1977). The formation of pediments: Scarp back wearing or surface down wasting. In D. O. Doehring (Ed.), *Geomorphology of arid regions* (pp. 51–78). State University of New York.

Pannekoek, A. F. (1967). Generalized contour maps, summit level maps and streamline surface maps as geomorphological tools. *Zeitschrift für Geomorphologie, 11*, 169–182.

Penck, W. (1953). *Morphological analysis of landforms* (H. Czech & K. C. Boswell, Trans. & Eds.). Macmillan.

Pike, R. J., & Wilson, S. E. (1971). Elevation-relief ratio, hypsometric integral, and geomorphic area-altitude analysis. *Geological Society of America Bulletin, 82*(4), 1079–1084. https://doi.org/10.1130/0016-7606(1971)82%5B1079:ERHIAG%5D2.0.CO;2

Sarp, G., Toprak, V., & Düzgün, Ş. (2011). Hypsometric properties of the hydrologic basins located on the western part of NAFZ. In *Proceedings of the 34th International Symposium on Remote Sensing of Environment*. Sydney, Australia.

Scotti, V. N., Molin, P., Faccenna, C., Soligo, M., & Casas-Sainz, A. (2014). The influence of surface and tectonic processes on landscape evolution

of the Iberian Chain (Spain): Quantitative geomorphological analysis and geochronology. *Geomorphology, 206*, 37–57. https://doi.org/10.1016/j.geomorph.2013.09.017

Strahler, A. N. (1952). Hypsometric (area-altitude) analysis of erosional topography. *Geological Society of America Bulletin, 63*(11), 1117–1142. https://doi.org/10.1130/0016-7606(1952)63%5B1117:HAAOET%5D2.0.CO;2

Strahler, A. N. (1957). Quantitative analysis of watershed geomorphology. *Eos, Transactions American Geophysical Union, 38*(6), 913–920. https://doi.org/10.1029/TR038i006p00913

Summerfield, M. A. (1991). *Global geomorphology*. Longman Scientific & Technical.

Vasconcelos, P. M., & Carmo, I. de O. (2018). Calibrating denudation chronology through $^{40}Ar/^{39}Ar$ weathering geochronology. *Earth-Science Reviews, 179*, 411–435. https://doi.org/10.1016/j.earscirev.2018.01.003

Von Engeln, O. D. (1960). *Geomorphology*. The Macmillan Company.

Walley, C. D. (1998). *The geology of Lebanon*. American University of Beirut.

Worcester, P. G. (1958). *Textbook of geomorphology*. D. Van Nostrand Company.

Zevenbergen, L. W., & Thorne, C. R. (1987). Quantitative analysis of land surface topography. *Earth Surface Processes and Landforms, 12*, 47–56. https://doi.org/10.1002/esp.3290120107

INTERNATIONAL SCIENTIFIC JOURNAL | GEOGRAPHICA PANNONICA | Volume 30, Issue 2, 153–164 (June 2026)
Journal homepage: http://www.dgt.uns.ac.rs/en/homepage/pannonica/

Epikarst Springs as Atmospheric CO_2 Sinks in a Tropical Karst Environment: Evidence from the Gunungsewu Karst, Indonesia

Rasyiida Acintya[A], Tjahyo Nugroho Adji[A*], Ahmad Cahyadi[A], Wafiq Nur Azizah[A], Akhmad Singgih[A]

[A] *Karst Research Group, Faculty of Geography, Universitas Gadjah Mada, Sekip Utara, 55281, Yogyakarta, Indonesia.*

Received: March 28, 2026| Revised: July 7, 2026| Accepted: July 28, 2026
doi: 10.5937/gp30-66090

ABSTRACT

Karst ecosystems, covering 15% of global land, serve as vital carbon sinks, especially in the epikarst zone. This study examines the carbon sink capacity of epikarst spring catchments using field data from August 2022 to July 2023. Applying the hydrochem-discharge method, discharge and dissolved bicarbonate (HCO_3^-) concentrations were analyzed at two-week intervals. The results reveal that epikarst springs absorb atmospheric CO_2 at rates of 747.34–787.00 tons/km^2/year, significantly surpassing non-epikarst springs (576.92 tons/km^2/year). This sequestration capacity is driven by seasonal rainfall, discharge volume, and ion levels. Compared to other karst regions on Java Island, these springs demonstrate superior absorption, highlighting their critical importance in the global carbon cycle.

Keywords: epikarst springs; atmospheric CO_2 sequestration; Gunungsewu karst; dissolution processes

Introduction

According to Yoro and Daramola (2020), carbon dioxide (CO_2), as a greenhouse gas, accounts for 50% of the occurrence of global warming and climate change. The escalation of carbon dioxide emissions in the atmosphere exerts a detrimental influence on ecosystems, necessitating the implementation of a mechanism capable of regulating atmospheric carbon dioxide emissions (Kabir et al., 2023; Nunes, 2023). Chen et al. (2023) thus clarified that through the dissolution process of carbonate rocks, karst areas naturally absorb atmospheric carbon dioxide. Furthermore, Wu et al. (2023) clarify the difference between karst and other ecosystems, namely that in karst ecosystems all CO_2 generated from respiration is absorbed by the dissolution process whereas in non-karst ecosystems CO_2 emitted by respiration will remain as emissions in the atmosphere. In addition, the interaction of carbon dioxide (CO_2) from the atmosphere or soil with water (H_2O) will result in the formation of carbonic acid (H_2CO_3). The carbon value derived from titration of karst spring water represents approximately half of the total carbon, with the remaining half originating from the atmosphere and soi (Martin, 2017; Jiang, 2013).

Karst areas, which cover around 2.2×10^7 km^2 globally (15% of the Earth's total surface area), have the capacity to sequester carbon on land at a rate of approximately 2.5 Pg C/year (Pu et al., 2015). The absorption of CO_2 by the dissolution of limestone accounts for + 33% of worldwide forest carbon absorption, ± 68% of carbon in soil, ± 23% of the world's missing carbon

*Corresponding author: Tjahyo Nugroho Adji,; email: adji_tjahyo@ugm.ac.id

sink, and ± 7.5% - 8.3% of the total emissions produced by fossil fuels (Huang et al., 2024; Cao et al., 2018). Hence, it is imperative to acknowledge the significance of natural carbon absorption in this karst region into the foreseeable future, spanning hundreds of years or beyond (Xie et al., 2021).

Balazs (1968) estimates that Indonesia's karst region encompasses approximately 150,000 square kilometers. Karst areas are present on nearly all islands in Indonesia, including Sumatra, Java, Kalimantan, Sulawesi, and Papua. Additionally, Balazs (1971) elucidated that the Maros karst area in South Sulawesi and the Gunungsewu karst on Java Island are two karst areas in Indonesia that are considered prototypes of tropical karst. These areas are characterized by their unique topography. According to Haryono (2011)'s research, the estimated quantity of CO_2 that can be absorbed through the dissolution of carbonate rocks in Indonesia is 13,482 Gg/year.

Epikarst, also known as "karst layer skin", refers to a thin zone that is typically found near the surface of karst topography (Bakalowicz, 2019; Fu et al., 2015). The epikarst zone is distinguished by the extensive formation of fractures, which is influenced by factors such as the type of limestone rock, climate, hydrology, and vegetation (Pardo-Igúzquiza et al., 2018; Bakalowicz, 2013). From an ecological perspective, epikarst is regarded as a "reservoir" of biodiversity (Kozel & Pipan, 2020). Epikarst represents the uppermost weathered and highly fractured part of the karstified rock mass, where porosity and permeability are generally higher than in the deeper carbonate rocks. This zone plays an important role in storing and redistributing infiltrating water, regulating recharge to the vadose zone, and enhancing water–rock interaction (Klimchouk, 2004). Because epikarst is also a zone where geological, hydrological, biological, and chemical processes interact, its characteristics can vary greatly among karst systems (Milanović, 2025). In this study, such characteristics are important because they help explain the diffuse flow, prolonged carbonate dissolution, and atmospheric CO_2 sequestration observed in epikarst springs.

Furthermore, epikarst serves as a vertical extension of the soil and functions as a storage site for organic matter accumulation (Srivastava et al., 2012). Specifically, it is where CO_2 derived from the decomposition of organic matter is stored, making it the primary factor in the dissolution of carbonate rocks (Chen et al., 2021). Jiang (2013) discovered that epikarst plays a significant role in the production, storage, and distribution of carbon dioxide in karst aquifers. Epikarst functions as a reservoir for CO_2, gradually replenishing the infiltration zone through a slow infiltration process (Cheng et al., 2023). Specifically, this gradual infiltration results in the mixing of air and water in tiny cavities and pores, leading to the downward movement of CO_2-rich air into the soil system and its subsequent distribution across the infiltration zone (Williams, 2008; Trček, 2002). In this process, if there is a quick influx of water, whether from direct dispersion or point recharge, it will still have the ability to dissolve CO_2 (Jiang et al., 2013). Consequently, the carbonate rocks in the phreatic zone become more soluble (Jones, 2013). Hence, the storage of water in the epikarst plays a crucial role in the formation of karst landscapes and the capture of carbon, both in shallow and deep zones (Nannoni & Piccini, 2022; Yang et al., 2012).

Regarding the development of voids in karst aquifers, Fores et al. (2021) revealed that epikarst springs originate from water stored in undeveloped epikarst zones. Consequently, the flow in these springs is primarily recharged by slow-moving infiltration water (diffuse flow). The elevated levels of CO_2 in epikarst springs are a result of the extensive water-rock interaction process and the presence of mechanisms in the soil (Cahyadi et al., 2023a; Nurkholis et al., 2019). Conversely, non-epikarst springs have undergone significant void development resulting in faster and more turbulent water flow (Adji et al., 2017). As a consequence, there is a decrease in the absorption of carbon dioxide.

The Gunungsewu Karst area is characterized by the presence of epikarst springs in the Ponjong hydrogeological subsystem, which serve as the primary water source for the local people (Riyanto & Cahyadi, 2023). This subsystem exhibits a distinct pattern of groundwater movement in the direction of the west and south. It is noteworthy for its significant discharge and continuous flow throughout the year. The upstream part of this subsystem typically contains epikarst springs, while the downstream part is characterized by non-epikarst springs (Cahyadi et al., 2023b). The main objective of this study is to determine the carbon sink capacity of the epikarst spring catchment area. Furthermore, the carbon sequestration capacity of epikarst springs is compared to that of non-epikarst springs. At a broader scale, this study provides new evidence on the role of tropical karst systems in atmospheric CO_2 sequestration. The findings highlight how warm temperatures, seasonal rainfall, and epikarst hydrological processes can enhance carbonate dissolution and support natural carbon uptake in humid tropical environments.

Materials and Methods

Carbon sequestration studies were performed at three epikarst springs: Gedaren, Sulu, and Sumber Ponjong Springs, while the Seropan Underground River served as a non-epikarst spring sample (Figure 1). These four sites are part of the Ponjong hydrogeological subsystem, Gunungsewu Karst. The Ponjong hydrogeological subsystem is characterized by perennial springs and underground drainage systems, where groundwater

movement is mainly influenced by the local karst conduit–fracture network, catchment morphology, and recharge conditions (Cahyadi et al., 2023b).

Gunungsewu Karst is a part of the Southern Mountains on Java Island. It consists of a sequence of hills that create a highland landscape in the southern region of Java. The area extends from Ciletuh Bay in West Java to the Blambangan Peninsula in East Java (Reinhart et al., 2023). The Gunungsewu Karst is composed of the Wonosari-Punung Formation (Tmwl), which is a type of Neogene limestone. This limestone is characterized by extensive coral reef formations in the southern region and multiple layers of limestone in the northern region. The formation is classified as Middle Miocene and Upper Pliocene in terms of its age, and it is estimated to have a thickness exceeding 650 m, as reported by Hartawan et al. (2020). The terrain surrounding the main karst aquifer consists of several non-carbonate and mixed lithological units, including volcanic, volcaniclastic, siliciclastic, and Quaternary deposits. These surrounding formations form a contrasting geological setting because they are generally less soluble than limestone and tend to support more developed surface drainage.

The long-term rainfall data for 2002–2022 were used to describe the general climatic condition of the Gunungsewu Karst area. In addition, monthly rainfall data corresponding to the monitoring period were processed and used in the temporal analysis. These monitoring-period rainfall data were matched with the

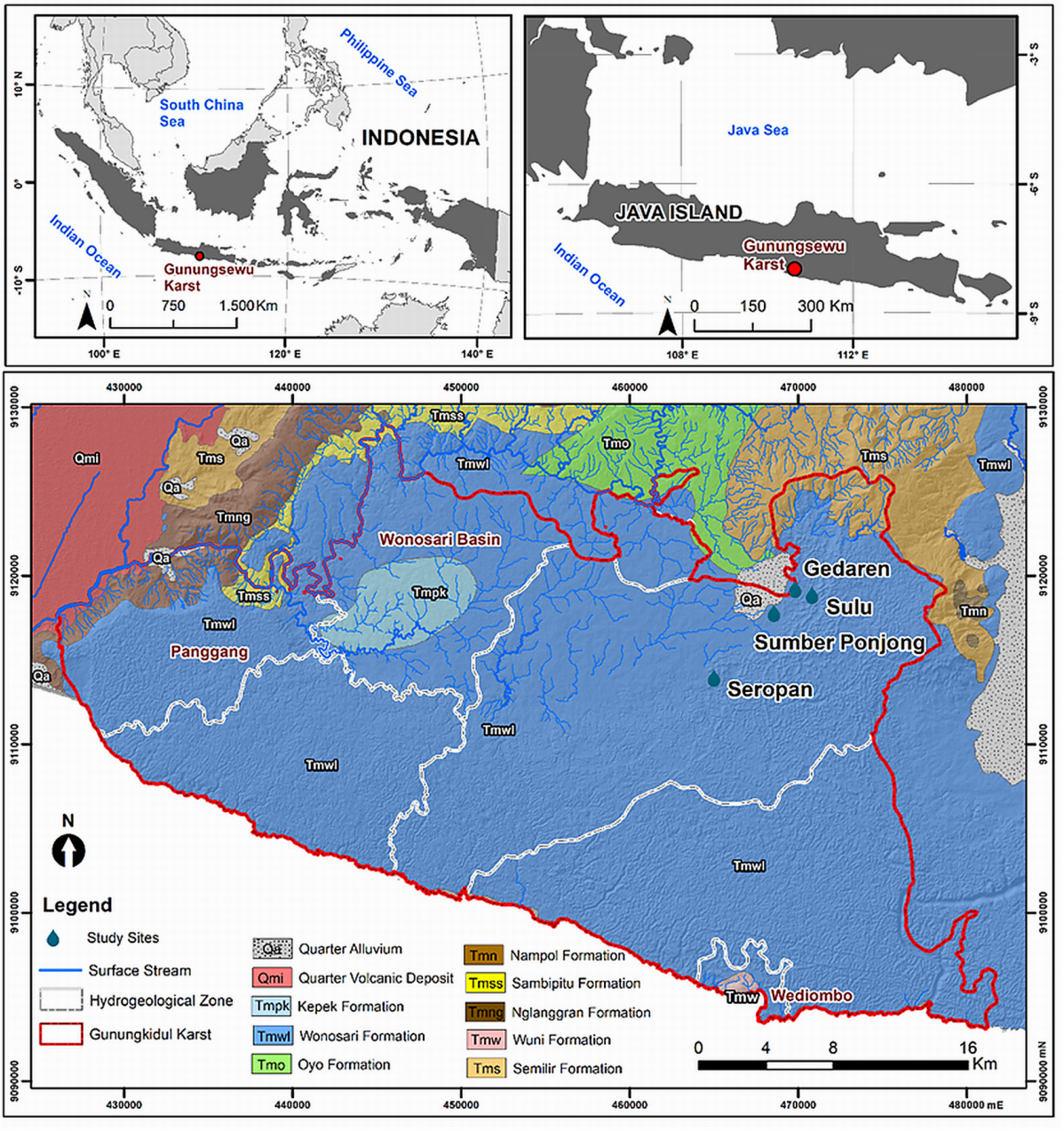

Figure 1. Location and geological setting of the studied epikarst springs and Seropan Underground River within the Gunungsewu Karst, Indonesia, including hydrogeological zones, surface rivers, and surrounding geological formations.

discharge, HCO_3^- concentration, and CO_2 sequestration records to evaluate the seasonal response of each spring system. Therefore, the long-term rainfall record represents the climatic background, whereas the monitoring-period rainfall data represent the hydrological forcing during the observation period.

The Gunungsewu Karst area has a distinct seasonal climate. Based on long-term data from 2002 to 2022, the area receives an average annual rainfall of about 2,355 mm, with rainfall mainly concentrated during the wet season. During the same period, the mean monthly air temperature was approximately 25.9 °C (Figure 2).

Temporal discharge data at each spring and the dissolved HCO_3^- concentration in mg/litre are required to calculate carbon sequestration accurately. The data were collected over one year, with samples collected every two weeks. The velocity-area method is employed to measure the discharge of springs and underground rivers, while a current meter is employed to measure the flow velocity. Meanwhile, the Alkalinity Test Kit MQuant® 1.11109 was employed to directly measure the dissolved HCO_3^- concentration in the field through titration. The catchment area is determined using the balance approach (Widyastuti et al., 2019) through evapotranspiration calculations:

$$V = (P - E) \times A \quad (1)$$

Where V is the discharge in volume (liter/year), P is precipitation (mm/year), E is evapotranspiration (mm/year), and A is the catchment area (m^2). The V value (total water volume) is obtained through the following equation (Widyastuti et al., 2019):

$$V = \left(\frac{Q(n)+Q(n+1)}{2} + \frac{Q(n+1)+Q(n+2)}{2} + \cdots + \frac{Q(m-1)+Q(m)}{2}\right) \times unit\ of\ time \quad (2)$$

$V = Q\ x\ unit\ of\ time$

Where V is total volume (liter), Q is total discharge (liter/year), Q(n) is the first discharge data (liter/second), Q(m) is the last discharge data (liter/second), and Unit of time is the time lapse of each recording (second).

Next, the rate of atmospheric carbon sequestration was determined using the hydrochem-discharge method (Liu & Zhao, 2000) with the following formula:

$$F = 0.5 \times [HCO_3-] \times Q \times (M_{CO2}/M_{HCO3}) \quad (3)$$

Where, F is the rate of atmospheric carbon sequestration (gram/year), HCO_3^- is the dissolved HCO_3^- (gram/liter), Q is the discharge (liter/year), M CO_2 is the Mr of CO_2 (44), and M HCO_3^- is the Mr of HCO_3^- (61.02). The F value in the formula given represents the quantity of carbon sequestration occurring in the catchment area of each spring/underground river. In order to convert carbon absorption into CO_2 absorption, a simple method is to use a stoichiometric equation with the formula:

$$CO_2 = F \times (atomic\ weight\ CO_2/atomic\ weight\ C) \quad (4)$$

Where, CO_2 is the atmospheric CO_2 sequestration rate (ton/year), F is the atmospheric C sequestration rate (ton/year), atomic weight of CO_2 is 44, and atomic weight of C is 12.

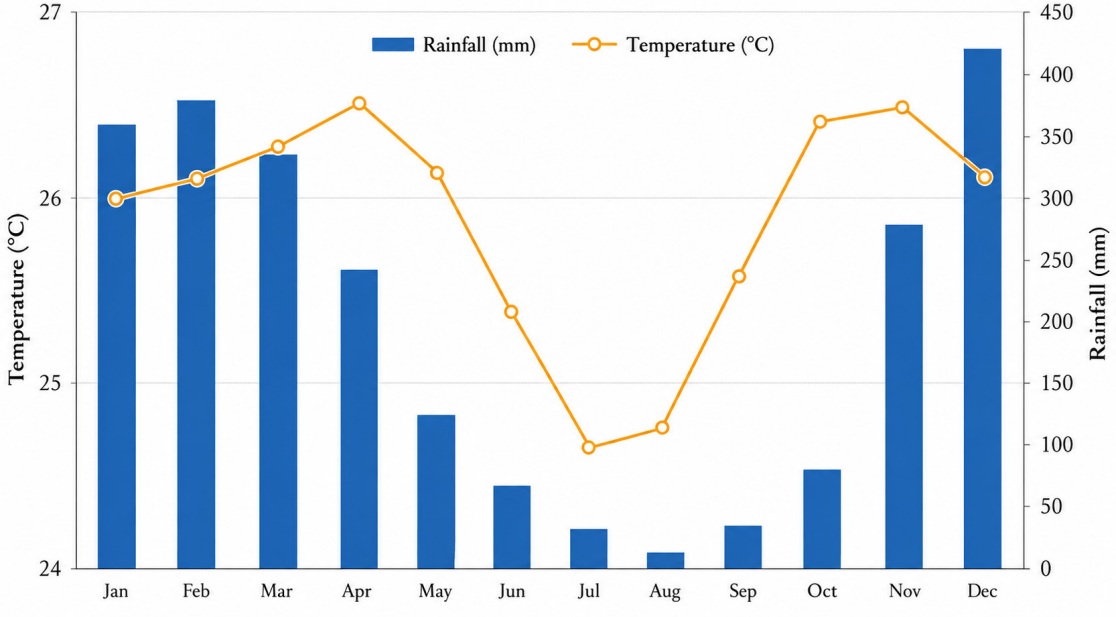

Figure 2. Long-term monthly rainfall and air temperature patterns in the Gunungsewu Karst area, based on climatic data used to describe the general climatic setting of the study area.

Results and Discussion

The sequestration of CO_2 is significantly affected by spring discharges and the concentration of dissolved bicarbonate ions (HCO_3^-). The discharge and HCO_3^- concentration measured at the spring outlet result from the accumulation of hydrological processes taking place in a water catchment area. The process of CO_2 absorption in karst springs begins with hydrological phenomena that include precipitation, infiltration, evapotranspiration, and the dissolution of carbonate rocks within a catchment area. Therefore, it is necessary to assess spring catchment requirements prior to estimating the absorption of atmospheric CO_2. Figure 3 displays the outcomes of estimating the catchment area using the water balance method. The Seropan Underground River has the most extensive catchment area, totalling 10.91 km^2. On the other hand, the Sumber Ponjong Springs has the smallest catchment area, measuring only 0.69 km^2.

The atmospheric carbon sequestration value obtained through the karstification process in epikarst and non-epikarst springs ranges from 157.33 to 214.62 tons/km^2/year, as determined by calculations and data analysis. Meanwhile, atmospheric CO_2 absorption values have a wider range of values, specifically from 576.92 to 787.00 tons/km^2/year (Table 1). CO_2 absorption rates in the three epikarst springs (Gedaren, Sulu, and Sumber Ponjong) are higher than that in the non-epikarst spring (Seropan).

Rainfall data for the monitoring period were processed and plotted together with discharge, HCO_3^- concentration, and CO_2 sequestration in Figure 4. This was done to ensure that the temporal variation of hydrochemical parameters could be interpreted in relation to the actual rainfall conditions during the observation period, rather than only from the long-term climatic average. The rainfall pattern shows clear seasonal variability, with higher rainfall during the wet season and lower rainfall during the dry season. This seasonal pattern helps explain the observed changes in spring discharge, bicarbonate concentration, and CO_2 sequestration. Collectively, the four springs show HCO_3^- concentration values ranging from 276 to 408 mg/litre. The HCO_3^- concentration in Seropan River is the lowest among the three epikarst springs. This is because the epikarst springs are primarily characterised by a diffuse flow type, which is typically highly saturated, resulting in a higher HCO_3^- concentration. Seasonally, the average absorption of atmospheric CO_2 in Sulu, Sumber Ponjong, and Seropan is greater during the dry season compared to the wet season (Figure 4). Here, due to the dilution effect of precipitation mechanism, high rainfall in the rainy season followed by an increase in spring discharge reduces HCO_3^- concentration and lowers CO_2 sequestration.

During the initial field measurement period, all springs exhibited significant fluctuation in CO_2 sequestration, particularly during the rainy season. The CO_2 levels during this time showed greater variability compared to the dry season. The temporal fluctuations in the rate at which atmospheric CO_2 is absorbed are primarily influenced by three key factors: rainfall, discharge, and the concentration of bicarbonate ions. In this scenario, the amount of rainfall is directly linked to the amount of discharge and is inversely linked to the concentration of HCO_3^-.

Table 1. CO_2 sequestration in epikarst and non-epikarst springs.

Location	Discharge (litre/year)	HCO_3^- (mg/litre)	Catchment area (km^2)	C (ton/km^2/year)	CO_2 (ton/km^2/year)
Gedaren	1,456,332,480.0	408.58	1.00	214.62	787.00
Sulu	1,733,709,124.8	392.39	1.16	211.21	774.52
Sumber Ponjong	1,042,780,073.6	375.37	0.69	203.80	747.34
Seropan (non-epikarst)	17,235,370,080.0	275.97	10.9	157.33	576.92
Average				**196.74**	**721.45**

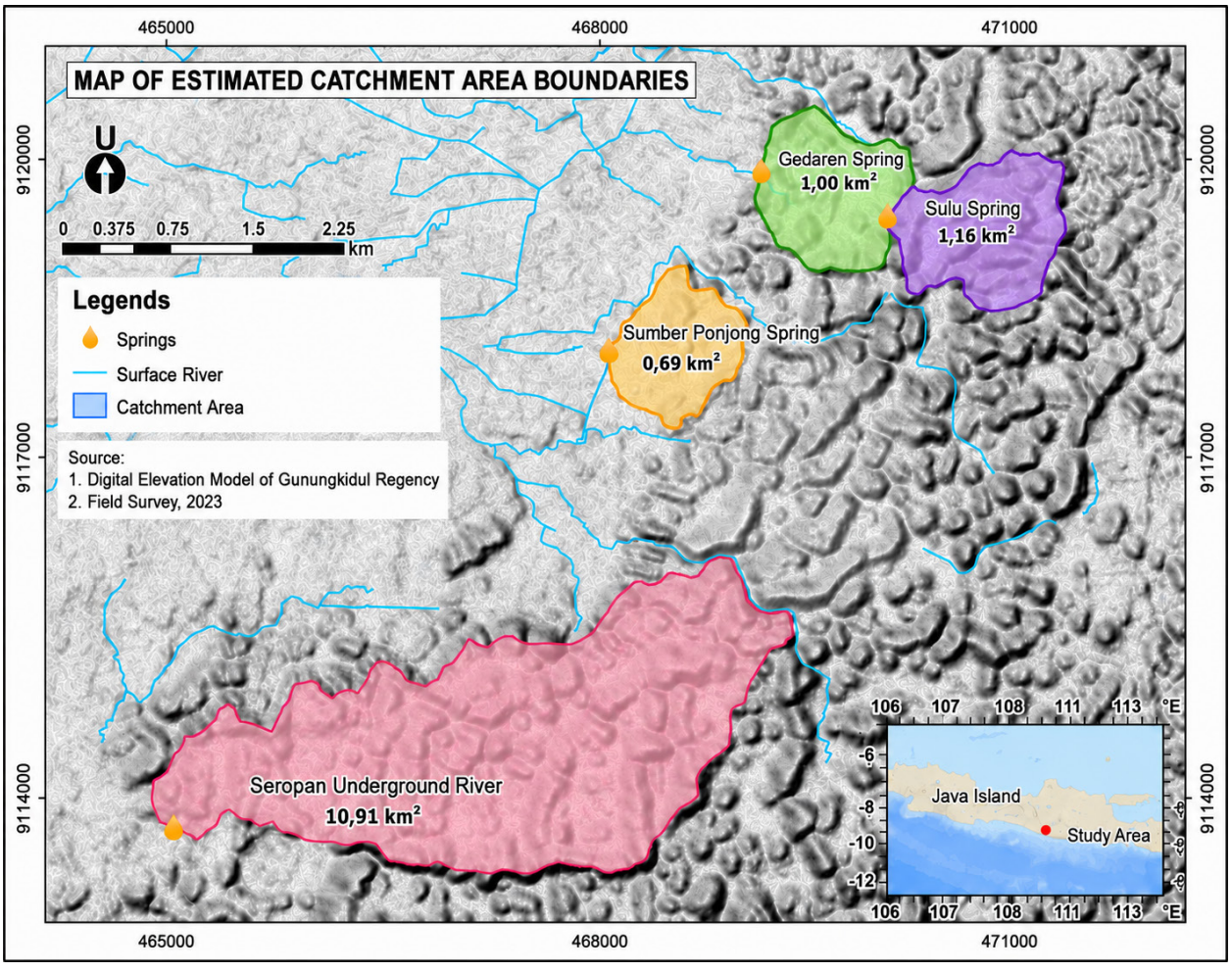

Figure 3. Estimated catchment boundaries of the studied epikarst springs and Seropan Underground River.

Nevertheless, there is no direct correlation between high rainfall and changes in discharge in epikarst springs. The phenomenon is attributed to a time delay, or time lag between precipitation and spring-discharge response that occurs in the catchment area. This delay is a result of the dominant diffuse flow characteristic of the epikarst spring type, which causes a slow response to rainfall (Adji et al., 2023). The duration of delay in the epikarst zone is affected by the changing intensity of rainfall, the thickness of the epikarst layer, the porosity, and the hydraulic conductivity (Aquilina et al., 2006; Zhang et al., 2013). It is evident that the rainy season reaches its peak in November 2022, while the flow discharge tends to be highest in January 2023. Despite the absence of rainfall in June 2023, the spring flow discharge can still be quantified as it originates from the accumulated rainwater from the preceding period.

The discharge observed at the springs in the study area is affected by the size of the spring catchment area. The larger the catchment area, the higher the capacity of water it can retain. The respective catchment areas of Gedaren, Sulu, Sumber, and Seropan Springs are 1.00 km², 1.16 km², 0.69 km², and 10.9 km², respectively. The size of the Seropan catchment area is directly correlated with the highest discharge value. Overall, the catchment area shows that Seropan has the highest atmospheric CO_2 absorption value, specifically 6,288.45 tons per year, while Sulu Springs follows with 899.39 tons per year. The Gedaren spring has a carbon dioxide absorption capacity of 786.68 tons per year, whereas the Sumber Ponjong spring has a capacity of 517.5 tons per year. These findings indicate that the Seropan catchment area has the highest capacity for absorbing atmospheric CO_2 among the three epikarst springs observed (Figure 5).

However, when viewed in units per km², epikarst springs have the greatest capacity to absorb CO_2 from the atmosphere. The epikarst zone, located in the upper soil layer, is directly influenced by vegetation and receives a large CO_2 input from respiration. This condition enhances CO_2 input to the epikarst zone. Meanwhile, the diffuse flow type in epikarst springs causes the water in this zone to move slowly, resulting in prolonged contact with carbonate rocks. This results in more saturated water and higher CO_2 absorption (Zeng et al., 2015). Furthermore, the epikarst zone is typically distinguished by a substantial layer of soil and abundant vegetation, which promotes elevated concentrations and pressures of CO_2 in the soil, consequently enhancing CO_2 absorption. The carbon cycle in the soil layer is recognized as a significant contributor to the process of karstification, despite its complexity re-

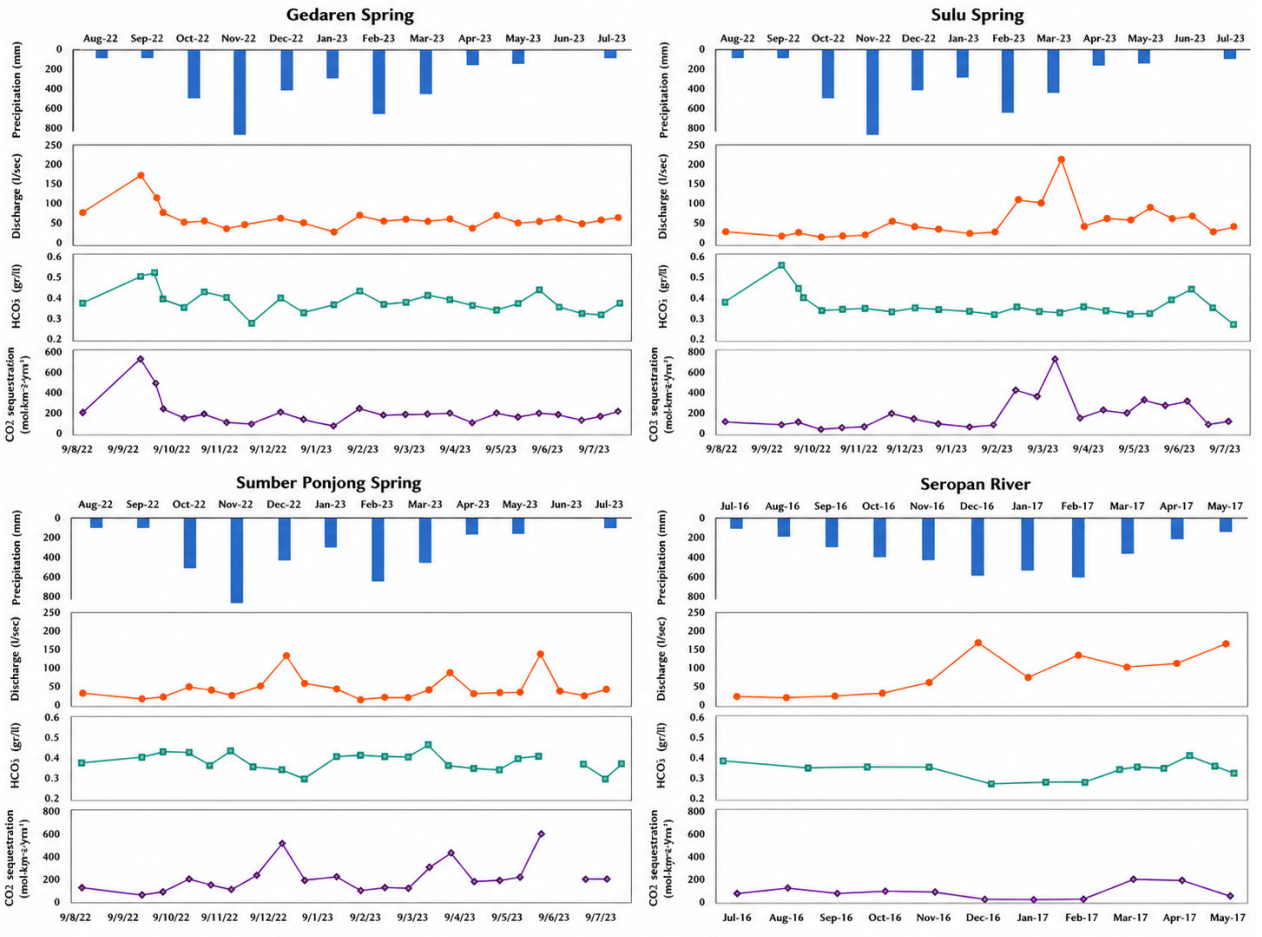

Figure 4. Temporal variations in precipitation, discharge, HCO_3^- concentration, and CO_2 sequestration at Gedar en, Sulu, Sumber Ponjong, and Seropan.

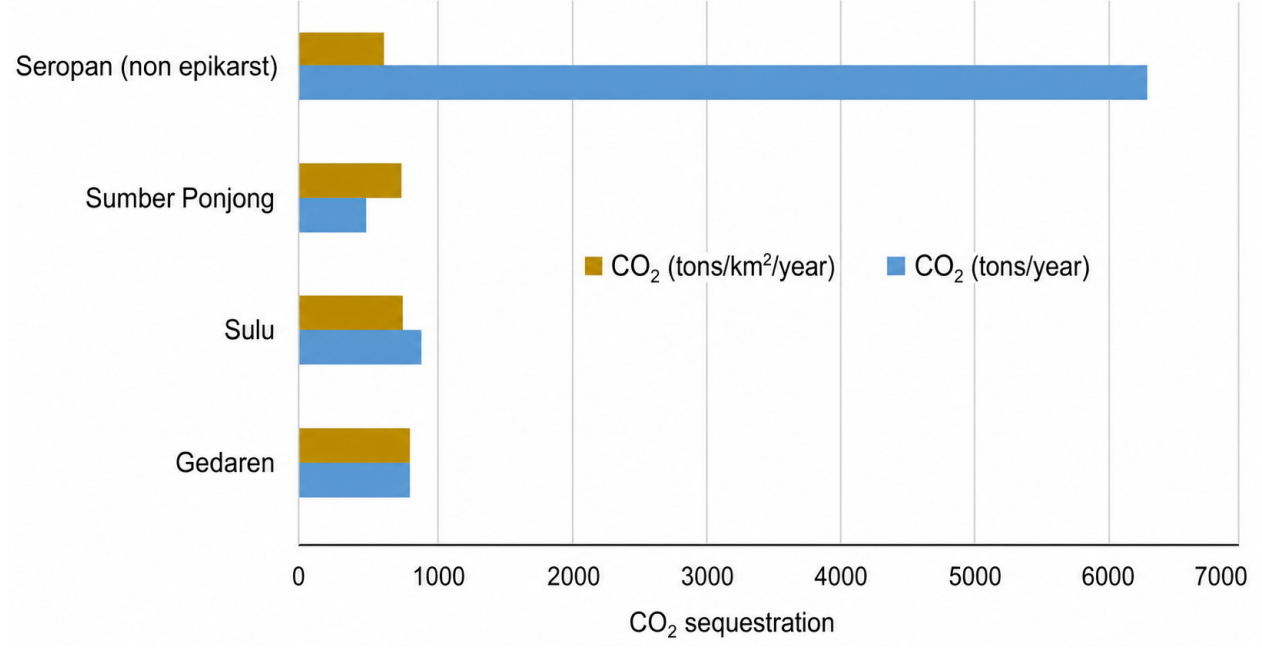

Figure 5. Comparison of total and area-normalized CO_2 absorption among epikarst springs and the non-epikarst Seropan Underground River.

sulting from soil limitations and moisture conditions (Jiang et al., 2013).

Figure 6 illustrates the conceptual position and function of epikarst in the Gunungsewu Karst system. The epikarst zone occurs near the surface, beneath the soil or regolith layer, and is characterized by intensive weathering, fractures, enhanced porosity, and higher permeability. Rainfall infiltrates diffusely into this zone, where part of the water may be temporarily stored, redistributed laterally, and then released slowly through epikarst springs such as Gedaren, Sulu, and Sumber Ponjong. In contrast, deeper conduit flow is represented by the underground river outlet, such as Seropan.

In the humid tropical setting of Gunungsewu, intensive karstification, strong weathering, and active soil formation may promote a more developed and locally thicker epikarst. These conditions increase water storage, prolong water–rock interaction, and enhance carbonate dissolution, helping explain the higher area-normalized CO_2 sequestration observed in the epikarst springs.

Compared to other tropical karst areas in Indonesia, epikarst springs have a higher capacity for absorbing CO_2. In the Jonggrangan karst area of Central Java, Dwiputra (2019) conducted an estimation of the amount of CO_2 sequestration in three springs: Mudal, Anjani, and Kiskendo springs. Table 2 presents a comparison of CO_2 absorption in two tropical karst areas in Indonesia.

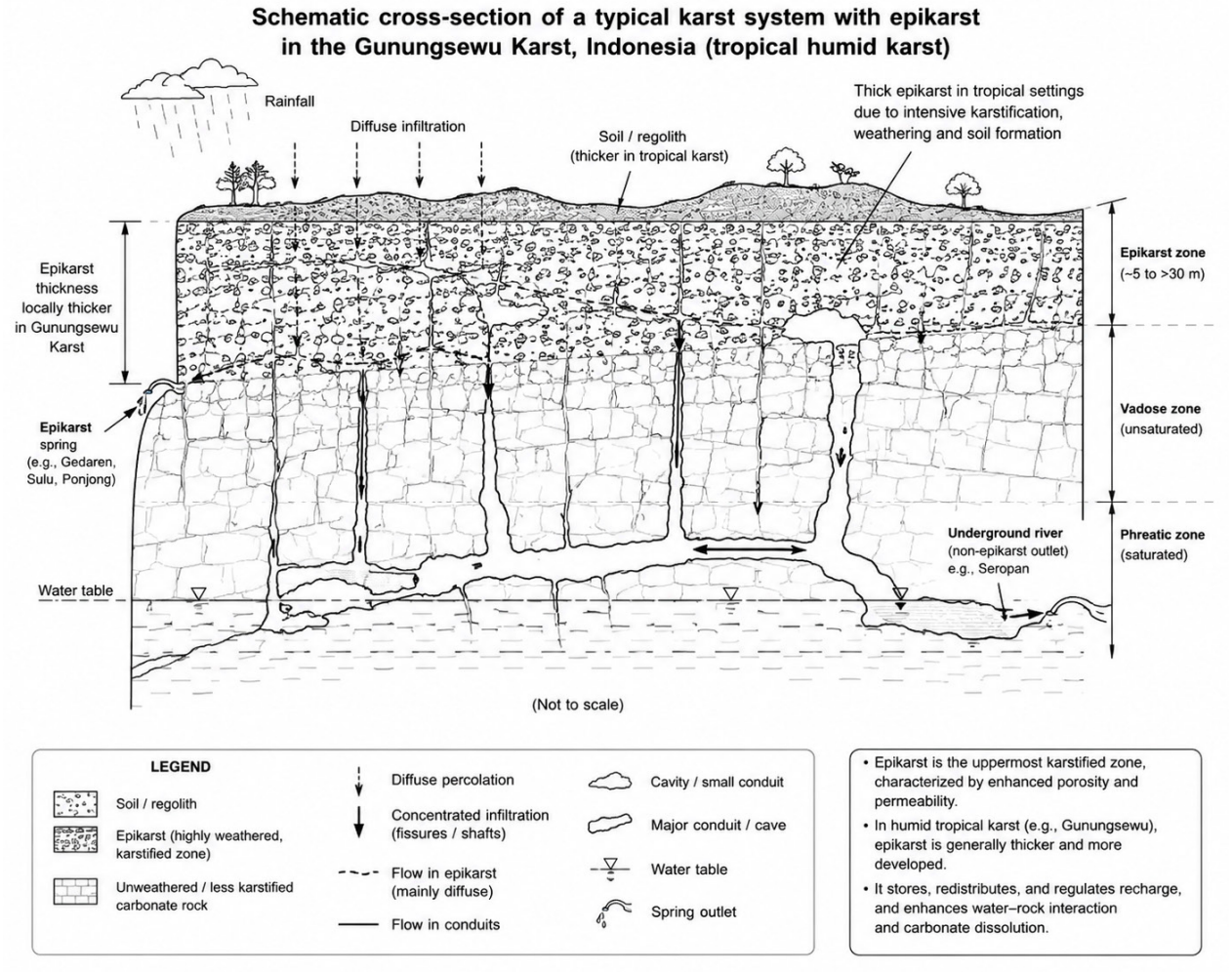

Figure 6. Conceptual cross-section of a typical tropical karst system in the Gunungsewu Karst, showing the po sition of the epikarst zone, diffuse infiltration, temporary storage, focused recharge, vadose and phreatic zones, epikarst springs, and the underground river outlet.

Table 2. CO_2 sequestration in Gunungsewu and Jonggrangan karst

Karst Area	Springs	Discharge (litre/year)	HCO_3^- (mg/litre)	Catchment area (km²)	CO_2 (ton/km²/year)
Gunungsewu (DIY province)	Gedaren (epikarst)	1,456,332,480.00	408.58	1.00	787.00
	Sulu (epikarst)	1,733,709,124.80	392.39	1.16	774.52
	Sumber Ponjong (epikarst)	1,042,780,073.60	375.37	0.69	747.34
	Seropan (non-epikarst)	17,235,370,080.00	275.97	10.9	576.92
Jonggran-gan-(Central Java province)	Mudal (non-epikarst)	10,379,559,298.60	290.00	7.05	564.48
	Anjani (non-epikarst)	4,818,823,835.75	210.00	4.00	334.47
	Kiskendo (non-epikarst)	8,627,129,496.38	260.00	6.90	429.79

The springs in the Jonggrangan karst are classified as non-epikarst springs. Generally, their absorption of CO_2 is lower than the epikarst springs found in the Gunungsewu karst. Furthermore, their absorption is even lower than that of the non-epikarst springs in Seropan. This comparison reveals that the catchment of epikarst springs plays a crucial role in the process of absorbing CO_2. This is due to the slow and diffuse flow in the aquifer, as well as the respiration mechanism of vegetation, which absorbs carbon dioxide from the air through the dissolution process. In addition, within the epikarst zone, carbon dioxide (CO_2) produced from the decomposition of organic material is retained, making it the main contributor to the dissolution of carbonate rocks.

The results of this study can also be placed in the broader context of karst carbon sink studies from other regions of the world. In subtropical karst regions of China, karst carbon sequestration has been shown to be strongly influenced by carbonate weathering, soil–vegetation processes, hydrological conditions, and human intervention in karst landscapes (Zhang et al., 2022). In contrast, high-alpine karst systems in Europe show different hydrological behavior because recharge, storage, and solute transport are strongly affected by snowmelt, seasonal flow dynamics, and clearly defined catchment conditions (Frank et al., 2021). Studies from stratigraphically complex karst areas in South Korea also show that hydrochemical and isotopic approaches are useful for identifying differences in spring-water flow types and groundwater pathways (Yu et al., 2021). These comparisons indicate that the hydrochem–discharge method is broadly applicable, but its results must be interpreted according to local climatic and hydrogeological conditions.

Compared with these karst environments, the relatively high CO_2 absorption per unit area in the Gunungsewu epikarst springs highlights the important role of tropical epikarst systems. Warm and humid conditions, active soil respiration, vegetation cover, diffuse flow, and longer water–rock interaction may support higher bicarbonate production and carbonate dissolution. Therefore, the Gunungsewu results provide useful evidence from tropical karst and strengthen the view that epikarst springs can play an important role in natural atmospheric CO_2 sequestration.

Conclusions

This study confirms that epikarst is a crucial zone in the carbon sequestration mechanism in tropical karst areas. Epikarst springs in Gunungsewu have been shown to have a higher CO_2 absorption capacity per unit area than non-epikarst systems, ranging from 747.34 to 787.00 tons/km²/year, while Seropan only has 576.92 tons/km²/year. This high absorption indicates that the slow, diffuse flow character of epikarst creates more ideal conditions for carbonate dissolution and the absorption of atmospheric CO_2. This finding is further strengthened by the fact that the absorption value in Gunungsewu is also higher than that of several springs in Jonggrangan Karst, such as Mudal, Kiskendo, and Anjani. Therefore, epikarst not only functions as an important component of the karst hydrological system but also as a key element in karst's ecological role as a natural carbon sink. Although Seropan's total CO_2 uptake is greater due to its larger catchment area, these results indicate that carbon uptake efficiency is more determined by the karst system's hydrogeological characteristics than by catchment area alone. Thus, epikarst should be a key focus in tropical karst carbon studies and climate change mitigation.

Acknowledgements

The authors would like to thank the Karst Research Group, Faculty of Geography, UGM, for providing the necessary facilities and equipment for field data collection. Apart from that, the authors thank the Gunungkidul Regency government for providing permission to conduct this research.

References

Adji, T. N., Haryono, E., Fatchurohman, H., & Oktama, R. (2017). Spatial and temporal hydrochemistry variations of karst water in Gunung Sewu, Java, Indonesia. *Environmental Earth Sciences, 76*(20), Article 709. https://doi.org/10.1007/s12665-017-7057-z

Adji, T. N., Mujib, M. A., Haryono, E., Fatchurohman, H., & Kholis, A. N. (2023). Simplified approach in karst aquifer characterization by using discharge variability, storage capacity, and void development: A preliminary study in the tropical karst region. *Kuwait Journal of Science, 50*(4), 812–822. https://doi.org/10.1016/j.kjs.2023.05.012

Aquilina, L., Ladouche, B., & Dörfliger, N. (2006). Water storage and transfer in the epikarst of karstic systems during high flow periods. *Journal of Hydrology, 327*(3–4), 472–485. https://doi.org/10.1016/j.jhydrol.2005.11.054

Bakalowicz, M. (2013). Epikarst processes. In J. F. Shroder (Ed.), *Treatise on geomorphology* (1st ed., pp. 164–171). Academic Press. https://doi.org/10.1016/B978-0-12-374739-6.00100-7

Bakalowicz, M. (2019). Epikarst. In W. B. White, D. C. Culver, & T. Pipan (Eds.), *Encyclopedia of caves* (3rd ed., pp. 394–398). Academic Press. https://doi.org/10.1016/B978-0-12-814124-3.00045-5

Balazs, D. (1968). Karst regions in Indonesia: Karszt-Es Barlangkutatas (Vol. 5). Globus Nyomda.

Balazs, D. (1971). *Intensity of the tropical karst development based on cases of Indonesia: Karszt-Es Barlangkutatas (Vol. 6).* Globus Nyomda.

Cahyadi, A., Riyanto, I. A., Ramadhan, F., Widyastuti, M., Fatchurohman, H., & Adji, T. N. (2023a). Multitemporal water quality analysis of an epikarst spring for agricultural irrigation in the Gunungsewu Karst Area, Indonesia. *AIP Conference Proceedings*, *2683*(1), Article 030003. https://doi.org/10.1063/5.0145414

Cahyadi, A., Riyanto, I. A., & Adji, T. N. (2023b). Suitability of water from tropical epikarst spring for irrigation in the Gunungsewu Karst Area, Indonesia. *IOP Conference Series: Earth and Environmental Science*, *1268*(1), Article 012008. https://doi.org/10.1088/1755-1315/1268/1/012008

Cao, J., Wu, X., Huang, F., Hu, B., Groves, C., Yang, H., & Zhang, C. (2018). Global significance of the carbon cycle in the karst dynamic system: Evidence from geological and ecological processes. *China Geology, 1*(1), 17–27. https://doi.org/10.31035/cg2018004

Chen, B., Zhao, M., Yan, H., Yang, R., Li, H. C., & Hammond, D. E. (2021). Tracing source and transformation of carbon in an epikarst spring-pond system by dual carbon isotopes (^{13}C–^{14}C): Evidence of dissolved CO_2 uptake as a carbon sink. *Journal of Hydrology, 593*, Article 125766. https://doi.org/10.1016/j.jhydrol.2020.125766

Chen, L., Tan, L., Zhao, M., Sinha, A., Wang, T., & Gao, Y. (2023). Karst carbon sink processes and effects: A review. *Quaternary International, 652*, 63–73. https://doi.org/10.1016/j.quaint.2023.02.009

Cheng, K., Liu, Z., Xiong, K., He, Q., Li, Y., Cai, L., & Chen, Y. (2023). Migration of dissolved organic matter in the epikarst fissured soil of South China Karst. *Land, 12*(4), Article 887. https://doi.org/10.3390/land12040887

Dwiputra, D. S. (2019). *Estimasi laju penyerapan karbon dioksida atmosfer melalui proses pelarutan batuan karbonat di kawasan karst Jonggrangan, Kulonprogo-Purworejo* [Undergraduate thesis, Universitas Gadjah Mada]. https://etd.repository.ugm.ac.id/penelitian/detail/176652

Fores, B., Champollion, C., Lesparre, N., Pasquet, S., Martin, A., & Nguyen, F. (2021). Variability of the water stock dynamics in karst: Insights from surface-to-tunnel geophysics. *Hydrogeology Journal, 29*(6), 2077–2089. https://doi.org/10.1007/s10040-021-02365-5

Frank, S., Goeppert, N., & Goldscheider, N. (2021). Improved understanding of dynamic water and mass budgets of high-alpine karst systems obtained from studying a well-defined catchment area. *Hydrological Processes, 35*(4), Article e14033. https://doi.org/10.1002/hyp.14033

Fu, Z., Chen, H., Zhang, W., Xu, Q., Wang, S., & Wang, K. (2015). Subsurface flow in a soil-mantled subtropical dolomite karst slope: A field rainfall simulation study. *Geomorphology, 250*, 1–14. https://doi.org/10.1016/j.geomorph.2015.08.012

Hartawan, B. S., Erwandha, R., Sholih, D., Hidayat, M. R. A., & Irsyadi, M. B. (2020). Characteristics of Sewu Mountain Karst as geopark area. *Journal of Global Environmental Dynamics, 1*(1), 7–12. Journal article

Haryono, E. (2011). Atmospheric carbon dioxide sequestration through karst denudation processes estimated from Indonesian karst region. In *Proceedings of the Asian Trans-Disciplinary Karst Conference* (pp. 203–207).

Huang, W., Wang, X., & Zhang, D. (2024). The estima-

tion of forest carbon sink potential and influencing factors in Huangshan National Forest Park in China. *Sustainability, 16*(3), Article 1351. https://doi.org/10.3390/su16031351

Jiang, Y. (2013). The contribution of human activities to dissolved inorganic carbon fluxes in a karst underground river system: Evidence from major elements and δ13CDIC in Nandong, Southwest China. *Journal of Contaminant Hydrology, 152*, 1–11. https://doi.org/10.1016/j.jconhyd.2013.05.010

Jiang, Z., Lian, Y., & Qin, X. (2013). Carbon cycle in the epikarst systems and its ecological effects in South China. *Environmental Earth Sciences, 68*(1), 151–158. https://doi.org/10.1007/s12665-012-1724-x

Jones, W. K. (2013). Physical structure of the epikarst. *Acta Carsologica, 42*(2–3), 311–314. https://doi.org/10.3986/ac.v42i2-3.672

Kabir, M., Habiba, U. E., Khan, W., Shah, A., Rahim, S., Rios-Escalante, P. R. D. L., Farooqi, Z., Ali, L., & Shafiq, M. (2023). Climate change due to increasing concentration of carbon dioxide and its impacts on environment in 21st century: A mini review. *Journal of King Saud University - Science, 35*(5), Article 102693. https://doi.org/10.1016/j.jksus.2023.102693

Klimchouk, A. B. (2004). Towards defining, delimiting and classifying epikarst: Its origin, processes and variants of geomorphic evolution. *Speleogenesis and Evolution of Karst Aquifers, 2*(1), 1–13. https://digitalcommons.usf.edu/kip_articles/5335

Kozel, P., & Pipan, T. (2020). Specialized aquatic subterranean communities are probably most species-rich in the thickest epikarst. *Limnologica, 81*, Article 125756. https://doi.org/10.1016/j.limno.2020.125756

Liu, Z., & Zhao, J. (2000). Contribution of carbonate rock weathering to the atmospheric CO_2 sink. *Environmental Geology, 39*, 1053–1058. https://doi.org/10.1007/s002549900072

Martin, J. B. (2017). Carbonate minerals in the global carbon cycle. *Chemical Geology, 449*, 58–72. https://doi.org/10.1016/j.chemgeo.2016.11.029

Milanović, P. T. (2025). The complexity of epikarst: Definitions and observations. *Carbonates and Evaporites, 40*, Article 127. https://doi.org/10.1007/s13146-025-01162-5

Nannoni, A., & Piccini, L. (2022). Mixed recharge and epikarst role in a complex metamorphic karst aquifer: The Pollaccia System, Apuan Alps (Tuscany, Italy). *Hydrology, 9*(5), Article 83. https://doi.org/10.3390/hydrology9050083

Nunes, L. J. (2023). The rising threat of atmospheric CO_2: A review on the causes, impacts, and mitigation strategies. *Environments, 10*(4), Article 66. https://doi.org/10.3390/environments10040066

Nurkholis, A., Adji, T. N., Haryono, E., Cahyadi, A., Waskito, W. A., Fathoni, H., Kurniawan, I. A., & Agniy, R. F. (2019). Analysis of master recession curve (MRC) and flood hydrograph components for karstification degree estimation in Kiskendo Cave, Jonggrangan Karst System, Indonesia. *IOP Conference Series: Earth and Environmental Science, 256*, Article 012011. https://doi.org/10.1088/1755-1315/256/1/012011

Pardo-Igúzquiza, E., Dowd, P. A., Ruiz-Constán, A., Martos-Rosillo, S., Luque-Espinar, J. A., Rodríguez-Galiano, V., & Pedrera, A. (2018). Epikarst mapping by remote sensing. *CATENA, 165*, 1–11. https://doi.org/10.1016/j.catena.2018.01.026

Pu, J. B., Jiang, Z. C., Yuan, D. X., & Zhang, C. (2015). Some opinions on rock-weathering-related carbon sinks from the IPCC Fifth Assessment Report. *Advances in Earth Science, 30*(10), 1081–1090. https://doi.org/10.11867/j.issn.1001-8166.2015.10.1081

Reinhart, H., Putra, R. D., Rafida, M. R., Majiid, M. A., & Maulita, N. S. (2023). Karst of Gunung Sewu land use and land covers dynamics: Spatio-temporal analysis. *Forum Geografi, 36*(2), 98–109. https://doi.org/10.23917/forgeo.v36i2.19868

Riyanto, I. A., & Cahyadi, A. (2023). Anthropogenic activity effect on water quality of epikarst spring in the western part of Gunungsewu Karst Area, Java Island, Indonesia. *Journal of Degraded and Mining Lands Management, 11*(1), 4899–4908. https://doi.org/10.15243/jdmlm.2023.111.4899

Srivastava, P., Kumar, A., Behera, S. K., Sharma, Y. K., & Singh, N. (2012). Soil carbon sequestration: An innovative strategy for reducing atmospheric carbon dioxide concentration. *Biodiversity and Conservation, 21*(5), 1343–1358. https://doi.org/10.1007/s10531-012-0229-y

Trček, B. (2002). Epikarst zone of a karst aquifer – Its characteristics and importance in karst hydrogeology. *Geologija, 45*(2), 573–578. https://doi.org/10.5474/geologija.2002.067

Widyastuti, M., Riyanto, I. A., Naufal, M., Ramadhan, F., & Rahmawati, N. (2019). Catchment area analysis of Guntur Karst Spring Gunung Kidul Regency, Java, Indonesia. *IOP Conference Series: Earth and Environmental Science, 256*(1), Article 012008. https://doi.org/10.1088/1755-1315/256/1/012008

Williams, P. (2008). The role of the epikarst in karst and cave hydrogeology: A review. *International Journal of Speleology, 37*(1), 1–10. https://doi.org/10.5038/1827-806X.37.1.1

Wu, L., Zhang, Y., Luo, G., Chen, D., Yang, D., Yang, Y., & Tian, F. (2023). Characteristics of vegetation carbon sink carrying capacity and restoration potential of China in recent 40 years. *Frontiers in Forests and Global Change, 6*, Article 1266688. https://doi.org/10.3389/ffgc.2023.1266688

Xie, Y., Huang, F., Yang, H., & Yu, S. (2021). Role of anthropogenic sulfuric and nitric acids in carbonate weathering and associated carbon sink budget in a karst catchment (Guohua), southwestern China. *Journal of Hydrology, 599*, Article 126287. https://doi.org/10.1016/j.jhydrol.2021.126287

Yang, R., Liu, Z., Zeng, C., & Zhao, M. (2012). Response of epikarst hydrochemical changes to soil CO_2 and weather conditions at Chenqi, Puding, SW China. *Journal of Hydrology, 468–469*, 151–158. https://doi.org/10.1016/j.jhydrol.2012.08.029

Yoro, K. O., & Daramola, M. O. (2020). CO_2 emission sources, greenhouse gases, and the global warming effect. In M. R. Rahimpour, M. Farsi, & M. A. Makarem (Eds.), *Advances in carbon capture: Methods, technologies and applications* (pp. 3–28). Woodhead Publishing. https://doi.org/10.1016/B978-0-12-819657-1.00001-3

Yu, S., Chae, G., Oh, J., Kim, S.-H., Kim, D.-I., & Yun, S.-T. (2021). Hydrochemical and isotopic difference of spring water depending on flow type in a stratigraphically complex karst area of South Korea. *Frontiers in Earth Science, 9*, Article 712865. https://doi.org/10.3389/feart.2021.712865

Zeng, C., Liu, Z., Yang, J., & Yang, R. (2015). A groundwater conceptual model and karst-related carbon sink for a glacierized alpine karst aquifer, Southwestern China. *Journal of Hydrology, 529*, 120–133. https://doi.org/10.1016/j.jhydrol.2015.07.027

Zhang, M., Yang, W., Yang, M., & Yan, J. (2022). Guizhou karst carbon sink and sustainability—An overview. *Sustainability, 14*(18), Article 11518. https://doi.org/10.3390/su141811518

Zhang, Z., Chen, X., Chen, X., & Shi, P. (2013). Quantifying time lag of epikarst-spring hydrograph response to rainfall using correlation and spectral analyses. *Hydrogeology Journal, 21*(7), 1619–1631. https://doi.org/10.1007/s10040-013-1041-9